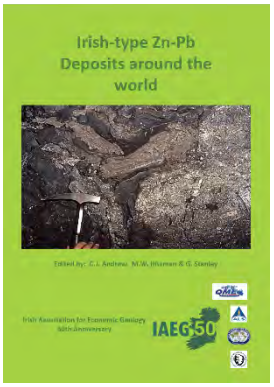

Irish Association for Economic Geology

(founded 1973)

Home Page: https://www.iaeg.ie

Global Irish – Diversity of the diaspora

Neal A. Reynolds[1], R. Mark Allen[1], Peter Muhling[2] & Charlie Gianfriddo[1]

[1] *CSA Global, Perth, Western Australia*
[2] *Perth, Western Australia*

Corresponding Author: Neal Reynolds Neal.Reynolds@erm.com

To cite this article: Reynolds, N.A., Allen, M.A., Muhling, P. & Gianfriddo, C. (2023) Global Irish – Diversity of the diaspora. In: Andrew, C.J., Hitzman, M.W. & Stanley, G. '*Irish-type Deposits around the world*', Irish Association for Economic Geology, Dublin. 45-94. DOI: https://doi.org/10.61153/TAYM1799

To link to this article: https://doi.org/10.61153/TAYM1799

Global Irish – Diversity of the diaspora

Neal A. Reynolds[1], R. Mark Allen[1], Peter Muhling[2] & Charlie Gianfriddo[1]

[1] *CSA Global, Perth, Western Australia*
[2] *Perth, Western Australia*

Abstract: The spectrum of zinc-lead deposits formed in basinal mineral systems encompasses VMS (volcanogenic massive sulphide), SHMS (shale-hosted massive sulphide), Irish-type and MVT (Mississippi valley Type) deposits. The platform carbonate-hosted part of that spectrum, the Irish-type and MVT deposits, has created the greatest challenges to pigeonholing approaches and the Irish Midland deposits have been variably considered as unique, "SedEx" variants, or MVT variants. In fact, the Irish-type spectrum of deposits can be considered as a global diaspora of diverse deposits that, nonetheless, show a number of distinct and economically significant characteristics in style and setting. For this reason, they warrant consideration as a discrete deposit type, though not in a neat pigeonhole, that is best considered in a mineralizing system context.

The distinguishing features of Irish-type mineral systems can be considered in terms of source, trigger, pathway, trap, and preservation. The key features that distinguish Irish-type from 'typical' MVT and SHMS deposits are related to basin type and setting, timing of the mineralization event, mineralization style and chemistry, and deposit geometry. Empirically, these characteristic basin to deposit scale features overlap both MVT and SHMS but, together, are unique to Irish-type systems. This gives rise to criteria that can be applied to determine prospectivity of basins for Irish-type deposits and to target deposits within these basins.

It is important to distinguish Irish-type from MVT systems because their economic characteristics are different. However, it is also important to recognise that there is great variability within the broad basinal carbonate-hosted zinc-lead deposit family and that each basin, and indeed each trend and deposit, are to some extent unique. It is therefore extremely important to avoid model-driven exploration and to develop a targeting understanding that acknowledges the model framework but is based on actual observations and data.

To understand this diversity and targeting context, it is pertinent to consider the wide range of carbonate-hosted deposits that do not fit into the published MVT pigeonhole, including the Irish Midlands deposits; the Alpine deposits; deposits in the Basque-Cantabria Basin; deposits on the Gondwana margin including a number of deposits in North African,, southeast Turkey, Iran, and Duddar in Pakistan; the Early Cretaceous deposits on the Atlantic margin in Gabon; the Ordovician of the Sibumasu terrane (Tibet to Southeast Asia); Polaris in the Franklinian Basin; Nanisivik in the Borden Basin; and the Devonian Lennard Shelf deposits of Western Australia. All of these deposits occur in rift-sag basins with carbonate platforms, in some cases with multiple rift-sag cycles or with successor basins and, where constrained, the mineralization event is syn-basinal and typically related to early extension or inversion events. The deposits are stratabound and mostly tabular and continuous, often show strong direct control by extensional structures, are typically dominated by replacement, and commonly have significantly higher grades than 'typical' MVT deposits such as those in the mid-continent US, Silesia (Poland) and Pine Point (Canada).

Keywords: Mineral systems, classifications, Irish-type, MVT-type, SHMS, rift-sag basins, carbonate platforms

Introduction

The discovery and development of the Tynagh and Silvermines zinc-lead deposits in the 1960s sparked a renaissance in the Irish exploration and mining industry and, in the 1960s to 1980s, a succession of publications on the geology and origin of Irish zinc-lead deposits. Early work interpreted the deposits to have formed by replacement early in the sedimentary history of the Irish Midlands Basin, for example at Tynagh (Schultz, 1966; Boast *et al*., 1981), where the geometry of mineralization alone precluded a syngenetic exhalative origin. However, amidst the global syngenetic exhalative revolution of the 1970s and 1980s, numerous publications placed the Irish deposits within the emerging 'SedEx' family, notably Russell and co-

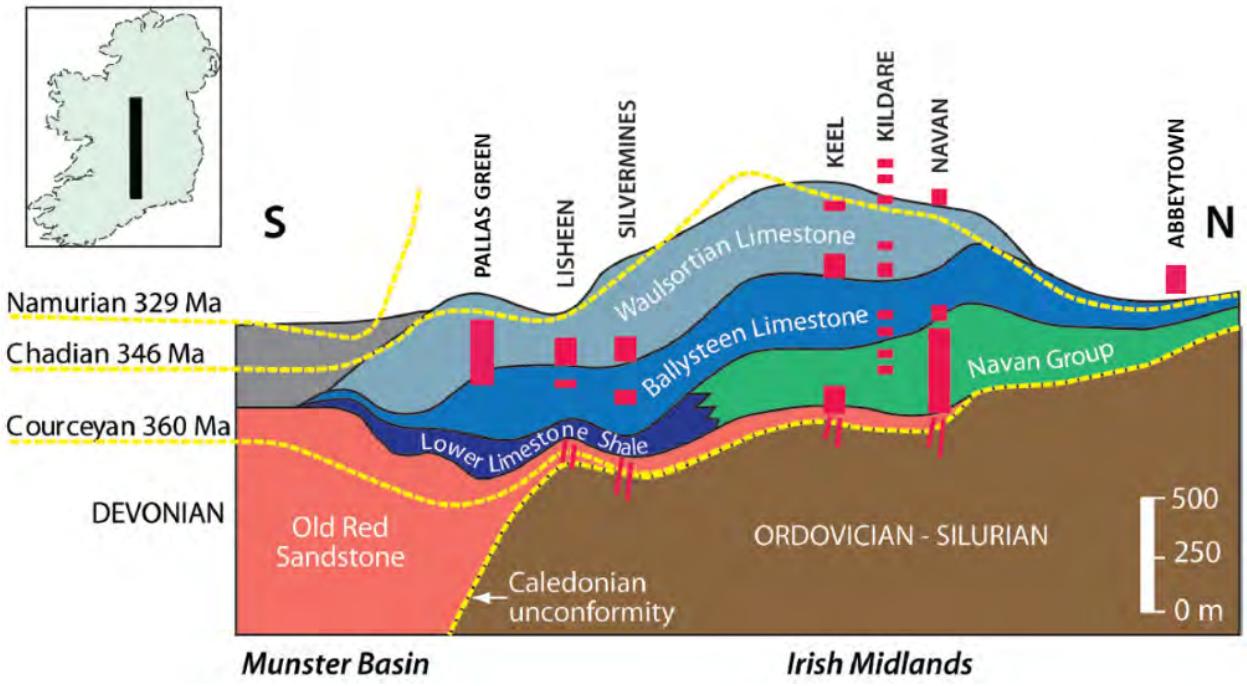

Figure 1: *Simplified stratigraphic section showing diachronous nature of sediment facies from south to north across the Irish Midlands and the stratigraphic location of mineralization in a number of deposits and footwall veins. Modified from Andrew (1993).*

workers (e.g., Russell, 1972; Boyce, *et al.*, 1983; Mills *et al.*, 1987, Boyce, 1990).

The pendulum swung back slowly over time with the recognition that most mineralization in the Irish deposits is replacive, sometimes considering them as MVTs, but generally towards an understanding that the Irish deposits should be considered as neither SHMS nor MVT (e.g., Wilkinson, 2014). The term 'Irish-type' was reportedly first used in 1977 and recognised the distinct nature of the Irish Midlands deposits. Although there is still some disagreement over the timing of mineralization, there is general agreement that mineralization largely post-dated early diagenesis and, in the Limerick Basin, post-dated the main stage emplacement of diatremes of the early Visean (Chadian to Arundian) Knockroe Formation volcanic suite (Elliott *et al.*, 2019), while at Navan, it at least in a minor part post-dated the Arundian Boulder Conglomerate (e.g. Peace & Wallace, 2000; Walker, 2005; Ashton *et al.*, 2015).

Despite the development of this more nuanced understanding of the Irish deposits, globally many economic geologists still carry the understanding that Irish deposits are syngenetic. The other aspect of Irish deposits that is not widely understood globally is the variability in mineralization style and controls, where imagery of stratabound Navan or Lisheen mineralization geometry prevails over geometries of Tynagh, Pallas Green, Keel, or Harberton Bridge. Perhaps these perceptions have hindered the recognition of other global examples of the Irish-type family. Certainly, some deposits have been suggested as analogues previously, for example Morro Agudo in the Vazante Group in Brazil (Misi *et al.*, 2005), Gays River in the Mississippian of Nova Scotia (Akande & Zentilli, 1984), Prairie Creek in the Lower Palaeozoic Mackenzie carbonate platform of the Northwest Territories (Paradis, 2007), and the Triassic Alpine zinc-lead deposits (Schroll & Rantitsch, 2005).

In this review, we summarise the key characteristics of the Irish Midlands deposits and 'typical' MVT deposits, describe some other districts that do not conform to 'typical MVT' characteristics, and discuss the genetic and economic implications.

Zinc-Lead mineralizing systems and deposits in sedimentary-volcanic basins

Mineralizing systems in sedimentary basins give rise to deposits hosted within the basin in fine-grained, often calkcatreous or dolomitic, siliciclastic sediments and/or volcanics, SHMS and VMS, and deposits hosted in carbonate platforms that mark the edge of basins, MVT and Irish-type. The ideas regarding formation of SHMS and VMS systems are reasonably well constrained, including the increasing recognition that SHMS deposits formed by replacement (e.g., Blevings *et al.*, 2013; Magnall *et al.*, 2020; Spinks *et al.*, 2021), and acceptance of the existence of transitional 'hybrid' deposits in the spectrum (e.g. Rammelsberg; Mueller, 2022). Platform carbonate-hosted deposits however have generally been grouped into a unifying MVT model (e.g., Bradley & Leach, 2003; Leach *et al.*, 2001), with the sometime exception of the Irish Midlands deposits which have been considered as an 'Irish-type' MVT sub-type or a 'SedEx' sub-type (e.g., Sangster, 1990). As a result, deposits globally with widely differing features have generally been assigned to the MVT class and many reviews have highlighted this variability (e.g., Sangster, 1983; Leach *et al.*, 2005; Wilkinson, 2014).

Irish-type deposits of the Irish Midlands basin

It is instructive when considering the Irish Midlands deposits to consider the empirical and interpreted characteristics that encompass all the deposits and not just the type examples. This is considered an appropriate approach considering the

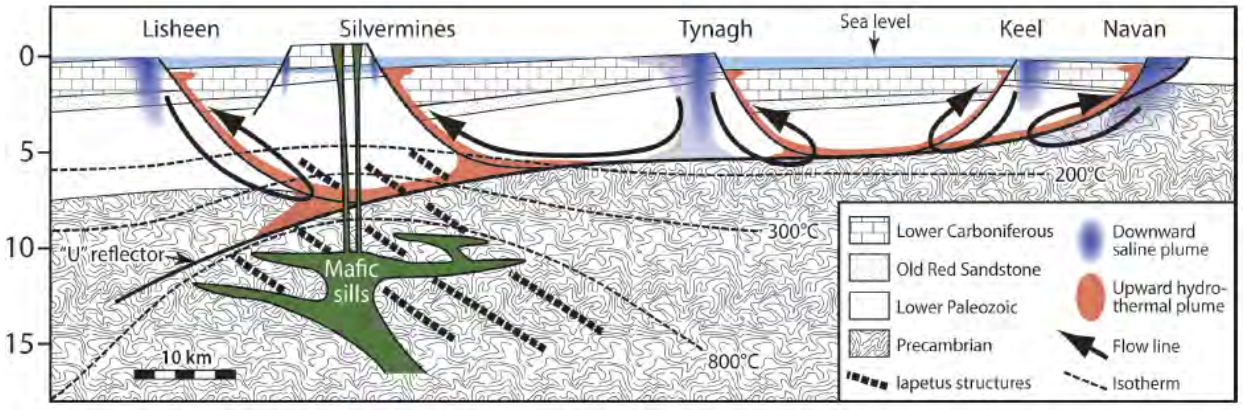

Figure 2: *Model for fluid systems forming deposits in the Irish Midlands. From Wilkinson & Hitzman, 2015.*

evidence provided by lead isotope data (e.g., O'Keefe, 1986; *et al*., 1987) that mineralization occurred in a single event, albeit potentially prolonged.

The key characteristics that are generally highlighted in distinguishing Irish-type deposits from MVT deposits include the dominantly replacive style, structural control, stratabound geometry, the relatively higher temperature and content of silver and other elements like antimony, arsenic and thallium, and the dominance of negative sulphur isotopic composition indicative of bacteriogenic sulphur reduction (BSR). Deposits occur within a mixed carbonate sequence with a variable input of siliciclastic sediment, deposited in a tectonically active platform and basin setting. The close association with syn-sedimentary extensional faults is not clearly defined in all deposits, for example the Pallas Green – Stonepark deposits and the Kildare deposits. Lead isotope signatures are broadly conformable in terms of model ages with indications of mixing of lead sources (LeHuray *et al.*, 1987). The main interpreted characteristic is that mineralization occurred early in basin history, during early to late diagenesis.

The Irish Midlands model should also accommodate 'atypical' deposits including Harberton Bridge, characterized by replacive, vein- and breccia-hosted mineralization in the Waulsortian extending up into Arundian shelf limestone (Allenwood Beds), Keel encompassing vein-hosted and replacive mineralization in the Pale Beds extending down into the transitional siliciclastics and basal conglomerates, and Abbeytown where stratabound and cross-cutting mineralization is associated with dolomitization of Chadian platform limestones. Considering all deposits, mineralization straddles a significant time interval despite the diachronous sedimentary facies across the Irish Midlands (Figure 1).

From the perspective of a basinal mineral system, the Irish-type deposits occur within a broad platform, marginal to a rift-sag basin that evolved to a passive margin and underwent inversion and deformation in the Upper Carboniferous Variscan orogeny. Additionally, the basin and platform can be considered as a successor basin to the underlying Ordovician-Silurian flysch, deformed at sub-greenschist during the Caledonian orogeny. Following Courceyan (Tournaisian) transgression and deepening, a major extensional event in the Chadian to Arundian (Visean) resulted in development of fault-controlled sub-basins within the platform, including rapid deepening in the Limerick and Dublin Basins (Morton *et al*., 2015). This was accompanied by significant mafic alkaline volcanism, best developed in the Limerick Basin (Strogen, 1995; Slezak *et al*., 2022). Mineralization is mainly hosted within Courceyan carbonates, including marginal marine sequences at Navan and deeper water Waulsortian mudbanks at most of the other significant deposits and prospects. There is substantial evidence at most deposits for two fluids, a deep-sourced metal-bearing oxidi*zed* moderately saline brine and a shallowly sourced more saline brine carrying bacterially reduced sulphur (Wilkinson & Hitzman, 2015; Torremans *et al*, 2018), supporting the interpretation of relatively early mineralization.

A working mineral system model considers: a thermally-mature metal source region encompassing the older flysch basin and, in the south, the Devonian Old Red Sandstone (Figure 2) but potentially also incorporating input from the Lower Carboniferous Munster Basin to the south; sulphur source from Carboniferous seawater, which was entrained in the carbonate sequence as dense evaporated brines, via a combination of BSR and thermochemical sulphur reduction (TSR); a trigger event for mineralizing fluid-flow resulting from Chadian-Arundian tectonism in a high-heat-flow environment, as evidenced by synchronous volcanism; fluid-flow pathways provided by syn-sedimentary faulting and dolomitized aquifers in the Waulsortian; and traps related to mixing of metal and sulphur-bearing fluids and reaction with favourable clean limestone units, especially micritic limestone which presented an abundance of reactive grain surfaces.

This system model can accommodate mineralization in rocks from Courceyan to Arundian age related to a major district-scale fluid-flow event. This system generated huge replacive deposits like Navan in optimal circumstances due to the combination of major structures, favourable host rocks, and shallow sulphur-bearing brines (Ashton *et al.*, 2015) due to uplift and tectonic erosion on the northern edge of the Dublin Basin. It also generated lower-grade more dispersed deposits like Pallas Green where multiple structures facilitated fluid flow into a thick Waulsortian interval without aquicludes, smaller deposits like Tynagh where the Waulsortian development was discontinuous, and deposits like Keel where the favourable Navan Beds host units are less well developed than at Navan. It can also accommodate the Kildare deposits which have often

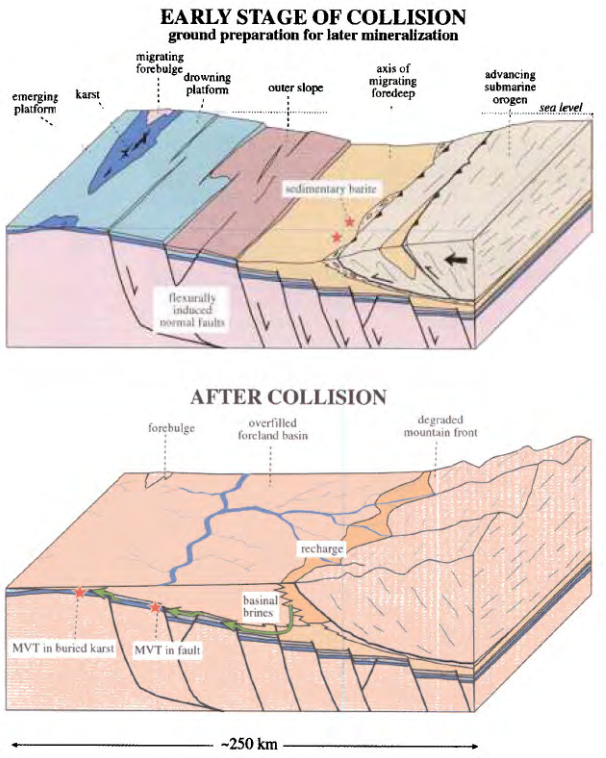

Figure 3: *Model for MVT mineralization in palaeokarst in foreland basins during collisional orogeny, from Bradley & Leach, 2003.*

been considered as younger MVT deposits and which are characterized by generally higher sulphur isotope ratios suggestive of TSR rather than the BSR; the Kildare mineralization occurs as stacked lenses in the Waulsortian and in the overlying shelf limestones (Allenwood Beds), both affected by regional dolomitization resulting in less constrained mineralization.

The key point is that multiple deposit types, or target plays, exist within the Irish Midlands mineral system, related to different fluid focus and trap environments, of which two have been demonstrated to host economic mineralization. The economic deposits have favourable characteristics including relatively high grades, laterally extensive and continuous mineralized zones of mineable thickness, and favourable metallurgy including relatively low comminution energy requirements, good recoveries, high-grade low-iron zinc concentrates, and lead concentrates with payable silver.

In terms of project-scale exploration characteristics, Irish Midland deposits are typically characterized by a recognised lithostructural setting, an alteration halo of black-matrix breccia and/or iron-bearing dolomite that may extend significantly beyond economic mineralization, and a geophysical response to Induced Polarization methods and, in some cases, electromagnetic detection.

Mississippi-Valley type deposits

In this review, we consider as 'typical' a number of MVT systems that have been a foundation for the unifying models for mineralization during contractional tectonic events, especially within orogenic foreland basins (e.g., Leach & Sangster, 1993; Leach *et al.*, 2001; Bradley & Leach, 2003). These include the mid-continent US districts (Viburnum/Old Lead Belt, Tristate, East and Central Tennessee), Silesia, and Pine Point, as well as numerous other districts globally such as the Earaheedy Basin in Western Australia, the Cambrian of South China, and most deposits of the Atlas orogen in North Africa. These deposits are characteri*zed* by mineralization within thick, clean carbonate sequences deposited on stable platforms and predominant open-space fill of meteoric palaeokarst and/or hydrothermal karst. Mineralogy and chemistry are simple with generally low grades of Ag, low temperature of formation, and sulphide sulphur with a TSR isotopic signature. Lead isotope signatures are typically anomalously radiogenic ('J-type'). The key interpreted characteristic is that mineralization is late and often substantially younger than the host rocks, following complete lithification and typically after uplift, meteoric karst formation, and re-burial.

The Bradley & Leach (2003) mineral system model envisages large-scale fluid-flow events within foreland basins, caused by collisional compression and uplift in the adjacent orogen and resulting in expulsion of mineralizing metal- and sulphur-bearing brines onto carbonate platforms in passive margin or intracratonic basin settings (Figure 3). In this system, the metal source may be the passive margin flysch outboard of the carbonate platform and/or basal siliciclastic sedimentary rocks underlying the carbonate platform, the sulphur source may be brines and hydrocarbons forming part of the fluid-flow event, the trigger is compressional orogeny, the pathway and focus is typically envisaged as a formational aquifer with faults present but often of lesser importance, and the trap is typically meteoric karst with hydrocarbons commonly invoked as a reductant. Failure to explain some features of even the mid-continent US deposits have been pointed out by Wilkinson (2014), invoking the possibility of more local metal sources, but the broad model is generally accepted and applied to most deposits described as MVT.

Economic characteristics of these MVT systems are generally less favourable than Irish-type deposits, typically with lower zinc and lead grades and with no silver credits, and commonly occurring as irregular discontinuous mineralization with a geometry comparable to karst systems controlled by jointing. However, the negative features are countered by some deposits, or rather interconnected districts, being very large, and by having favourable metallurgical characteristics, producing very clean concentrates at high recoveries and without the deleterious elements that can occur in Irish-type and SHMS deposits.

A spectrum of districts and deposits

The variability and complexity of settings and environments hosting low-temperature carbonate-hosted deposits can be illustrated through examples that do not readily fit a unifying MVT model and that can be alternatively considered as forming within Irish-type systems. The examples presented here are all interpreted to reflect intra-basin mineralizing systems that developed during basin formation, with typically replacive mineralization occurring during diagenesis of the host sequence. They include low-temperature systems with mineralization that shows close similarities to 'typical' MVT (e.g.,

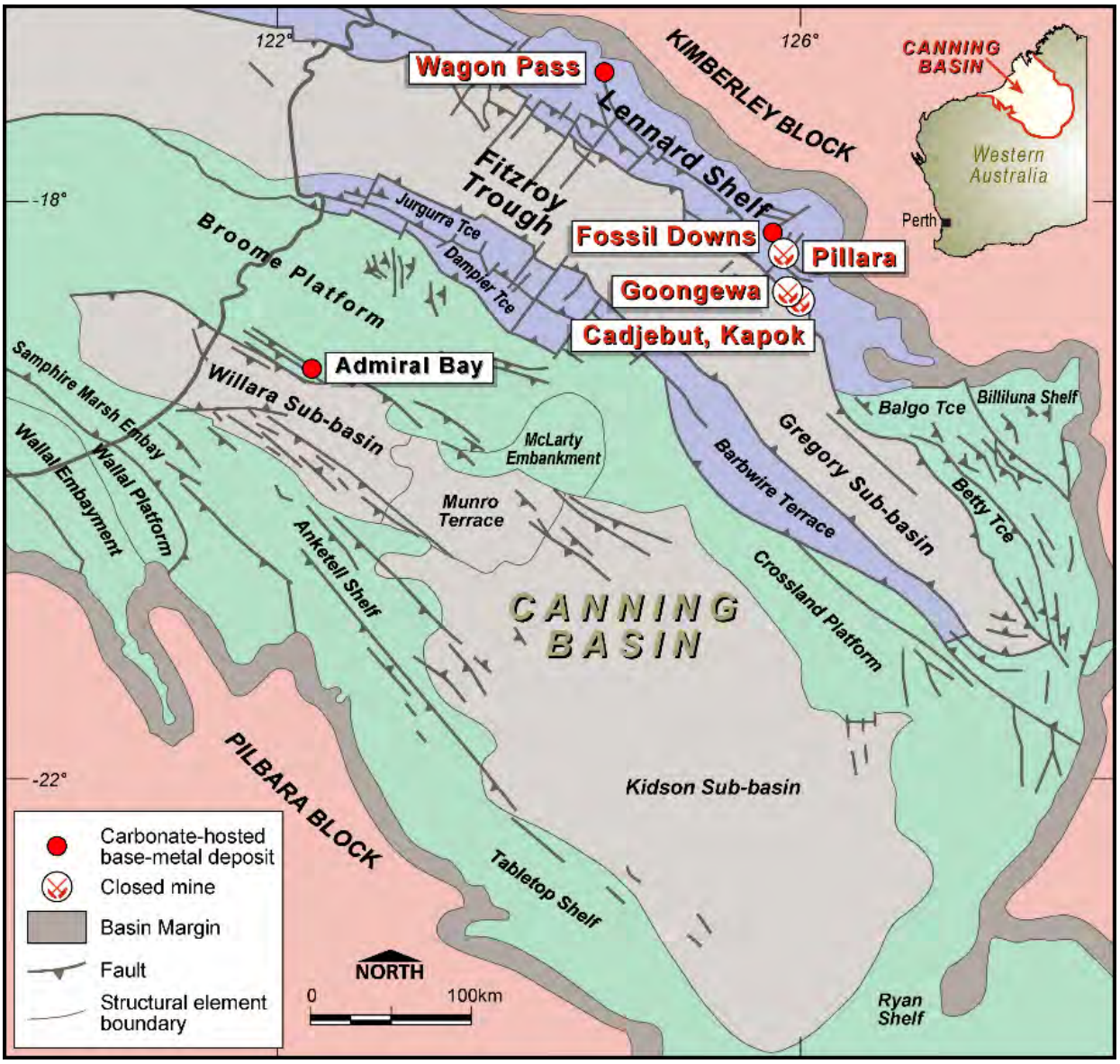

***Figure 4**: Regional geological setting of the Canning Basin and location of Zn–Pb deposits. Modified from Shaw et al., 1995.*

Lennard Shelf, Australia) and higher-temperature systems where mineralization shows closer similarities to the Irish Midlands that have been considered as SHMS (e.g., Duddar, Pakistan).

The examples that have been addressed in some detail are all districts where the authors have direct experience, some other deposits have been discussed in less detail. The deposits are presented in order of the age of the host rocks rather than attempting to further subdivide the spectrum that is illustrated.

Admiral Bay

The carbonate-hosted Admiral Bay zinc-lead-silver deposit is located at depths of 1200-1500m in the southern Canning Basin of northwest Australia (McCracken *et al.*, 1996). Mineralization was discovered in 1981 in petroleum well Great Sandy 1 and three other wells (Ferguson, 1999). Twenty-four diamond drillholes were completed between 1986 and1991 with a further twelve drillholes in 2007 and 2008 in the central 2.5-kilometre part of the deposit. Mineralization has been intersected for approximately 20 kilometres along the fault zone, with potential ore-grade mineralization in drillholes 14 kilometres apart.

Regional Geology

The Canning Basin is a long-lived intracratonic rift-sag basin developed between the Archean Pilbara craton to the southwest and the Proterozoic Kimberly craton to the northeast (Shaw, *et al.*, 1995; Parra-Garcia *et al.*, 2014). The basin underwent successive episodes of subsidence and deposition in four major tectono-stratigraphic sequences from the Ordovician to Early Cretaceous (Kennard *et al.*, 1994), resulting in a complex architecture of sub-basins, platforms, and terraces, bounded by fault systems (Figure 4). The first major rift-sag cycle occurred in the Lower Ordovician to Silurian Willara–Kidson Sub-basin, accompanied by rift-stage tuffs (Mory, 2017).

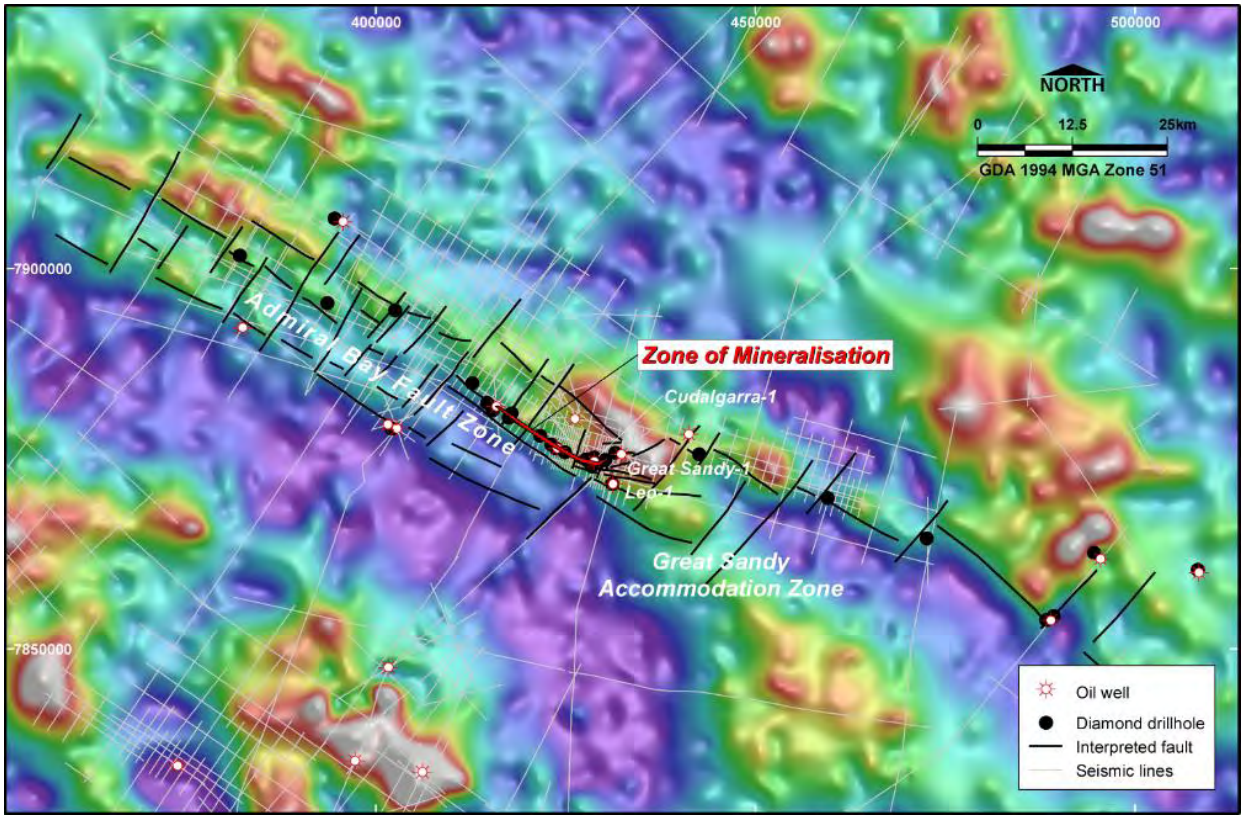

Figure 5: *Structural framework of the Admiral Bay Fault Zone on regional Bouguer gravity image; the main part of the Admiral Bay deposit is in the southeast of the mineralized zone. From Reynolds & Copp, 2017a.*

Structural and Lithostratigraphic Setting

The Admiral Bay deposit is located within the Admiral Bay Fault Zone which originated during the Lower Ordovician rift event as an extensional fault zone separating the Willara Sub-basin half-graben to the south from the Broome Platform to the north (Shaw *et al.,* 1995). Ordovician extension resulted in a series of complex fault relays and terraces along the fault zone. The deposit is localised on a fault-controlled palaeo-topographic high in the footwall of the fault zone adjacent to a left-stepping relay, the Great Sandy Accommodation Zone, and the associated basement ridge (Figure 5).

The stratigraphy at Admiral Bay comprises an upward-shallowing sag-phase succession from outer- to mid-ramp siliciclastic-dominated facies with variable carbonate content (Willara and Goldwyer Formations); through inner-ramp carbonate facies with increasing siliciclastics (Nita Formation: Leo and Cudalgarra Members); to intertidal/lagoonal/supratidal facies (Bongabinni Formation of the Carribuddy Group) (Figure 7). Tuffs are present in the Willara Formation and the Goldwyer Formation, in which tuff has been dated at 467 ± 6Ma (Mory, 2017). Distinct local facies variations are present along the Admiral Bay Fault Zone, notably the development of debrites in the upper Goldwyer Formation, and the development of extensive microbial boundstone (bioherms) in the Leo Member (Reynolds & Copp, 2017a).

Mineralization

Mineralization extends through up to 450 metres of stratigraphy, mainly hosted by the Nita Formation but extends down into the Goldwyer Formation and up into the Bongabinni Formation beneath the evaporitic interval of the Carribuddy Group. The deposit coincides with the strongly dolomitized biohermal facies of the Leo Member in the footwall of the fault zone, which hosts significant lead-barite mineralization. Zinc mineralization is mainly hosted in undolomitized limestone in the lower part of the overlying Cudalgarra Member (Figure 6). The highest-grade mineralization (>5% Zn) is localised at discrete stratigraphic levels where favourable host lithofacies of bioclastic and micritic limestone are developed.

Pale low-iron sphalerite and galena are the main sulphide minerals, while the pyrite content is low. The zinc-rich mineralization in the Cudalgarra Member is characterized by replacement and small-scale open-space fill, with veinlet-hosted sphalerite-galena ±barite mineralization in bioclastic and micritic limestone beds. Mineralization in the Bongabinni Formation is similar in style but typically low-grade (<3% Zn) and limited in extent. Veinlet and crackle-breccia mineralization is indicative of fluid over-pressuring. Folding of mineralized veins is interpreted to represent compaction continuing after mineralization and is only seen in the upper part of the deposit within the more argillaceous Bongabinni Member (Figure 7A).

The lower mineralized zones are dominated by barite and lead and display variable styles. Medium- to coarse-grained, massive replacement barite-siderite with galena and minor sphalerite occurs in the Leo Member (Figure 7B, Figure 8) and in carbonate facies in the underlying Goldwyer Formation, with

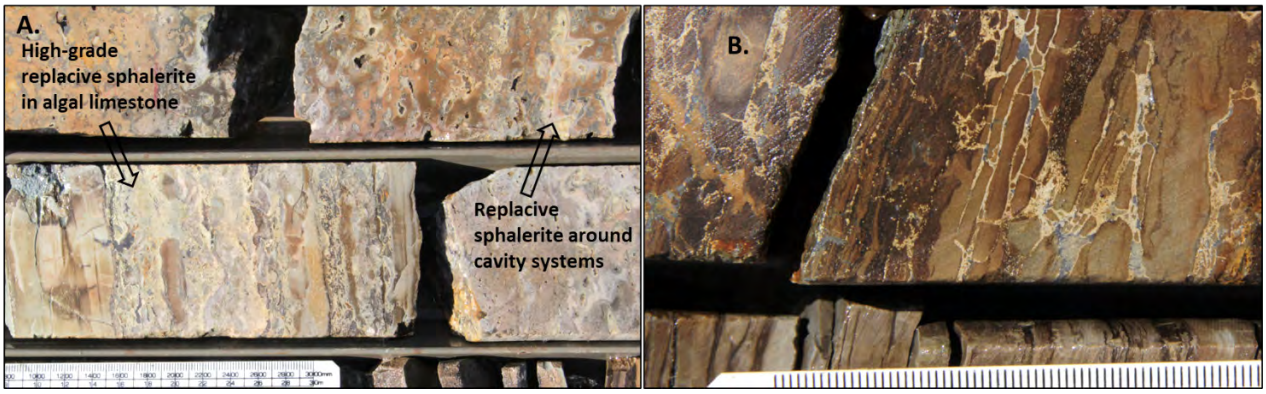

Figure 6: A). *Cudalgarra Member microbial boundstone with replacement of algal limestone by pale sphalerite at lower left and, at upper right, replacement rims to cavity systems which could represent dissolution or partial preservation of primary porosity.* ***)B.*** *Pale sphalerite-galena mineralization as lamination-parallel jack-apart veins and 'breakthrough' fluid-escape veinlets and microbreccias cutting lamination in Cudalgarra Member algal limestone and mudstone. Both examples are un-dolomitized.*

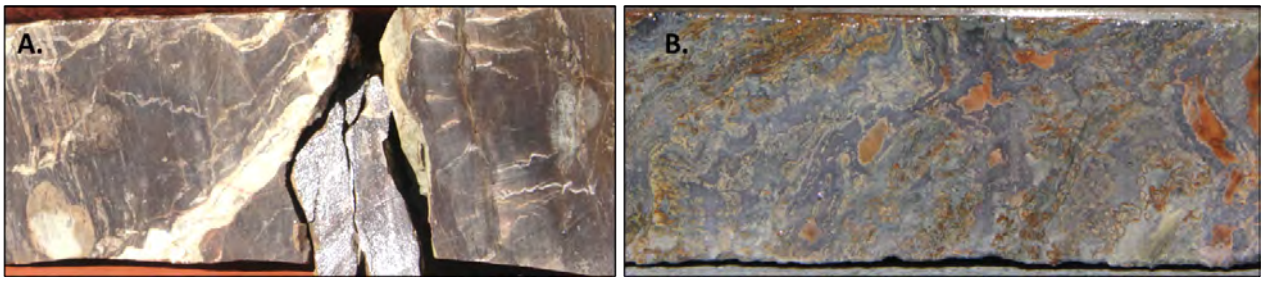

Figure 7: A)*. Bongabinni Formation algal organic carbon-rich horizon cut by pale sphalerite veinlets which are contorted by differential compaction and terminate against lamination planes enhanced by dissolution.* ***B)****. Leo Member microbial limestone replaced by galena with intergrown pale sphalerite and marcasite.*

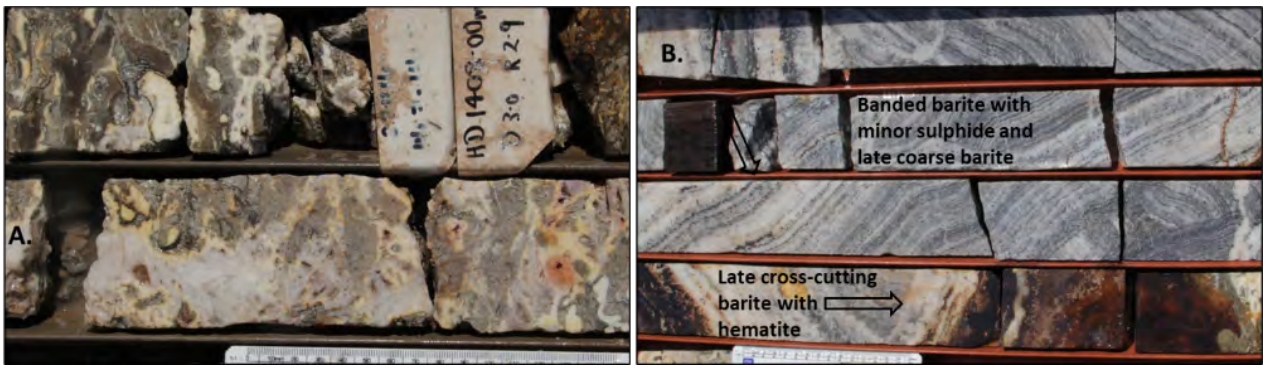

Figure 8. A)*. Bladed barite veining overprinting ferroan dolomite in cavity fill systems in the Leo Member bioherm.* ***B)****. Laminated barite veining, dark bands with minor pyrite and galena, and late white crystalline barite, and latest bladed barite veins with haematite*

localised haematite and magnetite. Mineralization is lead-dominant and generally low grade (1-5% Pb) but locally high grade (10-16% Pb). Sphalerite with minor galena in silicified Goldwyer Formation is locally present in the deeper parts of the deposit and overprints replacive barite mineralization.

The most widespread mineralization is low-grade barite-galena in small irregular veins and vugs in the dolomitized Leo Member bioherm (Figure 8A) which overprints the replacive lead-rich mineralization and locally overprints replacive sphalerite-rich mineralization near the base of the upper zinc zone. Later large-scale massive and banded barite veins contain only minor galena and sphalerite (Figure 8B). The latest mineralization stage consists of minor chalcopyrite and sphalerite in fault zones and late calcite veins.

The upper zinc mineralization is laterally extensive and consistent in style over approximately 14 kilometres along the

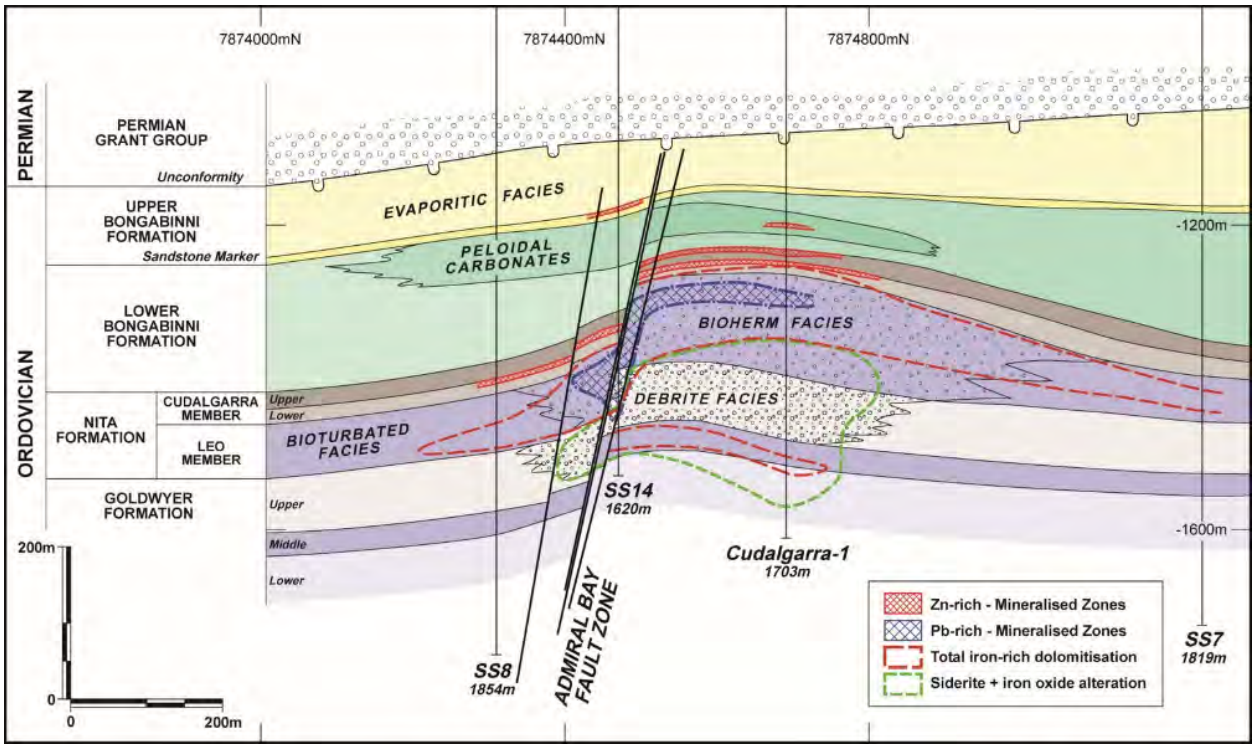

Figure 9: *Lithostratigraphy, mineralized and altered zones in the central part of the Admiral Bay deposit. From Reynolds & Copp, 2017a.*

fault zone, but of variable grade. Continuity is poorly constrained because of wide-spaced drilling, but it is likely that discrete zones of higher-grade mineralization occur within a largely continuous halo of low-grade mineralization. In the central deposit area, mineralization extends at least 900 metres across strike with potentially ore-grade mineralization up to 340 metres wide. Small-scale barite–galena veining in dolomitized Nita Formation is laterally extensive, occurring in an oil well, Leo-1, three kilometres southeast of the main fault (Figure 5). High-grade replacive lead-rich barite mineralization appears to be localised close to feeder zones.

Interpretation

The lateral and vertical extent of dolomitization and mineralization at Admiral Bay indicates a large-scale hydrothermal fluid-flow event, and homogenization of a large metal source area is supported by the homogenous lead isotope signature (McCracken, 1997) and broadly conformable model age. Textural evidence supports mineralization during diagenesis prior to complete compaction, including the contortion of mineralized veinlets and barite crystals in argillaceous horizons. The extensive mineralized fluid-escape veinlets and micro-breccias in argillaceous horizons are compatible with low lithostatic and hydrostatic pressure, allowing mineralizing fluids to infiltrate a large rock mass laterally and vertically to generate extensive mineralization. Based on cement history and stylolite relationships, McCracken (1997) interpreted that mineralization occurred at about 800 metres of burial and accompanied hydrocarbon migration.

The sulphur isotope signature is compatible with TSR and an Ordovician seawater source (McCracken, 1997) and fluid inclusion data suggest mineralization in the temperature range of 66 to 156°C (Etminan *et al.*, 1995).

Mineralizing fluid flow out of the Willara and Kidson sub-basins may have been triggered by extension, although initial stages of the Late Silurian Prices Creek inversion event cannot be ruled out. Fluids would have been focused through the Great Sandy relay zone onto the Admiral Bay palaeohigh (Figure 9), with fluid focus along the fault zone enhanced by dolomitization of the Leo bioherm before mineralization. Trapping of mineralization reflects the interplay of structure, favourable permeable and reactive host rocks, and shaley aquiclude horizons within the Bongabinni Formation. Fluid mixing may have played an important role, potentially including the interaction of metal-bearing brines with hydrocarbon or sour-gas moving through the structural and formational aquifers (McCracken, 1997).

Sibumasu Ordovician

The Sibumasu (or Shan-Thai) terrane encompasses northeast Sumatra, western peninsular Malaysia, western Thailand, eastern Myanmar including the Shan plateau and part of western Yunnan in China (Metcalfe, 2011; Figure 10). The terrane is interpreted to have rifted from the northwestern Australian part of Gondwana in the early Permian, drifted as the Palaeotethys Ocean closed, and collided with the Indochina terrane in the Upper Triassic Indosinian orogeny (Metcalfe, 2009). Lower Ordovician limestones of the Sibumasu terrane host extensive zinc-lead-silver mineralization, including the Kanchanaburi and Li districts in western Thailand, the Bawsaing district in Shan State of Myanmar, and the Baoshan district of southwest Yunnan in China. Oxide and sulphide mineralization has been

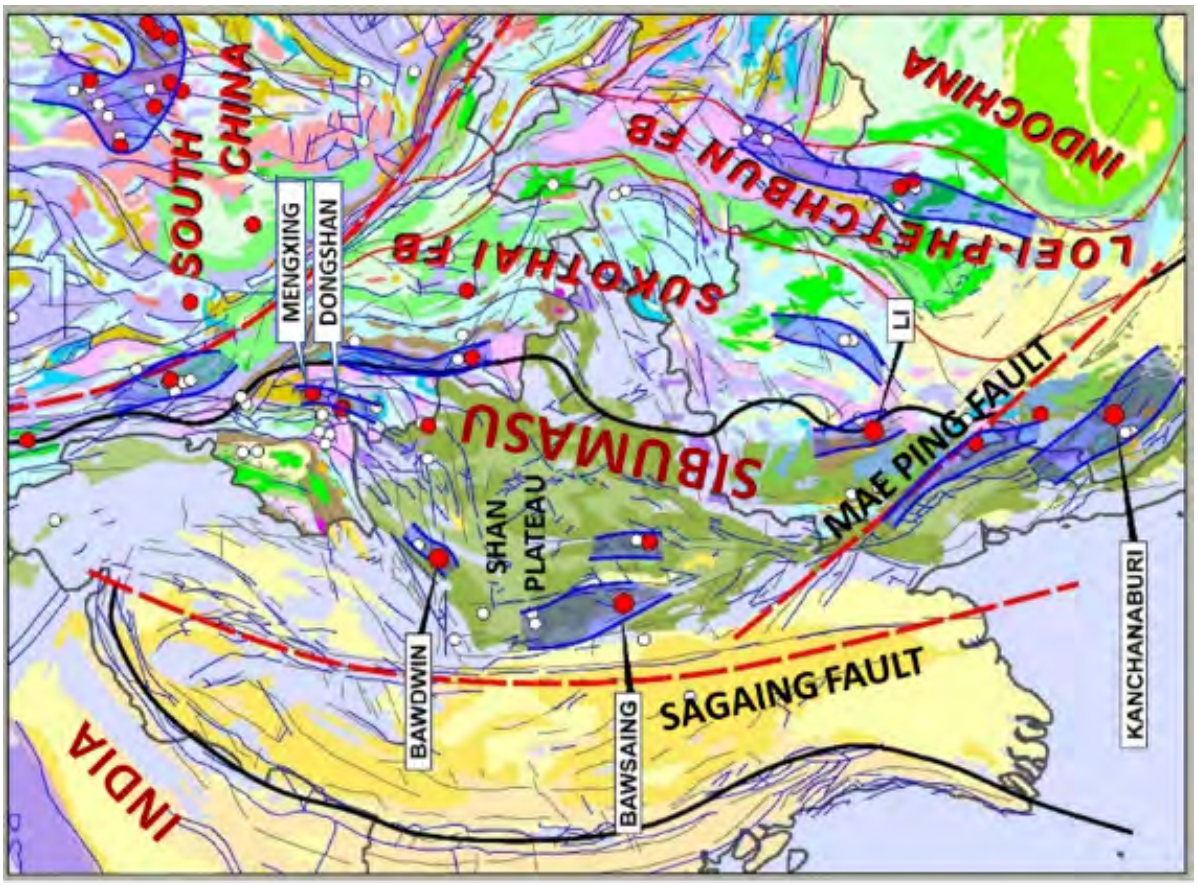

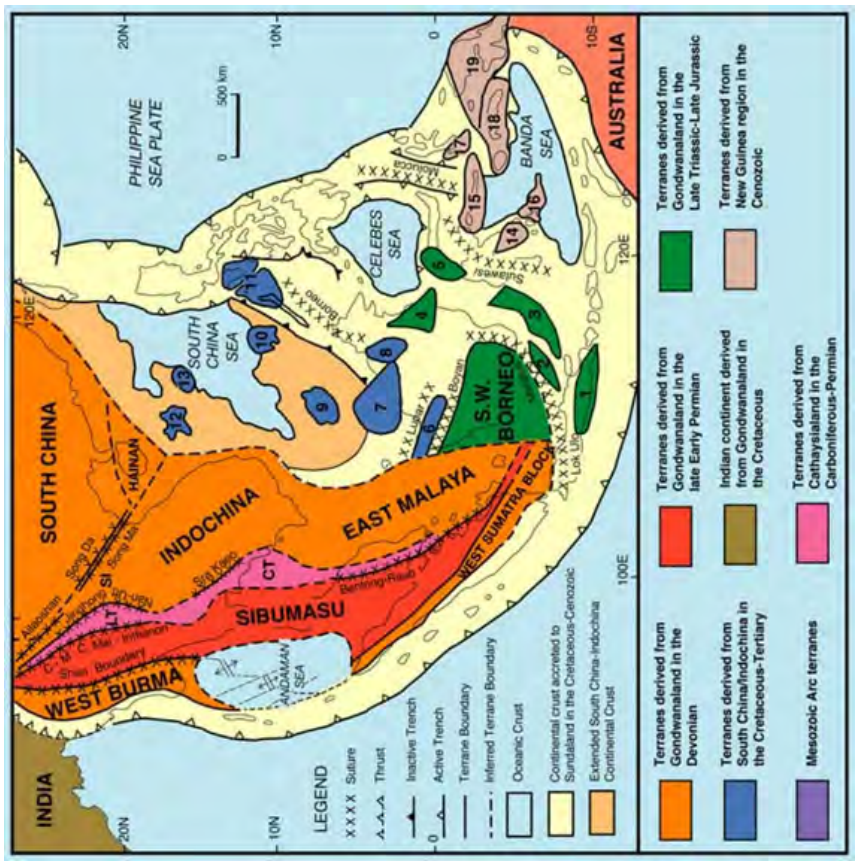

Figure 10: *Left, terranes in Southeast Asia (From Metcalfe, 2011). Right, significant zinc occurrences (red spots) and belts (blue shade) in Southeast Asia showing the Ordovician carbonate-hosted Bawsaing, Li, Kanchanaburi and Baoshan (Menxing, Dongshan) districts and the Bawdwin volcanic-hosted deposit. The background imagery is summary geology where Lower Palaeozoic rocks are lilac shades. (From Reynolds, 2017).*

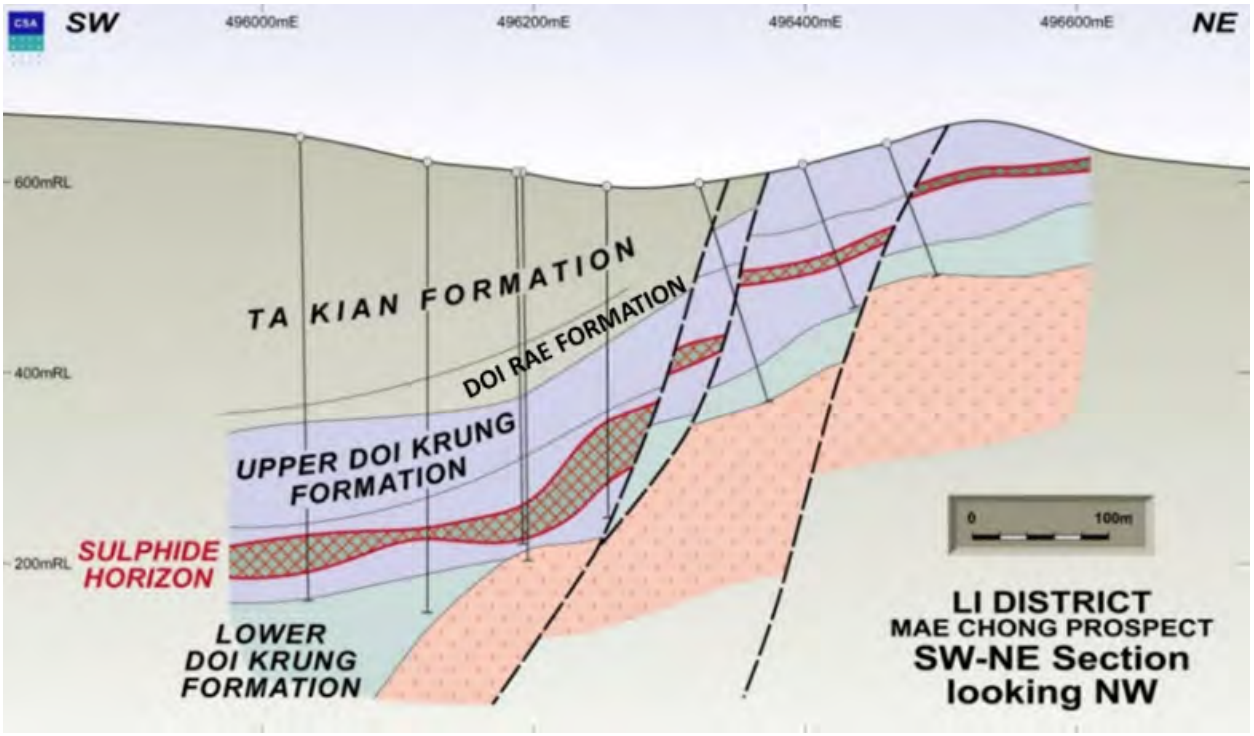

Figure 11: *Schematic section through the Doi Krung prospect at Mae Chong, showing host units and mineralization.*

mined historically in all these districts, and two mines are currently operational in Yunnan (Mengxing and Dongshan; Reynolds, 2017). This discussion focuses on the Li district in Thailand with reference to other districts.,

Regional Geology

The oldest rocks of the Sibumasu terrane consists of late Neoproterozoic to Cambrian Chaung Magyi Group which is interpreted as turbiditic in the northern Shan State and shallow marine to deltaic in the southern Shan State, with interbedded dolostone (Bender, 1983). These are overlain in the northern Shan State by shelf siliciclastic rocks, indicating a regressive sequence after late Neoproterozoic to Cambrian rifting. In western and southern Thailand, Middle Cambrian shelf sandstones and shales with minor carbonates (Tarutao Group) pass up into ramp and platform rocks of the Lower to Middle Ordovician Thung Song Group, recognised from the northern Shan State south to northern Malaysia (Hahn *et al.*, 1986; Wogwanich, 1990; Charusiri *et al.*, 2002). The Thung Song Group consists of up to 1400 metres of mixed carbonate-siliciclastic rocks overlain by platform carbonate-dominated sequences. Facies range from shallow water oolitic to deep-water argillaceous limestones, which may reflect rifted sub-basins. The Middle Ordovician is less well developed and generally more argillaceous.

In western Thailand, tuff horizons are common within the Lower Ordovician carbonate sequence. A Cambro-Ordovician calc-alkaline arc is interpreted on the eastern margin of Sibumasu in peninsular Malaysia (Kuala Lumpur volcanics; Hutchison, 1989), which would place western Thailand in a broadly continental back-arc basin setting on the northern margin of Gondwana. The Late Cambrian to Early Ordovician Bawdwin volcanic centre on the northern edge of the Shan Plateau may be related to the arc. Alternatively, these sub-alkaline volcanic centres may be related to rifting in northern Gondwana, at the same time as initial opening of the Canning Basin.

Li District

Mineralization in the Li district (*Figure* 10) of northwest Thailand has been evaluated during exploration by Thai company, Padaeng Public Company Limited, from the 1980s to 2009 and shows strong similarities to the better known Kanchanaburi district. Exploration outlined extensive zinc-lead mineralization within a belt of metamorphosed carbonate and siliciclastic rocks in three prospect areas at Mae Chong. In 2009, Padaeng estimated a 'resource' of 2.15 Mt at 7.25% Zn and 1.26% Pb for Doi Kung (not compliant with international reporting codes). Drill intersections at the Doi Krung prospect included 24 m at 13.5% Zn and 2.4% Pb, 19 m at 5.4% Zn and 1.4% Pb, and 6.5 m at 7.8% Zn and 0.8% Pb. Reconnaissance drilling between the prospects indicated that alteration and mineralization occur in the same stratigraphy over a strike of 7 kilometres in a zone up to 2 kilometres wide.

The Li district also hosts thick stratiform barite mineralization within fine-grained Ordovician siliciclastic rocks at Phu Mai Tong, which was the largest barite mine in Thailand with a 1978 'resource' estimate of about 7 Mt of barite.

Structural and Lithostratigraphic Setting

At Mae Chong, Ordovician calc-silicate, limestone and siliciclastic rocks overlie Cambrian sandstone and are overlain by Silurian-Devonian fine-grained siliciclastic rocks. The

Figure 12: A). *High-grade banded and brecciated sphalerite in pale green/white diopsidic calc-silicate and medium-grey fine-grained cherty silica.* ***B).*** *Laminated sphalerite parallel to S0/1 folded by F2 with small-scale mobilization into S2 fabric.*

sequence has been metamorphosed at greenschist facies and intruded by granite. At the Doi Krung prospect, zinc-lead and barite mineralization occurs in the Lower Doi Krung unit, comprised of recrystallized massive to banded limestone and abundant diopsidic calc-silicate rock, with subordinate laminated fine grained siliciclastic rocks and minor tuff. The Upper Doi Krung has less calc-silicate rock and is overlain by the arenaceous and pelitic Doi Rae unit, in turn overlain by more massive limestone in the Ta Kian unit. Detrital zircons from tuff in the Doi Rae unit have been U-Pb dated at 464.2 ± 8.5 Ma (Middle Ordovician; S. Meffre, *pers comm*. 2008).

Deformation and metamorphism have destroyed most depositional features. Major lateral stratigraphic thickness variations have not been recogniz*ed* and there is no direct evidence for reefal build-ups. The Doi Kung unit probably represents shallow shelf carbonates and siliciclastics, with the Doi Rae unit recording an influx of coarser sand and tuffaceous detritus on to the platform, before deposition of the Ta Kian limestones which become cleaner and more massive upwards. The sequence suggests a deepening shelf with increasing isolation from siliciclastic sediment sources.

The rocks at Mae Chong have been affected by two major compressive deformation events, D1 with a penetrative S1 fabric generally parallel to bedding and small-scale folding, and D2 with thrusting and southwest verging F2 folding and a variably developed S2 crenulation of S1. Deformation was accompanied by upper greenschist facies metamorphism, with calc-silicate growth in argillaceous limestone and calcareous mudstone. The sedimentary sequence is cut by a Late Triassic granite in the east (dated by zircon U-Pb at 216.0 ± 2.1 Ma; *pers comm.* S. Meffre, 2008). Hornfels occurs close to the granite, but there is no metasomatic skarn.

Mineralization

Zinc-lead mineralization is strongly stratabound in the Doi Krung unit in three prospect areas at Mae Chong and is best developed in the lower part of the unit, within medium- to dark grey limestone with zones of pale green diopsidic calc-silicate and grey silicified cherty limestone. Mineralization is characterized by reddish to pale brown sphalerite and galena with variable amounts of pyrrhotite or pyrite. The highest-grade mineralization is massive to semi-massive sphalerite with minor galena and pyrrhotite, commonly grading into sulphide-matrix breccia mineralization that predates deformation and metamorphism (Figure 12). Laminated to thinly bedded sphalerite is generally low to moderate grade. Zones of semi-massive to banded or sheared pyrrhotite without zinc mineralization is interpreted as a halo to the zinc-lead mineralization.

Thin bands of sphalerite are often sheared out in the S1 fabric, and primary sphalerite bands parallel to S0/1 may be folded and cleaved by F2/S2 (Figure 12). Syn-deformational durchbewegung breccias also occur in high-grade semi-massive sulphide. Mineralization is locally remobilised by deformation with sulphide along deformation fabrics and remobilised into veins with calc-silicates cutting across all penetrative fabrics. Limited multi-element data indicate elevated silver (max. 187 ppm) and antimony (max. 383 ppm) with zinc-lead mineralization. Minor barite is typically coarsely recrystallized and interbanded with sulphide. Barite is generally more abundant at higher stratigraphic levels where it may be massive and banded with low sulphide content.

Other Ordovician Zinc-lead Districts

The best-known zinc-lead districts are Kanchanaburi in Thailand (Diehl &Kern, 1981) and Bawsaing in Myanmar (Khin Zaw *et al.*, 1984; Than Htun *et al*., 2017), which lie about 700 kilometres apart along the same Ordovician belt (Figure 10).

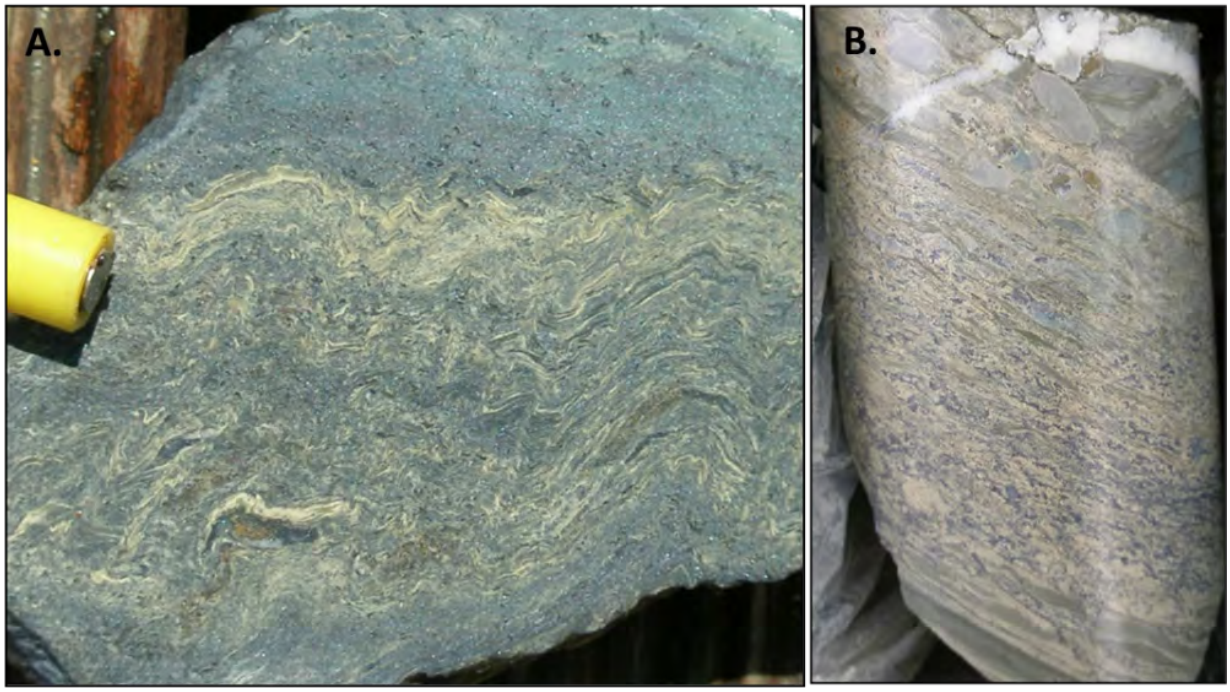

Figure 13: A). *High grade laminated sphalerite-galena mineralization at Song Tho showing F2 folding and S2 cleavage.* ***B).*** *High-grade pale sphalerite-rich mineralization replacing coarse intraclastic limestone breccia horizon at the Thong Pha Phum prospect 14 km northwest of Song Tho.*

Removing later sinistral offset of c. 500 kilometres along the Mae Ping Fault zone (Jitpiromsri & Kanjanapayont, 2012) would more closely juxtapose the two districts. A number of stratabound zinc-lead deposits in the Ordovician of the Baoshan block of far western Yunnan are likely correlatives, but available data are limited.

In Kanchanaburi, a number of deposits and prospects are known in Lower Ordovician limestone along a trend of over 30 kilometres. Mining was active from 1979 to 1995, mostly from the lead-rich Song Tho deposit which is reported to have produced 5.4 Mt from global 'resources' of c. 8 Mt at grades of c. 7% Pb, 3% Zn and 100g/t Ag. In 2012, a Mineral Resource for Song Tho and Bo Yai was reported as 2.90 Mt at 3.6% Pb, 2.8% Zn and 73 g/t Ag Indicated and 1.96 Mt at 3.0% Pb, 3.1% Zn and 49 g/t Ag Inferred (Parker *et al.*, 2013).

Replacive mineralization is stratabound within limestone horizons in a mixed carbonate and siliciclastic sequence with minor thin tuff horizons. Diehl & Kern (1981) described pale bedded limestone, pale massive limestone, interpreted as biohermal, and dark argillaceous limestone. All mineralization occurs in the pale massive facies within the argillaceous limestone sequence. Mineralization is dominated by galena, sphalerite and pyrite with reported minor sulphides including tetrahedrite-tennantite, sulphosalts, and arsenopyrite. Minor barite is also reported. No dolomitization has been recorded and calc-silicates are not present. Mineralization is enriched in silver, antimony, and mercury.

Mineralization has been deformed, isoclinally folded, and metamorphosed to lower greenschist facies with the host rock. At Song Tho, for example, multiple mineralized lodes are folded around the nose of a south-plunging overturned antiform. Massive to semi-massive fine- to medium-grained sulphide horizons are cleaved, folded and cut by remobilized lead-rich sulphide vein zones. At Bo Yai, the mineralized unit is repeated by large scale folding at a kilometre scale.

The Bawsaing - Pindaya district in the eastern Shan State was the second most important zinc-lead mining district in the British colonial period in Burma, notably from the Theingon mine (Khin Zaw *et al.*, 1984). Mining exploited stratabound mineralization hosted by the Lower Ordovician Wunbye Formation (Goosens, 1978), consisting of limestone or dolostone, including oolitic and bioturbated facies, interbedded with siltstone and overlain by mudstone and siltstone of the Nan-on Formation (Khin Zaw *et al.*, 1984). The host sequence is relatively undeformed compared to the host rocks at Li and Kanchanaburi. Mineralization is mostly localised near the top of the formation and is typically lead-rich and often associated with barite. Sulphides include galena, sphalerite, minor pyrite and tetrahedrite-tennantite, and trace argentite and chalcopyrite. The district is quite deeply weathered and much of the known mineralization has been partly oxidized, enhancing the apparent lead-rich character by preferential removal of zinc during weathering.

Interpretation

Stratabound zinc-lead mineralization within Lower Ordovician platform carbonates occurs at a number of localities in a belt of at least 1,400 kilometres from Kanchanaburi to Yunnan. The carbonates were deposited in shallow water, either in an intracratonic rift-sag basin or passive margin setting, with synchronous distal volcanism indicated by tuff horizons. The Ordovician platform carbonate and siliciclastic rocks were deposited on top of a thick late Neoproterozoic to Cambrian platform of

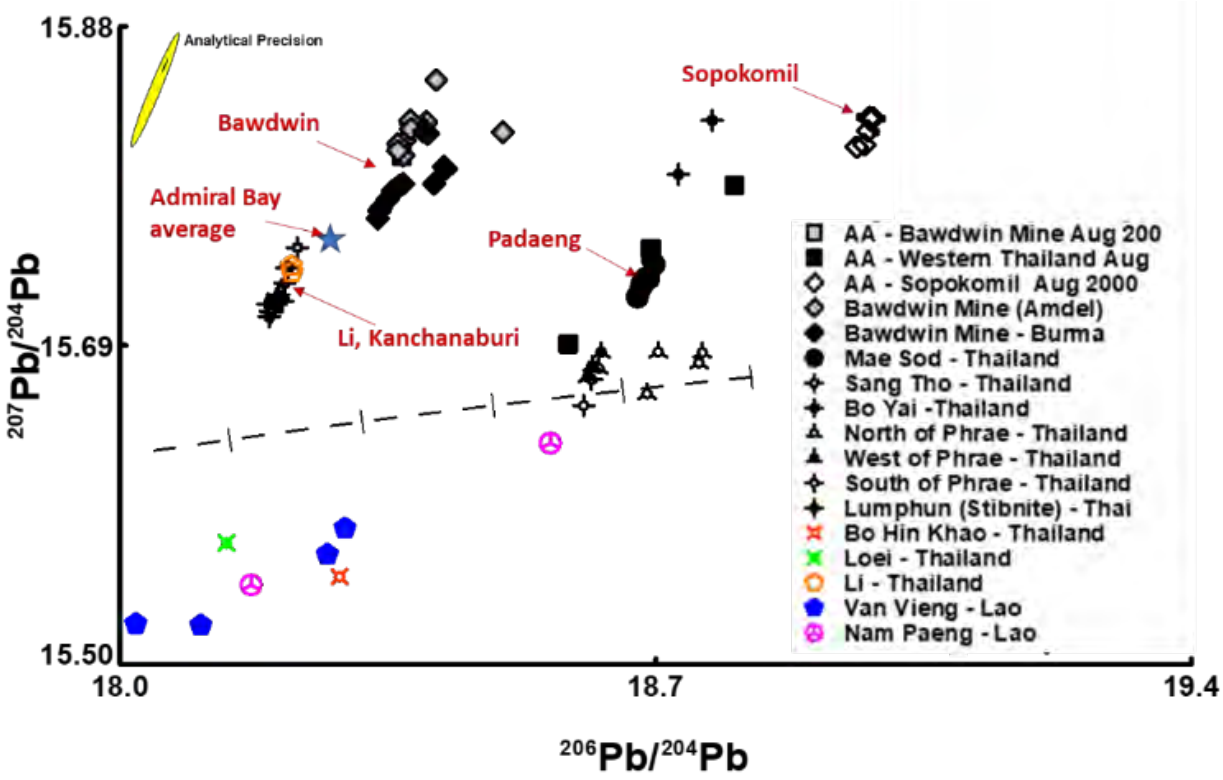

Figure 14: *Lead isotope signatures of selected Southeast Asia mineral deposits (G. Carr, pers. comm., 2005) and Admiral Bay.*

siliciclastic rocks and marginal to the thickest part of the Chaung Magyi flysch, interpreted to represent the upper rift to sag stage of basin development. The mineralization and host rocks were deformed during the Indosinian orogeny or an earlier Devonian event.

The style, setting, and chemistry of mineralization suggests an early replacement origin in an extensional basin. The widespread occurrence of very similar mineralization requires a large-scale basinal fluid-flow event initiated by a tectonic trigger. The broadly homogenous and conformable lead-isotope signature supports a large-scale homogenized basinal metal source (Figure 14). Tectonic reconstructions place Sibumasu within Gondwana and close to northwest Australia in the Ordovician, where the Admiral Bay deposit in the Canning Basin shows a similar lead isotope signature. Evidence of synchronous volcanism in the Sibumasu Ordovician suggests a high heat-flow setting, and a hot hydrothermal system may have contributed to the elevated Ag, Sb, and Hg content of mineralization, possibly also with magmatic inputs via source regions or fluids.

Lennard Shelf

The Lennard Shelf lies along the northern margin of the Canning Basin in northwestern Australia and hosts several zinc-lead deposits and mines, including Pillara (Blendevale), Cadjebut, Goongewa (Twelve Mile Bore) and Kapok (Figure 15). The Lennard Shelf deposits occur within Devonian carbonates and have generally been described as MVT deposits (Dörling *et al.*, 1998).

Regional Geology

The intracratonic Canning Basin underwent a multiphase depositional history from the Ordovician to the Cretaceous (Shaw *et al.*, 1995; Parra-Garcia *et al.*, 2014). The Lennard Shelf carbonate platform developed on the northeastern margin of the Fitzroy Trough rift during the Devonian Pillara Extension (Playford *et al.*, 2009). About 15 kilometres of sediment accumulated in the rift during the Middle to Upper Devonian, while only 1.5-2.5 kilometres of shallow marine carbonate and siliciclastic rocks were deposited on the platform on a basement of Proterozoic metamorphic rocks and Ordovician sedimentary rocks (Playford, 1980).

The carbonate platform developed in two cycles, the transgressive syn-rift Givetian to Frasnian Pillara Cycle, with retreating platform margins, and the sag-phase Famennian Nullara Cycle with prograding platform margins (Figure 16). The Pillara Cycle commenced with localised basal conglomerate and thin red-beds, overlain by the sabkha to barred lagoon facies algal dolostone, evaporites, and evaporite-dissolution breccias of the Cadjebut Formation (Hocking *et al.*, 1996). The overlying Pillara Formation was deposited on basement palaeohighs in the footwall of major extensional listric faults that controlled development of half-grabens within the platform where Gogo Formation calcareous mudstones were deposited (Figure 15, Figure 16). Geological mapping integrated with seismic interpretation shows that these faults were active during carbonate deposition, cut basement, and link with major faults defining the edge of the Fitzroy Trough (Dörling *et al.*, 1995). The Nullara Cycle carbonates were deposited during a period of reduced fault movement and subsidence in the sag phase and are

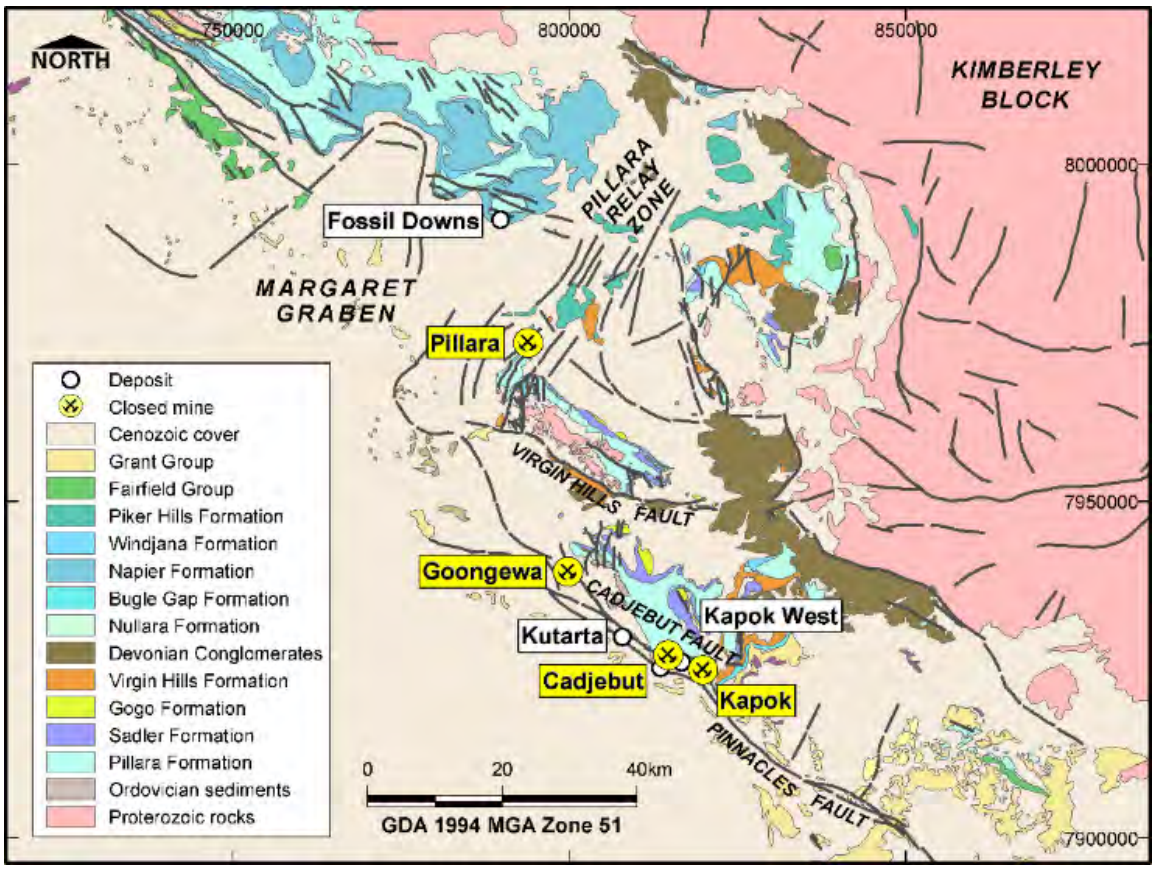

Figure 15: *Geology of the south-east Lennard Shelf showing the principal Zn–Pb deposits, major stratigraphic units and faults. The Emanuel Range platform lies immediately NE of the Cadjebut Fault, the Pillara Range platform is NE of the Virgin Hills Fault. From Reynolds & Copp, 2017b.*

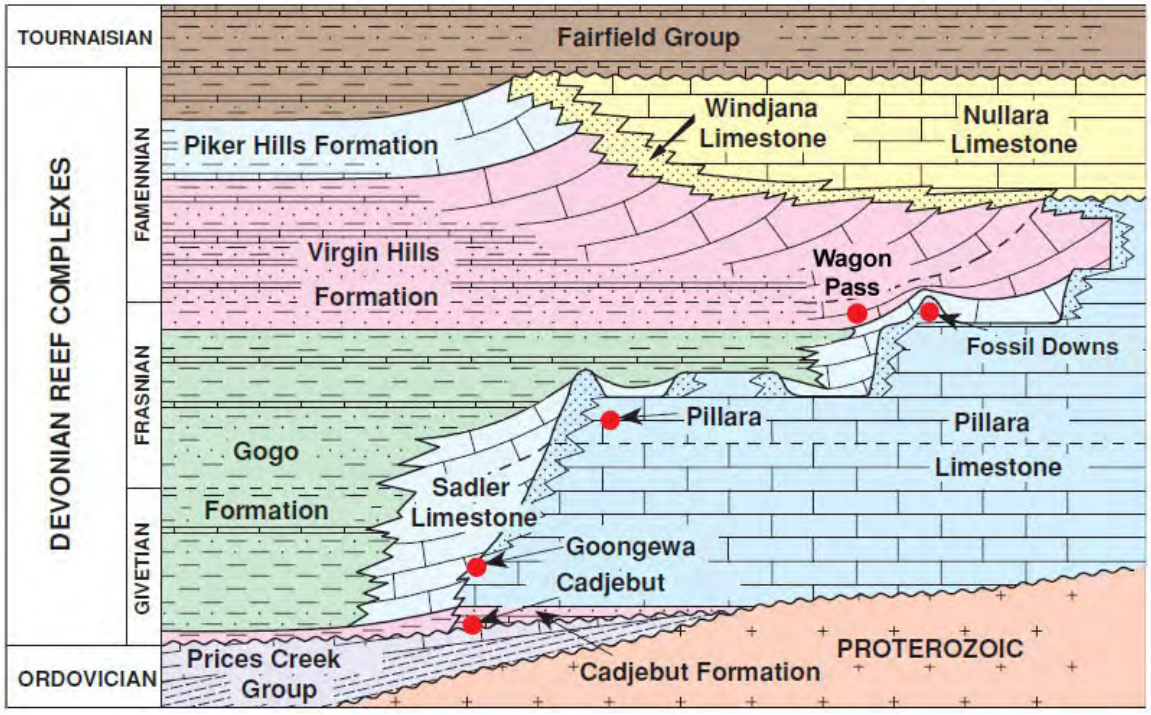

Figure 16: *Schematic stratigraphic units of the Lennard Shelf. The red dots mark Pb-Zn mineralization. Modified after Playford & Wallace, 2001.*

Figure 17: *Rhythmic-banded replacive and breccia-hosted mineralization at Cadjebut*

overlain by sandy grainstones of the Tournaisian Fairfield Group, deposited in a stable shelf setting.

Structural and Lithostratigraphic Setting

Most mineralization occurs within the Cadjebut Formation and the overlying Pillara Formation back-reef and reef and Sadler Formation fore-reef. Reefs were best developed on the topographic highs in the footwall of listric basin-facing normal faults and mark the transition from gently dipping back-reef facies to steeply dipping slope facies, thickening downslope to deeper water carbonate-siliciclastic facies. The overlying Nullara Cycle shows similar facies patterns but with little fault control, and hosts only minor mineralization.

The Pillara Cycle limestones are extensively dolomitized in a zone extending from the Pinnacle and Cadjebut faults into the adjacent platform of the Emanuel Range (Figure 15), however dolomitization is absent in the Pillara area. Cadjebut Formation evaporites are represented by evaporite dissolution breccias within the dolomitized zone, whereas anhydrite and gypsum evaporites are preserved in the northern part of the Emanuel Range platform.

Mineralization

All mined deposits occur within clean Pillara Cycle limestone or dolostone, close to syn-sedimentary basin-bounding faults or to transfer faults within relay zones. Most deposits are close

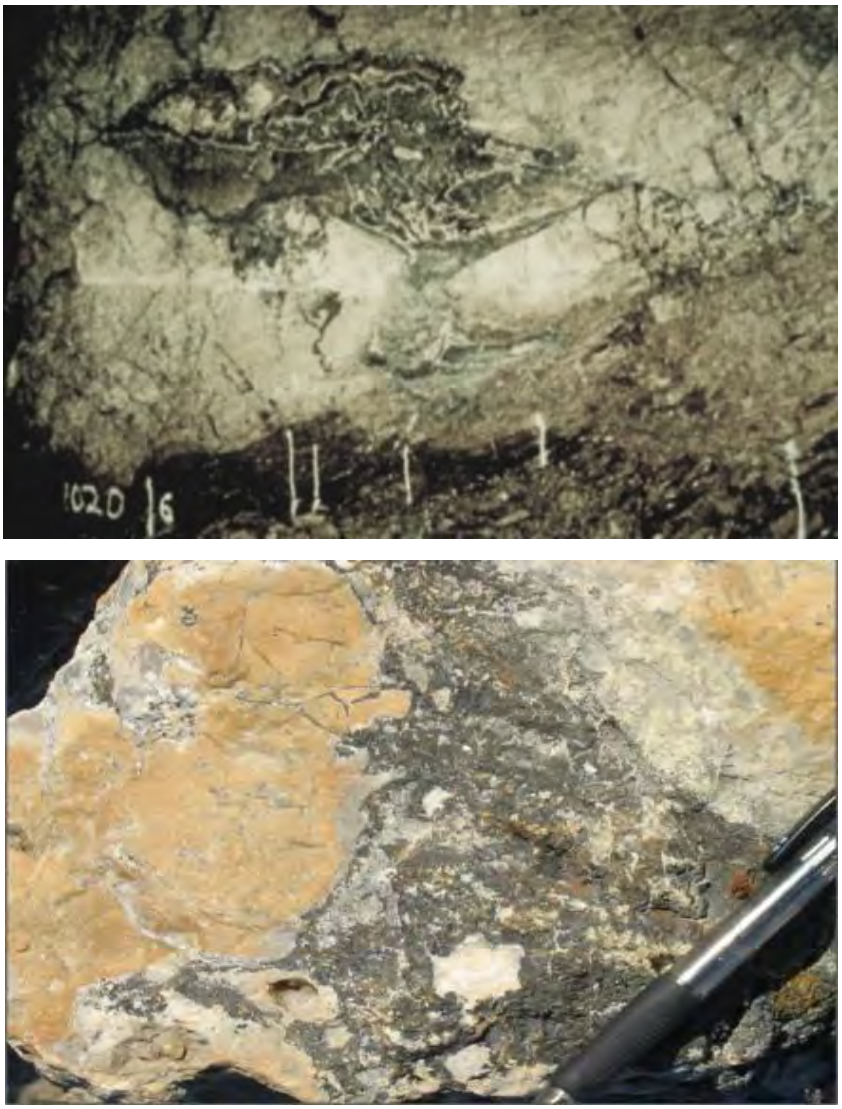

Figure 18: *At top, mineralized cavity system at Goongewa with late calcite fill and, at bottom, hydrothermal breccia with ferroan dolostone clasts de-dolomitized and replaced by sulphide at clast margins.*

to the basin parallel Cadjebut Fault zone, a splay from the Pinnacles Fault which marks the edge of the platform. The largest deposit, Pillara, occurs within the basin normal Pillara Fault zone, part of the Pillara relay controlling the Margaret Graben. Most mineralization occurs within clean and brittle reef and fenestral back-reef facies. Deposits show variable settings, styles and controls, including stratabound replacement, hydrothermal karst-hosted, and fault-hosted.

The Cadjebut deposit is characterized by high-grade zinc-rich replacement mineralization, stratabound in the Cadjebut Formation in the footwall of the Cadjebut Fault. The deposit consists of two stacked mineralized lenses that are 50–150 metres wide, 3–6 metres thick and 3.5 kilometres long, plunging gently to the south-east subparallel to the Cadjebut Fault. The lenses are at the stratigraphic level of evaporite solution-collapse breccia horizons outside the deposit, at the northern margin of the zone of hydrothermal ferroan dolomite that has spread from the Pinnacle–Cadjebut Fault zone (Tompkins *et al.*, 1994a, Warren & Kempton, 1997). Mineralization is predominantly rhythmically banded high-grade massive sulphide which is fringed by breccia and cut by breccia ore on the south side of the deposit (Figure 17). The zinc-lead mineralization is surrounded by a halo of banded marcasite in the same stratigraphic position, with banded barite on the north side of the orebody. A more extensive halo of disseminated and vein marcasite extends south to the Cadjebut Fault, which also contains sub-economic zinc-lead mineralization. Zinc-lead mineralization at Cadjebut shows simple low-iron sphalerite-galena-marcasite mineralogy with ore-stage calcite gangue. Zinc/lead ratios increase away from the Cadjebut Fault and towards the barite halo.

The Goongewa deposit is localised where steep north-striking hangingwall faults splay from a right-stepping bend in the Cadjebut Fault. A number of stacked ore lenses in reef and back-reef facies in the hangingwall consist of irregular, partly stratabound zones of dissolution, brecciation and open-space fill, with additional fault-controlled zones running south in

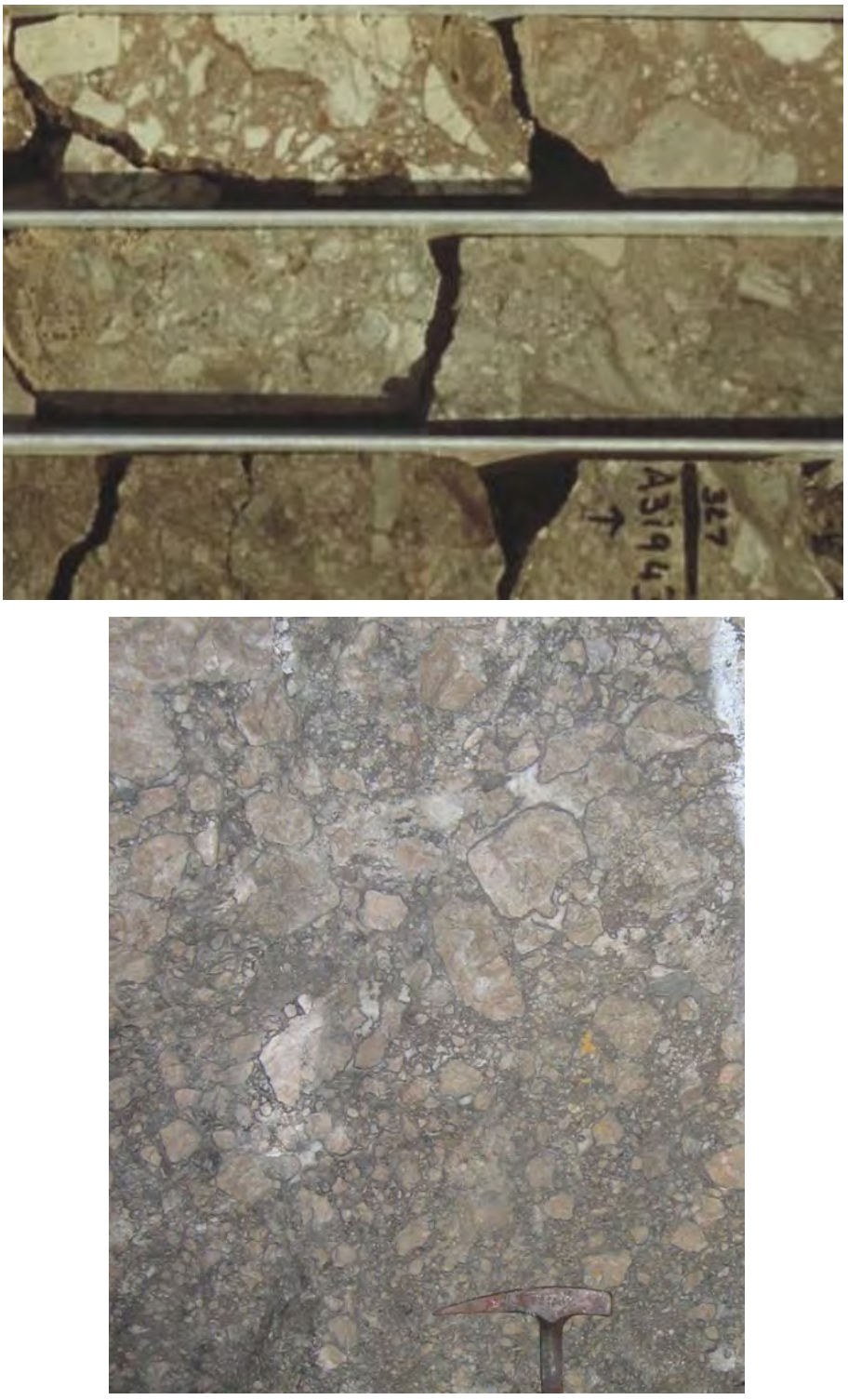

Figure 19: *At top hydrothermal breccia at Kutarta with clasts partly replaced by sphalerite. At bottom, hydraulic rubble to mosaic breccia in the hangingwall of the Pillara West Fault with matrix replaced by sphalerite-galena-marcasite, sub-angular clasts rimmed by sulphide, and late-stage open-space calcite fill.*

Sadler Limestone fore-reef. Mineralization occurs in limestone close to the contact with the ferroan dolostone zone to the south and within de-dolomitized zones. Sphalerite-galena-marcasite mineralization with calcite gangue is dominated by small-scale dissolution and open-space fill, but also occurs as fill in large metre-scale cavities (Figure 18). Mineralization shows multiple cycles of colloform sphalerite and galena, with hydrocarbon inclusions in dark brown late-stage sphalerite. Goongewa shows low-level enrichment in silver and is the only deposit where silver reached payable grades in concentrate.

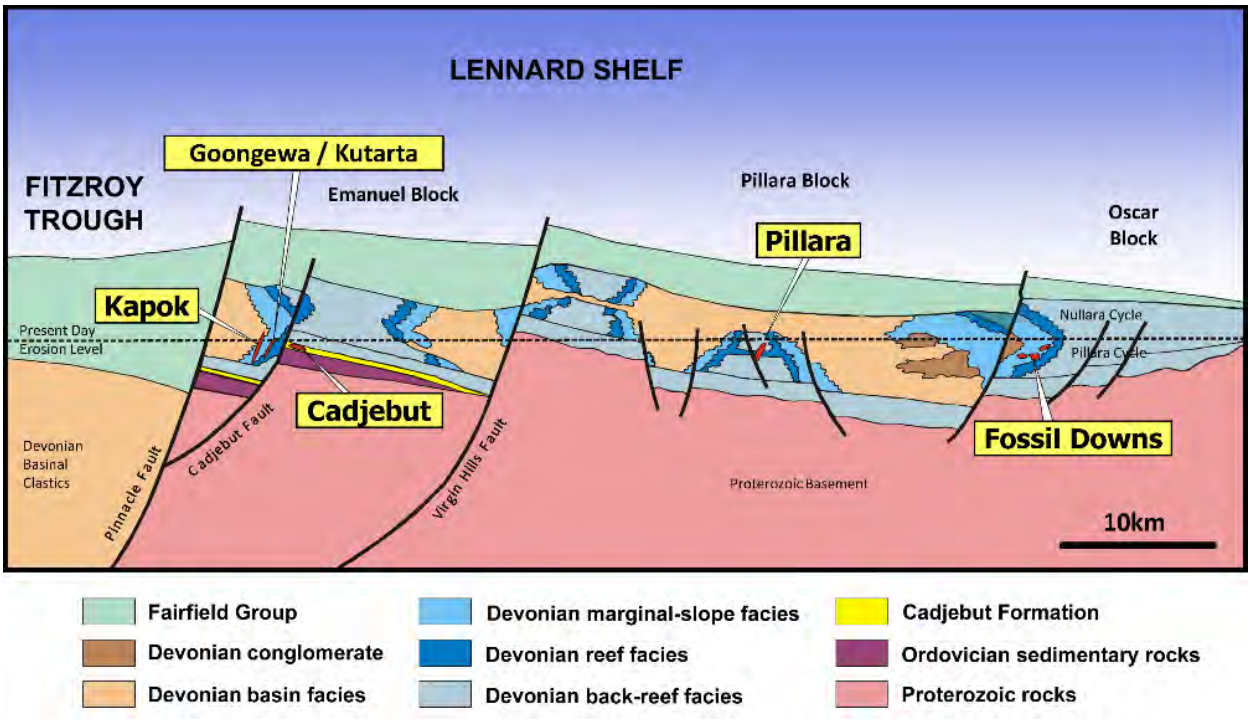

Figure 20: *Schematic SE–NW cross-section of the Lennard Shelf showing the district-scale structural and stratigraphic setting of the principal Zn–Pb deposits. From Reynolds & Copp, 2017b.*

Kutarta is also localised in the hangingwall of the Cadjebut Fault but is hosted within a hydrothermal breccia that is best developed as a partly stratabound wedge in dolomitized fenestral limestone of the Pillara Formation. Mineralization is zinc-rich with an extensive marcasite halo.

Fault-hosted mineralization in the Kapok Fault, a southwest-dipping splay between the Pinnacle and Cadjebut Faults, occurs in a single 0.5–3-metre-wide breccia zone with a strike of over two kilometres and a dip extent of up to 300 metres. Mineralization is thickest in dilational fault bends where fore-reef Sadler Limestone is present in the hangingwall and back-reef fenestral Pillara Limestone in the footwall, both relatively massive and brittle limestone facies. The mineralogy is the same as Cadjebut and Goongewa, but the deposit is distinguished by sub-equal zinc and lead content.

Pillara, the largest deposit on the Lennard Shelf, is localised in a north-south trending graben in the Pillara Relay Zone, defined by the east-dipping Western Fault and its west-dipping splay, the Eastern Fault. Extension across the graben increases from south to north, resulting in additional mineralized splays to the north. Each fault consists of a zigzag array with dilational bends and relay steps providing the locus for thickest mineralization. Mineralization occurs within fault zones and in broad hangingwall breccia zones that transition upward from rubble to mosaic to crackle breccia and are controlled by splays. Breccias are best developed in a brittle fenestral limestone unit in the Pillara Formation, resulting in a secondary stratabound control. Mineralization is characterized by colloform sphalerite, galena and marcasite with calcite gangue, replacing breccia matrix and as open-space fill, with multistage deposition and brecciation in the fault zones.

Interpretation

The Lennard Shelf is unusual amongst carbonate-hosted zinc-lead districts in that the age of mineralization is well constrained by isotopic and palaeomagnetic dating (Brannon *et al.*, 1996; Symons *et al.*, 2005) which also coincides with timing interpreted from cement history (Middleton and Wallace, 2003). This evidence places mineralization in the earliest Tournaisian, about 20 Ma after deposition of the host stratigraphy. Fluid inclusion data indicate saline brines and a low temperature system (70-130°C) and sulphur isotope data indicate sulphate reduction by TSR (Dörling *et al.*, 1998). Cadjebut and Pillara have similar radiogenic lead isotope signatures, while minor deposits are even more radiogenic (Tompkins *et al.*, 1994b), suggesting a single highly radiogenic upper crustal source for the two largest deposits.

The setting and characteristics are compatible with a large-scale hydrothermal fluid-flow system from the Fitzroy Trough into the adjacent Lennard Shelf, occurring about 20 Ma after rapid extension, subsidence and sedimentation in the Fitzroy Trough. Subsidence with consequent loading by rapid deposition of sediments may have been the driver, with the arrival of fluids onto the platform in the waning stages of the Pillara extension. The first stage of fluid-flow appears to have resulted in extensive pre-mineralization dolomitization along the Pinnacle-Cadjebut fault system. Mineralizing fluids may have partly exploited dolostone aquifers, however the localisation of deposits at relay zones suggests that faults provided the main fluid focus. Alteration in Proterozoic basement indicates that

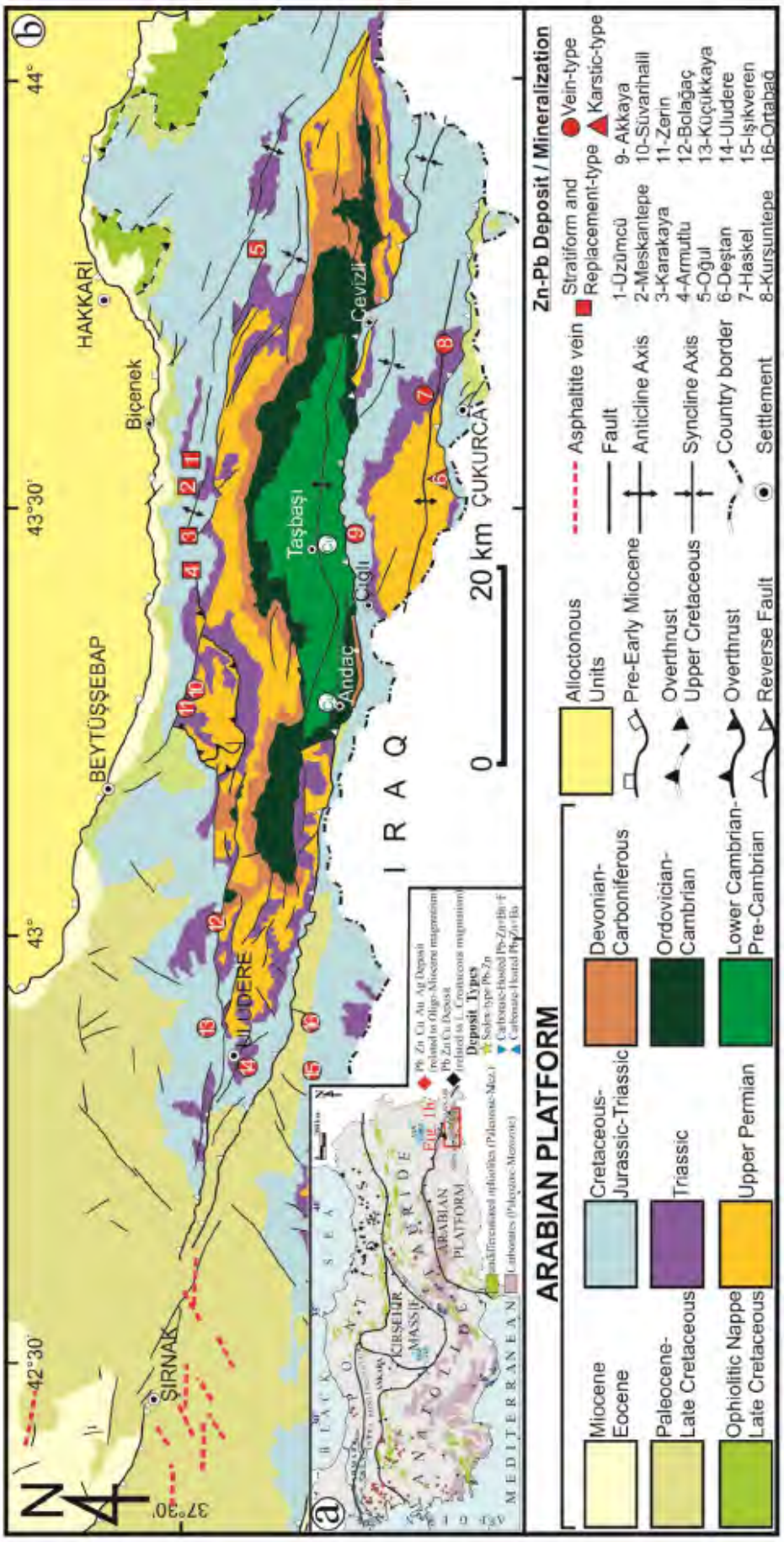

Figure 21: *Location and summary geology of the Hakkari region showing Zn-Pb deposits. From Hanilçi et al., 2020. The inset shows the main tectonic units.*

fluids penetrated basement in these fluid-flow corridors.

On a regional scale the setting of the deposits on the Lennard Shelf can be summarised as occurring close to major basin architecture faults that have splays leading onto palaeotopographic highs. On the scale of the deposits, diverse trap settings for mineralization have resulted in the wide range of deposit styles (Figure 20). Localisation of mineralization along dolomite fronts may reflect chemical and physical boundary effects, where mineralizing fluids exploiting dolostone aquifers encountered less permeable but more reactive limestone. Breccia-fill mineralization at Goongewa is interpreted to be related to hydrothermal karst formation in limestone. Mineralization in fault zones is best developed in dilational jogs in the most brittle host units. Stratigraphic and structural aquiclude seals commonly play a role in constraining fluid systems and trapping mineralization. At Cadjebut, hydrocarbons or sour gas have been suggested as a reductant that triggered precipitation of zinc and lead (Wallace *et al.*, 2002), and fluid mixing of oxidized basinal metalliferous brines with reduced sulphur- and hydrocarbon-bearing fluids may have played a role in all deposits. At Cadjebut, however, there is also evidence (Tompkins *et al.*, 1994b; Warren & Kempton, 1997) that mineralization was produced by reaction with evaporites.

Hakkâri District

The Hakkâri district in southeast Türkiye contains extensive stratabound zinc-lead mineralization in Triassic carbonate rocks, known from a number of prospects and small oxide workings over at least 25 kilometres of strike. The largest known deposit, Meskan, has been mined by local Turkish company Meskan Ölmez Madencilik, producing high-grade direct-shipping oxide ore. High-grade sulphide mineralization is known from deeper drilling and mine workings. The deposit is currently being evaluated by First Quantum Minerals.

Regional Geology

The Hakkâri zinc-lead district is located on the Arabian plate south of the Tauride Fold Belt (Figure 21), just south of the ophiolite-bearing Bitlis Belt which marks the Miocene collision zone between the Gondwanan Arabian plate to the south and the composite Central Anatolian/Asian terrane to the north. The Mesozoic sedimentary rocks in southeast Turkey are predominantly platform carbonates deposited on the northern passive margin of Gondwana following Permian rifting of Neotethys. These rocks extend in an arcuate belt west from Hakkâri and are mostly Permian and younger ages but with older Palaeozoic inliers.

The passive margin was deformed in the Neogene collision as an autochthonous southward-verging fold and thrust terrain, with southward transport of nappes on the Arabian plate following northward subduction beneath the Anatolian block. The Hakkâri district sedimentary sequence is unmetamorphosed but was affected by strong thin-skinned fold and thrust deformation.

Structural and Lithostratigraphic Setting

Mineralization in the Hakkâri district is hosted by carbonates of the Cudi Group which overlies reddish siliciclastic and minor carbonate rocks of the Çığlı Group. The Cudi Group was assigned a Triassic to Cretaceous age by Perinçek (1990). Stratabound mineralization was interpreted by Hanilçi *et al.* (2020) to be hosted by Upper Triassic rocks (Figure 22).

The local stratigraphic sequence in the Meskan area commences with siltstone and mudstone and passes up into thin-bedded dark reduced silty and argillaceous limestone. Beneath the mineralized unit, coarse clean dolostone appears to be discontinuous and may represent reef- or ramp-type build-ups. The overlying interval that hosts mineralization is marked by reduced bituminous peloidal wackestone and micrite, often fenestral, and algal-laminated limestone, with evidence for evaporites provided by pseudomorphed anhydrite nodules and laths and stratabound dissolution-collapse breccias. Above the mineralized interval, cyclic reduced silty limestone and mudstone passes progressively up into clean, thick-bedded platform limestone which often displays boundstone and stromatactis textures. The upper clean carbonates are pervasively dolomitized, but the underlying mixed sequence is largely undolomitized, including the mineralized unit. Based on the facies associations, the mineralized interval is interpreted to have been deposited in a barred lagoonal to sabkha environment, with the overlying sequence deposited in a deepening platform environment with decreasing siliciclastic input, evolving to open-shelf limestone deposition.

The almost complete absence of macrofossils suggests that much of the sequence was deposited in a restricted, stressed hypersaline environment. This accords with the extensive evaporites documented in the Cudi Group in the Cizre and Mardin area, 130 kilometres east of Hakkâri. Here, the Mesozoic is less deformed and extensive evaporitic intervals are recorded from oilwell drilling in the Triassic (Erik *et al.*, 2005). Across the Arabian platform, a broad arc of shallow water carbonate and evaporite deposition in the Triassic was followed by Middle Jurassic regression in northern Arabia (Ziegler, 2001).

The structure of the Meskan area is dominated by large-scale asymmetric south-verging folds, characterized by shallowly north-dipping northern limbs and steeply south-dipping southern limbs, consistent with Miocene, southward directed brittle-ductile deformation. The Meskan deposit occurs in the shallowly dipping northern limb of the Armutlu anticline (Figure 23). The host sequence is extensively faulted, notably by the northwest-trending Meskan Tepe Fault which dips north and separates mineralization at Meskan Tepe and Meskan Valley with an estimated normal throw of 500 metres.

Mineralization

The mineralized Meskan stratigraphy includes Meskan Tepe and Meskan Valley zones and continues east to the Karakaya deposit and west to the Üzümcü deposit, a strike of about 10 kilometres (Figure 23). At surface, all the mineralization in the district is oxidized. Sulphide mineralization is best known from mining and drilling at the Meskan deposit. At Meskan, zinc-lead mineralization occurs over a stratigraphic interval of up to 30 metres in reduced bituminous and algal-laminated limestone, typically with two main mineralized horizons from two to ten metres thick. Based on mapping and drilling, mineralization is continuous on either side of the Meskan Tepe fault over a strike of more than five kilometres and extends down dip at least 800 metres.

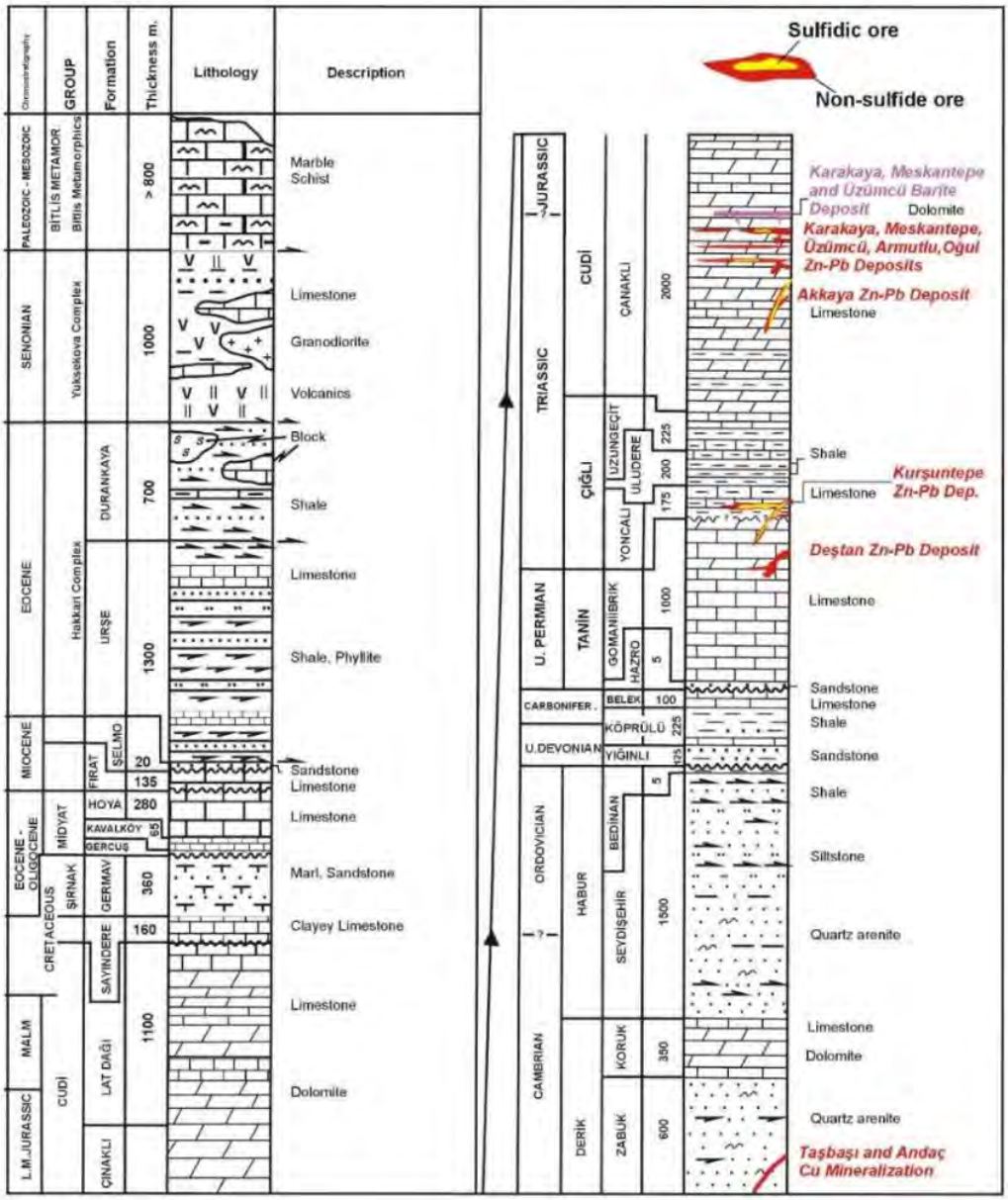

Figure 22: *Generalized stratigraphic column of the Hakkari region (after Perinçek, 1990) and stratigraphic positions of the Zn-Pb deposits. From Hanilçi et al., 2020.*

Mineralization appears to preferentially replace laminated algal limestone horizons within the bituminous to silty limestone sequence, often mimicking the laminated texture but with development of zebra textures representing generation of open space by dissolution. High-grade mineralization is dominated by pale to brown colloform sphalerite with galena, minor pyrite and calcite gangue (Figure 24A and B). Breccia- and vein-hosted mineralization occurs especially in dark-grey bituminous silty limestone that is interbedded with algal limestone that has been fully replaced. Pyritic mineralization displaying similar zebra textures is intersected above and below high-grade zinc-lead mineralization in drilling, and mapping suggests that banded pyritic mineralization also forms a lateral halo (Figure 24C). Mineralization predates extensive calcite and dolomite veining throughout the sequence that is interpreted to accompany late folding and faulting.

Geochemically, the mineralization has a moderate silver content and elevated arsenic, antimony and thallium. Sulphur isotope data from Hakkâri deposits are in the -4 to +5 per mil range (Hanilçi *et al.*, 2020) and may represent BSR from Triassic seawater sulphate composition of -20 per mil. Fluid inclusion data suggest that mineralizing fluids had moderate salinities (2 to 22 wt% equiv. NaCl) and an evaporated brine component, and mineralization temperatures in the 160 to 220°C range, possibly up to 280°C (Hanilçi *et al.*, 2020). Lead isotope data are homogenous with a broadly conformable model age, unlike more radiogenic, probably intrusive-related zinc-lead mineralization in Central Anatolia (Ceyhan, 2003).

Most oxidized mineralization shows similar laminated textures as the sulphide and is interpreted as direct replacement with minor local-scale remobilization into karst-like footwall feat

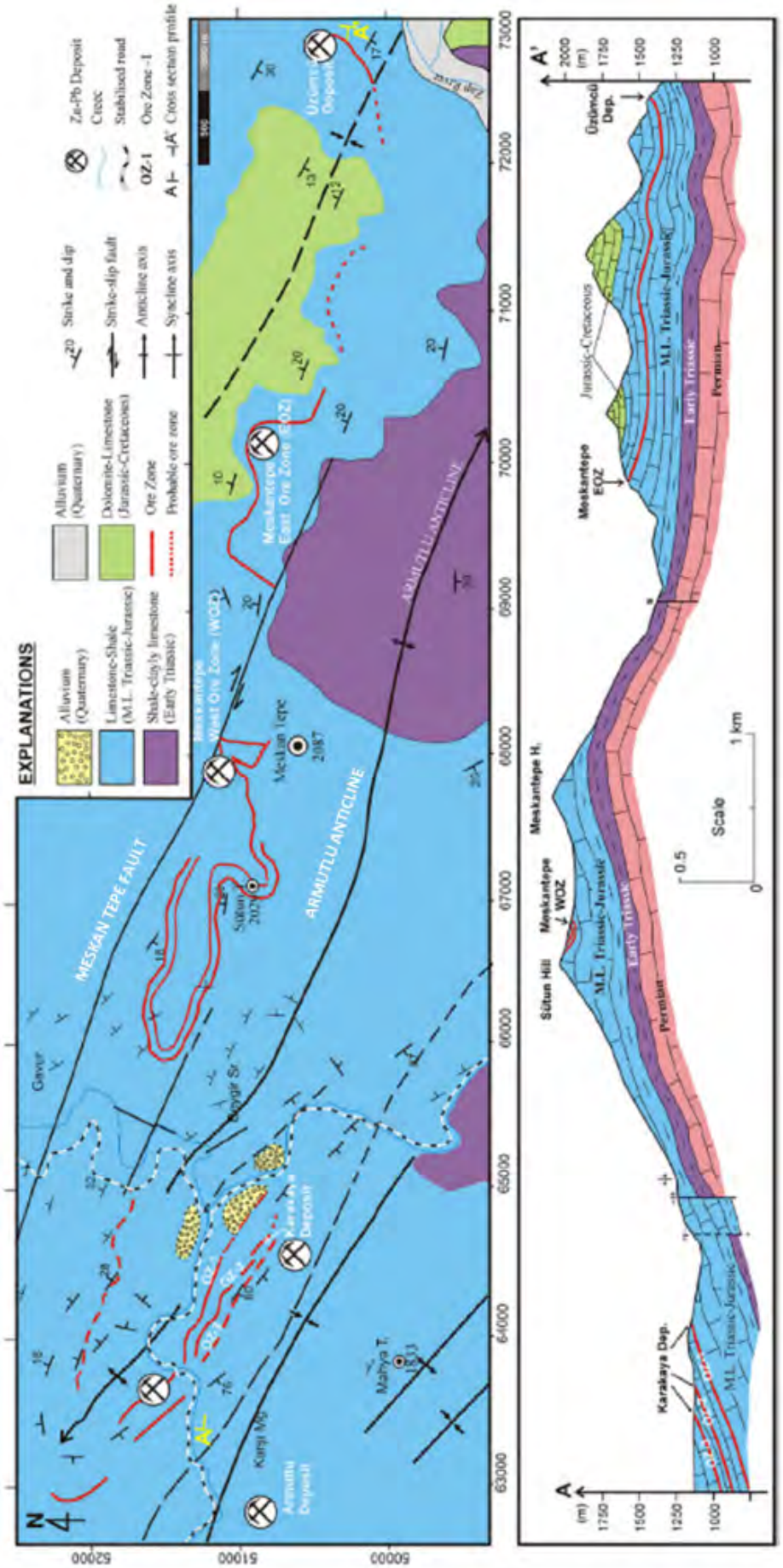

Figure 23: *Schematic east-west section through the Karakaya, Meskan and Üzümcü deposit area showing the Armutlu anticline and fault offset on the Meskan Tepe fault. From Hanilçi et al., 2020.*

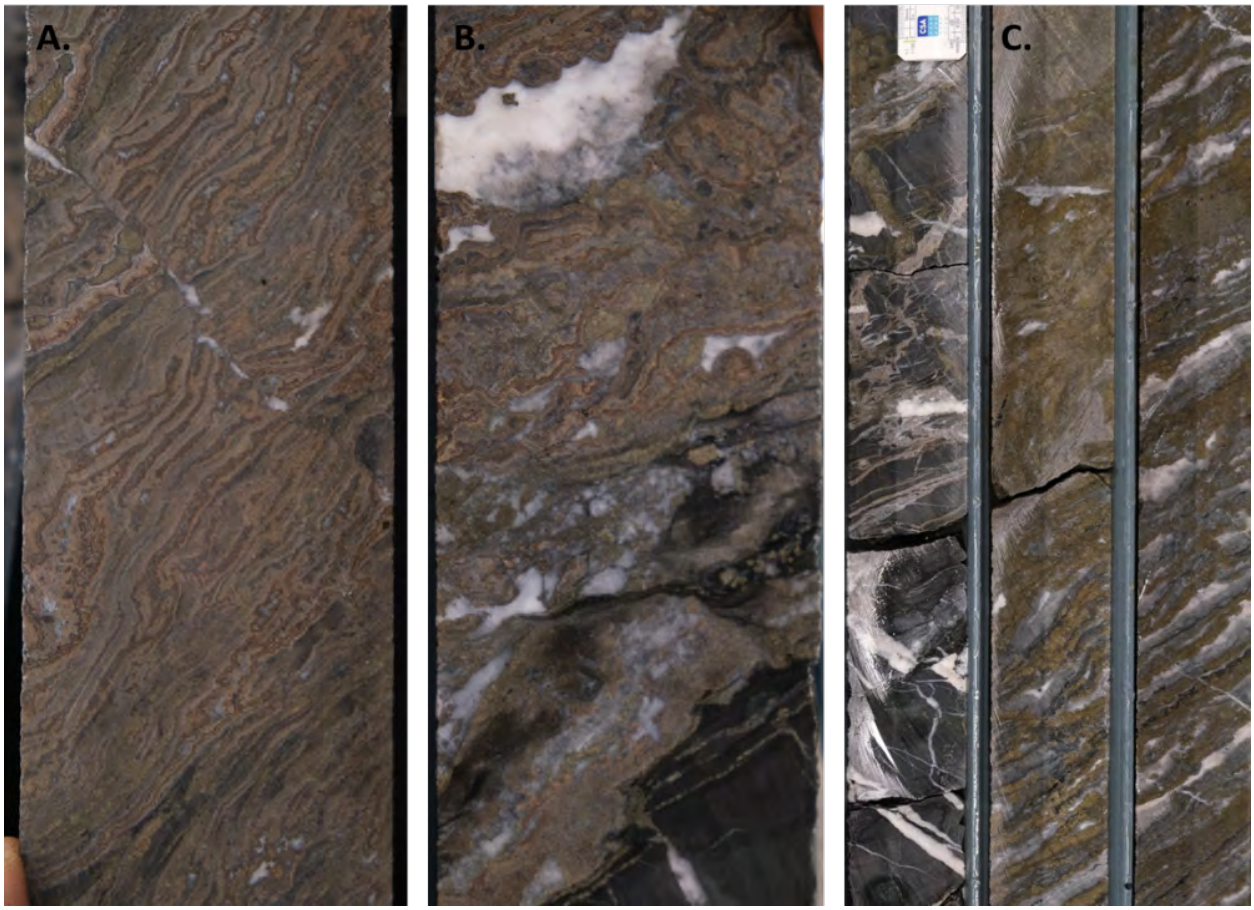

Figure 24: *Examples of mineralization from Meskan.* ***A).*** *High-grade colloform-banded sphalerite-rich mineralization cut by late calcite vein.* ***B).*** *High-grade colloform mineralization with late calcite gangue and mineralized veins cutting underlying dark-grey limestone.* ***C)****. Laminate pyrite-calcite fringing the main mineralized zone cut by zones and veins of later pale-brown sphalerite.*

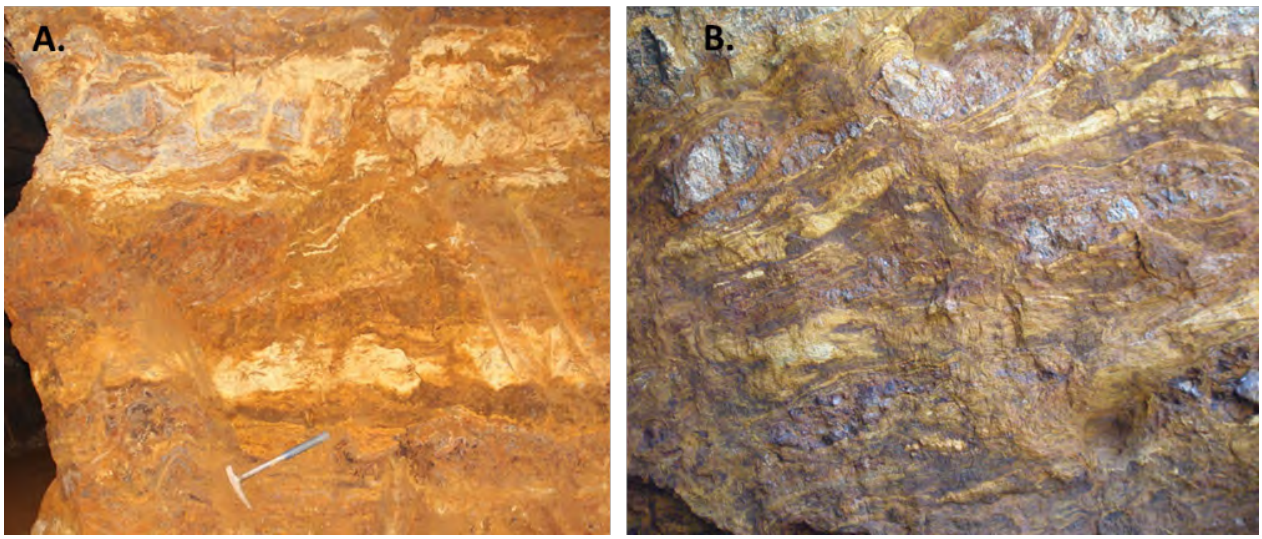

Figure 25*: Examples of oxidized mineralization from Meskan.* ***A).*** *Laminated oxidized mineralization preserving primary sulphide textures and cross-cutting relationships.* ***B)****. Boudinaged horizons of limestone within oxidized mineralization.*

ures (Figure 25A). Larger scale boudinage textures are evident in mined oxide faces, where more competent limestone blocks within sulphide have been isolated during deformation (Figure 25B).

Interpretation

The carbonate-hosted mineralization in the Hakkâri district replaces reduced bituminous and algal limestone prior to Neogene deformation. While there is no absolute control on the age of mineralization, the system is interpreted to have formed relatively early in basin history during extension on the Neotethys passive margin. The lead signature is compatible with a large, homogenizing basinal fluid system and the fluid inclusion and sulphur isotope data suggests conditions similar to the Irish Midlands. The trace element association including Ag, As, and Sb is typical of other Irish-type systems. Although volcanismis not documented in southeast Türkiye, Carnian volcanism related to renewed rifting is documented in the western Arabian platform in Syria (Ziegler, 2001) and Permian and Triassic volcanism was widespread across the belt of Neotethys opening (Chauvet *et al*., 2011).

The lateral extent and continuity of mineralization at Meskan is unusual in carbonate-hosted zinc-lead deposits and is more like a sedimentary copper deposit. The bituminous and algal host unit at Meskan may have been a particularly effective trap through a combination of availability of reduced sulphur and well-developed persistent shale aquicludes in the hangingwall. No definite fault control has been identified, but it is possible that the steep limb of the Armutlu anticline was localised by inversion of an earlier extensional structure that fed the system along its strike length. Clockwise splays like the Meskan Tepe fault also appear to control thicker zones of mineralization, although they have been substantially reactivated during compressional deformation.

The age, setting and style of the Hakkâri mineralization shows strong similarities to the Alpine deposits (below), despite occurring on opposite sides of the opening Neotethys. This suggests that similar conditions of formation developed in different locations during the extension and breakup of Pangea in the Triassic and may have implications for prospectivity in other parts of the Neotethyan realm.

Alpine District

The Alpine zinc-lead district is defined by deposits that occur within carbonates of Upper Triassic age in an extensive belt of the southern Alps over a distance of about 400 kilometres (Schroll, 1996; Leach *et al.*, 2003). Several deposits were historically mined, including Bleiberg in Austria, Mežica in Slovenia, and Raibl and Salafossa in Italy. Bleiberg had reported global resources of c. 2.5 Mt of zinc and lead metal (Leach *et al.*, 2003) while Mežica had a global resource of c. 19 Mt at 5.3% Zn, 2.7% Pb (Herlec *et al.*, 2010). Gorno in Italy was also mined historically and has a JORC-reported Mineral Resource in sulphide of 7.06 Mt at 6.9% zinc, 1.8% lead, and 33 g/t silver (https://www.altamin.com.au/).

Regional Geology

Mineralization in the Alpine district is hosted by Upper Triassic platform limestones within the autochthonous South Alpine block, south of the Peri-Adriatic Lineament, or within the South Alpine-derived allochthonous Austro-Alpine nappes north of the lineament. The South Alpine block is part of the Adria terrane which is interpreted to underlie much of northern and eastern Italy and the Adriatic Sea and forms part of the Hunic terranes that separated from Gondwana in the Palaeozoic to collide with Europe during the Variscan orogeny (Stampfli and Borel, 2002).

Lower Permian extension across Europe accompanied opening of the Neotethys to the south and was marked by widespread red-bed molasse and fluvio-deltaic sedimentation, succeeded by extensive evaporite deposition. Early Permian calc-alkaline volcanism within transtensional basins has been related to post-Variscan extensional collapse (Beltrán-Triviño *et al.*, 2016). Extension continued through the Triassic with opening of back-arc basins in the Carpathian-Tauride-Pontide-Caucasus Belt. Lower to Middle Triassic clastic lithologies were succeeded by widespread carbonate deposition in the Middle Triassic and mixed siliciclastics, carbonates and evaporites in the Upper Triassic, accompanied by minor volcanism. Renewed rifting in the early Jurassic resulted in the opening of the Alpine Tethys Ocean through Central Europe and coincided with rifting and spreading of the Central Atlantic (Mohn *et al.*, 2010).

Compression and orogeny commenced in the Late Cretaceous and culminated in Miocene collision between the Adria block and the main European terrane, resulting in extrusion and translation of nappe piles. The Periadriatic Lineament and Insubric line represent the final suture zone (Figure 26).

Structural and Lithostratigraphic Setting

The Alpine deposits are hosted by platform limestones of Carnian age overlying Permian and Lower to Middle Triassic siliciclastic rocks. Bleiberg and Mežica lie north of the Periadriatic Lineament within the upper Austroalpine nappe, which is unmetamorphosed and has suffered only minor deformation. Raibl and Salafossa lie south of the Periadriatic line in the Southern Alps nappes and have been more strongly modified by deformation.

At Bleiberg, mineralization occurs mainly in the upper part of the Ladinian to Lower Carnian Wetterstein Formation, comprising platformal carbonates about 400 metres thick deposited in reefal to lagoonal and peritidal environments (Cerny, 1989). The main host “Bleiberg facies” comprises lagoonal to tidal flat carbonates and marls with evidence of evaporites and interpreted emersion horizons with micro-karst. These units overlie Anisian shallow-marine marly limestone with minor tuff, and Permo-Triassic (Scythian) red-beds. Overlying the Wetterstein Formation, the Raibl Group comprises carbonate-evaporite units with interbedded terrigenous clastic rocks and hosts minor stratabound mineralization. The lagoonal facies limestones are anomalously thick at Bleiberg and are interpreted to have developed on a fault-controlled horst block with a reefal facies to the south passing further south into a deeper basinal environment (Bechstadt, 1979).

Mežica lies about 90 kilometres along strike to the east-southeast and occurs in a very similar stratigraphic and lithofacies setting to Bleiberg, mainly within Carnian “Bleiberg facies”

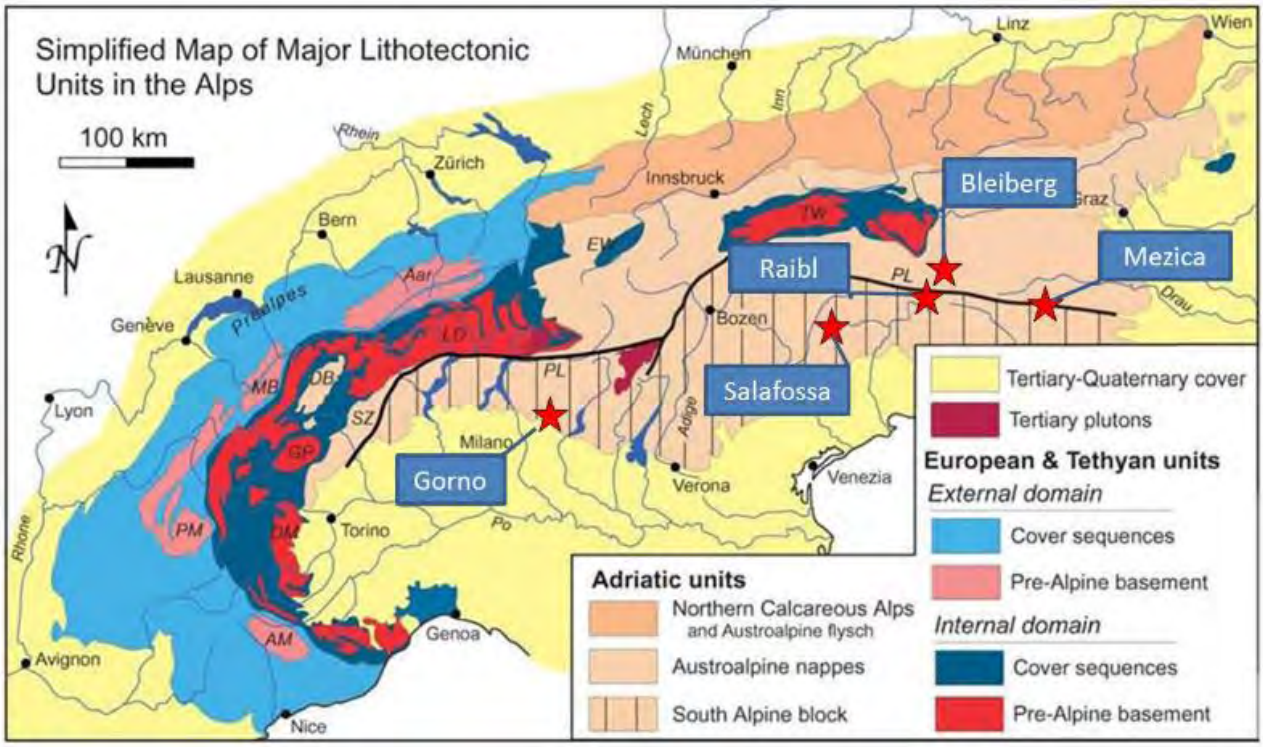

Figure 26: *Summary of the main tectonic units in the Alpine belt showing the main Alpine-type deposits straddling the Peri-adriatic lineament (PL). Modified from Selverstone, 2005.*

lagoonal sequences (Herlec *et al.*, 2010). Mineralization occurs in reefal facies carbonates and within shallow-marine carbonates of the overlying Raibl Group. Mineralization at Raibl and Salafossa is also hosted by early Carnian platform dolostone, the 'Dolomia Metallifera', overlain by bituminous basinal carbonates.

Gorno is located within the Brescian Alps in the Southern Alps tectonic unit. Mineralization is mainly stratabound within algal dark grey to black bituminous limestone of the Calcare Metallifero Bergamasco (CMB) unit which is 40 to 80 metres thick. In the broader district, mineralization is known in this unit over 300 kilometres of strike. The CMB was deposited in a tidal flat to lagoonal setting, overlain by alternating thinly bedded lagoonal black limestone and laminated marl of the Gorno Formation. These lagoonal units mark the transition between underlying shelf limestones and overlying paralic to continental clastic sedimentation. The underlying Late Permian to Middle Triassic sequence represents rift to platform sedimentation, with deep water Anisian-Ladinian limestone and localised subalkaline bimodal volcanism. Minor tuff horizons also occur within the mineralized stratigraphy.

Mineralization

At Bleiberg, stratabound or stratiform replacive mineralization occurs within the Bleiberg facies and Maxerbanke lagoonal carbonate-marl cycles, as well as in the Raibl Group carbonates. Stratabound mineralization includes replacement and cavity fill styles, interpreted to be early karst-fill structures, and mineralization in structures and discordant breccia bodies (Bechstadt, 1979; Cerny, 1989; Leach *et al.*, 2003). Mineralization is characteriz*ed* by colloform low-iron sphalerite with galena and pyrite. Kucha *et al.* (2010) interpreted nanotextures as biogenic sphalerite microglobules and filaments with associated pyrite framboids. This is consistent with the generally light sulphur isotopic compositions indicative of BSR at all deposits (Schroll and Rantitsch, 2005). The timing of mineralization relative to diagenetic cements also indicates early mineralization, accompanying clear saddle dolomite following shallow burial diagenesis (Kuhlemann and Zeeh, 1995).

Mineralization at Mežica is very similar to Bleiberg (Herlec *et al.*, 2010). At Raibl and Salafossa, mineralization occurs in stratabound horizons, columnar breccia zones, and faults within dolostone (Brigo & Omenetto, 1978; Leach *et al.*, 2003). At Gorno, mineralization in the upper Metallifero is strongly stratiform in style, associated with black shale interbedded with carbonate. "Columnar" mineralization in the middle to lower Metallifero forms south-plunging trends which may be 200 metres or more long, 50-100 metres wide and 3-20 metres thick. Columnar mineralization was more economically important and provided most historical production.

The principal sulphides at all deposits are low iron, typically colloform sphalerite, galena, and pyrite or marcasite with minor chalcopyrite, arsenopyrite, and sulphosalts. Ore stage carbonate is commonly early dolomite and later stage calcite (Kuhlemann *et al.*, 2001). Silver may be enriched to payable levels in concentrate. Minor late-stage fluorite is present, notably at Bleiberg, and minor barite is also recorded.

The lead isotope composition is similar for all deposits with a

homogenous signatures and broadly conformable model age (Schroll *et al.*, 2006). Sulphur isotope composition is negative for all deposits and interpreted to represent BSR processes (Leach *et al.*, 2003; Kuhlemann *et al.*, 2001). Fluid inclusion data suggest low to moderate mineralization temperatures (100-150°C, up to 200°C) and moderate salinities (Leach *et al*., 2003).

Interpretation

The Alpine deposits have often been assigned their own class of "Alpine-type" or "Bleiberg-type" (Sangster, 1976; Brigo *et al.*, 1977) or described as MVT deposits (Leach *et al*., 2003). The "Alpine-type" was originally considered to be seafloor sedimentary exhalative or related to early-formed micro-karstification resulting from periodic exposure of the shallow-water carbonate host sequence (Schulz, 1964; Maucher & Schneider, 1967; Brigo *et al.*, 1977). Later hydrothermal karstification was proposed by Dzulynski & Sass-Gustkiewicz (1985). Leach et al (2003) interpreted the deposits as MVT and related to an extensional Early Jurassic fluid-flow event. Schroll & Rantitsch (2005) interpreted mineralization as early syn-diagenetic replacement and cavity fill. Kucha *et al.* (2010) documented evidence for bacterial sulphate reduction during sedimentation or early diagenesis and Spangenberg & Herlec (2006) interpreted the hydrocarbon signature at Mežica as indicative of a high cyanobacterial biomass in the reduced host rocks that provided the sulphur source for mineralization through BSR.

Formation of the Alpine deposits within a large syn-basinal mineral system is supported by the broad extent of mineralization of similar style and setting with similar lead-isotope signatures, and the tectonic context of an extensional rift-sag basin predating the opening of Alpine Tethys. An early diagenetic timing for the mineralization is supported by the dominance of BSR and evidence for biogenic sphalerite. The association of mineralization with reduced bituminous and evaporitic host sequences is compatible with localisation through interaction of a metalliferous brine with a BSR sulphur source in a reducing environment. Rb-Sr ages for sphalerite at Bleiberg show a wide range from 195.1 ±2.6 Ma to 225 ±2.1 Ma (Henjes-Kunst *et al*., 2017), Norian to Sinemurian. The older ages are consistent with an early diagenetic timing for mineralization, and the younger ages may represent resetting.

Duddar

The Duddar carbonate-hosted zinc-lead deposit is located in the Mor Range of southwest Pakistan, one of a number of deposits in Jurassic carbonates of the Lasbela-Khuzdar belt also including Lasbela and Khuzdar (Arain *et al*., 2021). Following discovery in 1960 by the Geological Survey of Pakistan (GSP), Duddar was explored by GSP, United Nations Department of Development Support and Management Services (UNDDMS), Pakistan Mineral Development Corporation (PMDC) and Pasminco Ltd. (Ahsan & Quraishi, 1997). In 1998, Pasminco reported a pre-production resource of 14.3 Mt at 8.6% Zn and 3.2% Pb to a depth of 500m below surface, significant high-grade mineralization extended below this, down dip to a depth of at least 1,400m .

The deposit was developed by Metallurgical Construction Group (MCC) and Pakistan Mineral Development Corporation (PDMC) in 2005 and is currently producing 500 kt of ore per year by selective underground mining.

Regional Geological Setting

Duddar is located on the north-western passive margin of the Indian continental plate (Figure 27). The deposit lies in the Lasbela-Khuzdar belt, part of an easterly verging Palaeocene-Eocene collision zone between the Indian and the Iran-Afghanistan plates which includes the Bela Ophiolite. The current plate boundary is marked by the sinistral Ornach-Nal Fault, about 50 kilometres west of Duddar.

The Triassic-Jurassic sequence of the Lasbela-Khuzdar belt records the Triassic to Jurassic rifting and breakup of India from Gondwanaland. The original base of the Mesozoic sequence does not crop out, but work further north (Maldonado *et al*., 2011) indicates that the Mesozoic rocks structurally overlie the Cambrian Salt Range Group (gypsiferous marl, salt, gypsum and shale) which in turn structurally overlie the Neoproterozoic meta-igneous and metasedimentary rocks of the Indian shield. The Salt Range Formation is interpreted to have acted as a decollement between the Mesozoic rocks and the basement.

In the Quetta area north of Duddar, the oldest Mesozoic rocks are Lower to Middle Triassic clastic rocks and limestones of the Khanozai Group, with localised basalt flows in the Lower Triassic (Maldonado *et al*., 2011). The Khanozai Group is overlain by the carbonate dominated Ferozabad Group, which hosts the Duddar deposit. The lowest unit of this group comprises sandstone with occasional carbonate beds which passes upwards into shelly platform limestone and then peri-platform argillaceous limestone. A disconformity separates the Ferozabad Group from the overlying siltstone of the Late Jurassic-Cretaceous Mona Jhal Group.

Structural and Lithostratigraphic Setting

The Ferozabad Group is subdivided into three formations, from base the Spingwar (sandstone), Lorali (platform limestone) and Anjira Formations (peri-platform limestone). At Duddar, the Anjira Formation has been subdivided into (from base) the Bamph, Duddar and Kharrari Members (Allen, 1994; Table 1). At Duddar, stratigraphically controlled mineralization in the lower Duddar Member replaces thin bedded carbonaceous argillaceous limestone and mudstone, with algal or bacterial laminites and pseudomorphs after anhydrite and gypsum (Figure 28).

The Middle and Upper Duddar Members are made up of a wedge of mass flow sedimentary rocks which is over 600 metres thick above the northern part of the stratabound deposit and thins southwards over about two kilometres, pinching out completely at the south end of the deposit. This geometry is interpreted to result from deposition of the Duddar Member in a local sinistral strike-slip pull apart basin, with a northwest strike in the deposit area, about 50 degrees anticlockwise to the regional strike. Maximum displacement of the controlling fault at the north end of the deposit coincides with the thickest mass-flow sediments.

The structural elements in the Duddar area can be resolved into four groups resulting from specific events in the tectonic hist-

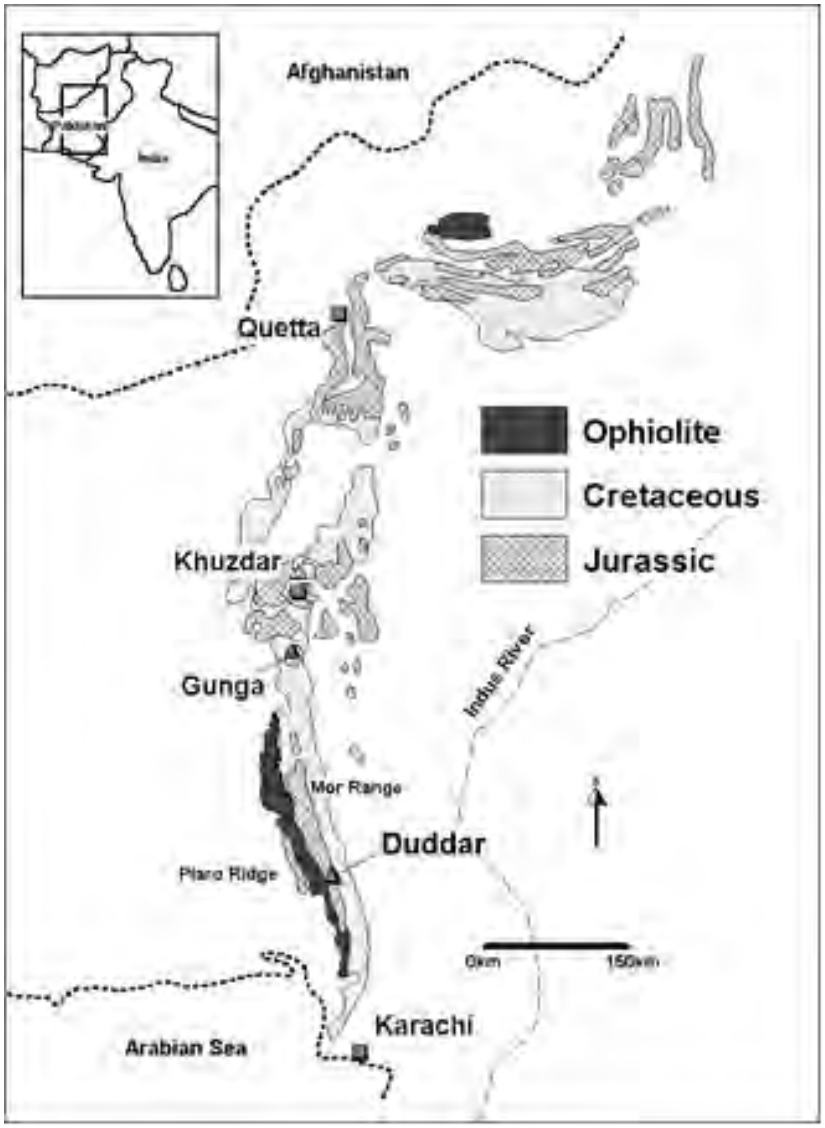

Figure 27: *Location of the Duddar Deposit, hosted in Jurassic rocks of the Mor Range.*

ory of the belt (Allen, 1994). Extensional faults related to the break-up of the Gondwana super-continent during the Jurassic are apparent from rapid thickness changes and the presence of reworked sedimentary rocks in the Anjira Formation. The area was then tectonically quiet until the Palaeocene when the basin experienced east-west compression and large-scale low angle reverse faults during initial collision of the Indian and Iran-Afghanistan plate. Renewed east-west compression during the early Oligocene produced the folds and high angle reverse faults that dominate the structure at Duddar. The direction of plate convergence changed to the present-day sinistral strike-slip in the late Oligocene as the Indian plate moved northwards under Asia.

Mineralization

Mineralization at Duddar is divided into two stratiform zones in the lower Duddar Member and a cross-cutting stockwork zone. The stratiform zones, the lower Zinc Zone and the upper Pyrite Zone, are separated by the Nodular Marker Unit (Jones and Sajjad, 1994).

The Zinc Zone consists of thin bedded carbonaceous limestone and mudstone with laminated algal or bacterial facies and pseudomorphs after gypsum or anhydrite. This unit is strongly replaced by sphalerite with subordinate galena (Figure 29). The nodular marker horizon consists of interbedded nodular limestones and calcareous mudstones about 8 to 10 metres in thickness. The Pyrite Zone consists of carbonaceous and calcareous mudstone with abundant framboidal to nodular to massive pyrite replacing more the 50% of the rock. The Pyrite Zone passes laterally into banded barite (Figure 30) towards the distal southern and western margins of the deposit and is progressively replaced with sphalerite to the north, with rims of sphalerite replacing pyrite nodules (Jones, 1994). In the northern part of the deposit, most or all of the pyrite is replaced by sphalerite.

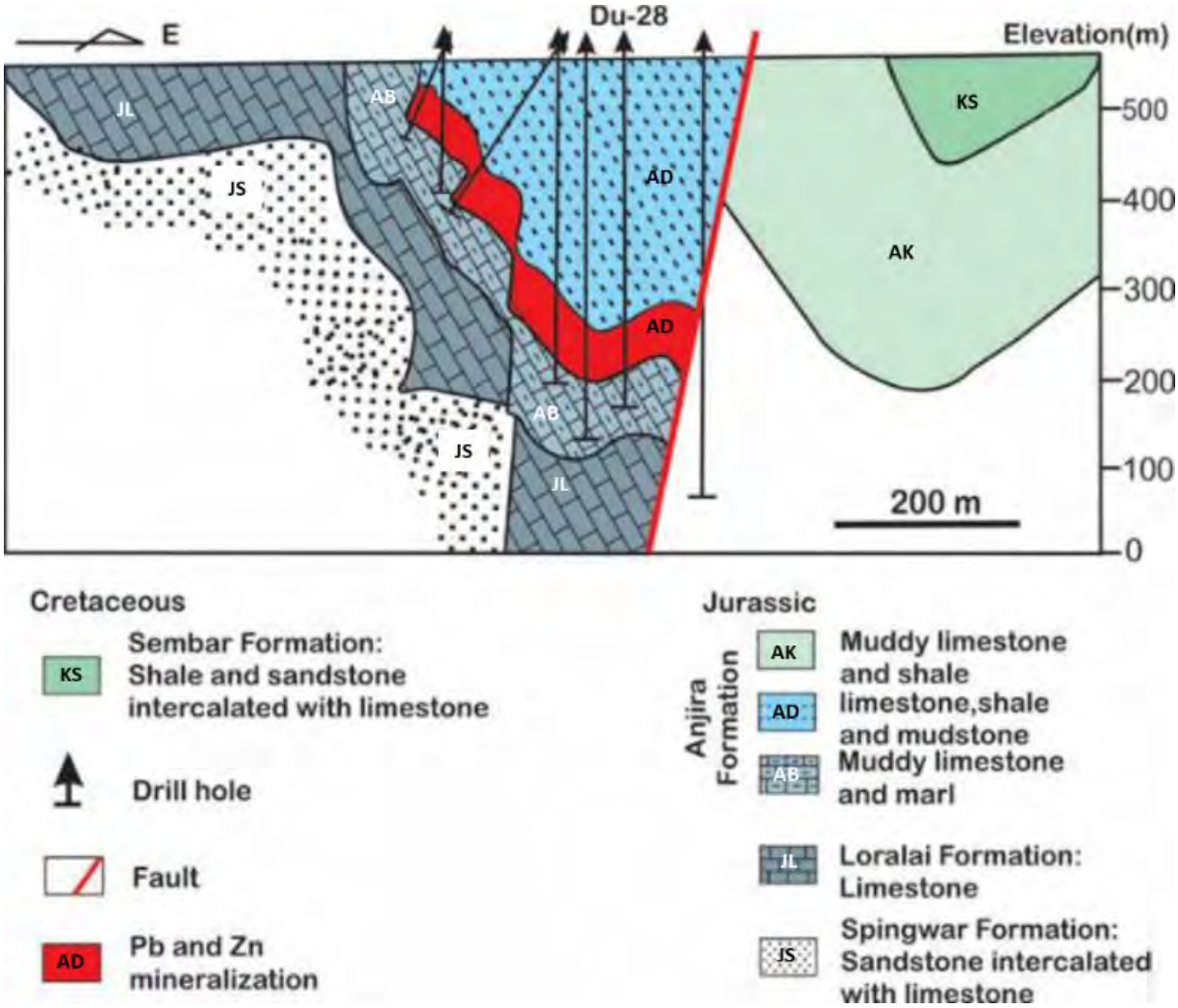

Figure 28: *East-west cross section of the Duddar deposit. Modified after Song et al. (2019).*

Group	Formation	Member	Lithology	Thickness	Age
Mona Jhal	Sember		Grey / green siltstone. Distal marine environment.	> 200 m	Late Jurassic-Cretaceous
			----- disconformity ------		
Ferozabad	Anjira	Kharrari	Peri-platform limestone and calcareous shale	130-200 m	Early-Middle Jurassic
		Upper Duddar	Peri-platform limestone and debris flow breccia	0-300 m	
		Middle Duddar	Peri-platform limestone and debris flow breccia. Platform limestone at top	0-300 m	
		Lower Duddar	**Mineralization** Thin bedded carbonaceous and pyritic limestone and mudstone	20-80 m	
		Bambh	Thin bedded nodular limestone and calcareous mudstone. Ammonites	50-75 m	
	Loralai		Fossiliferous micritic limestone and calcareous shale. Shelly fauna	> 200 m	
	Spingwar		Shallow marine x-bedded sandstone. Minor carbonate beds toward the top	> 400 m	Late Triassic-Early Jurassic

Table 1: *Stratigraphy of the Duddar area, after Allen and Anwar (1994)*

Figure 29 *High-grade zinc mineralization at Duddar, Pakistan. Pale fine-grained sphalerite replaces algal or bacterial laminite in bedded carbonaceous limestone and mudstone. DU-18 284m, NQ core.*

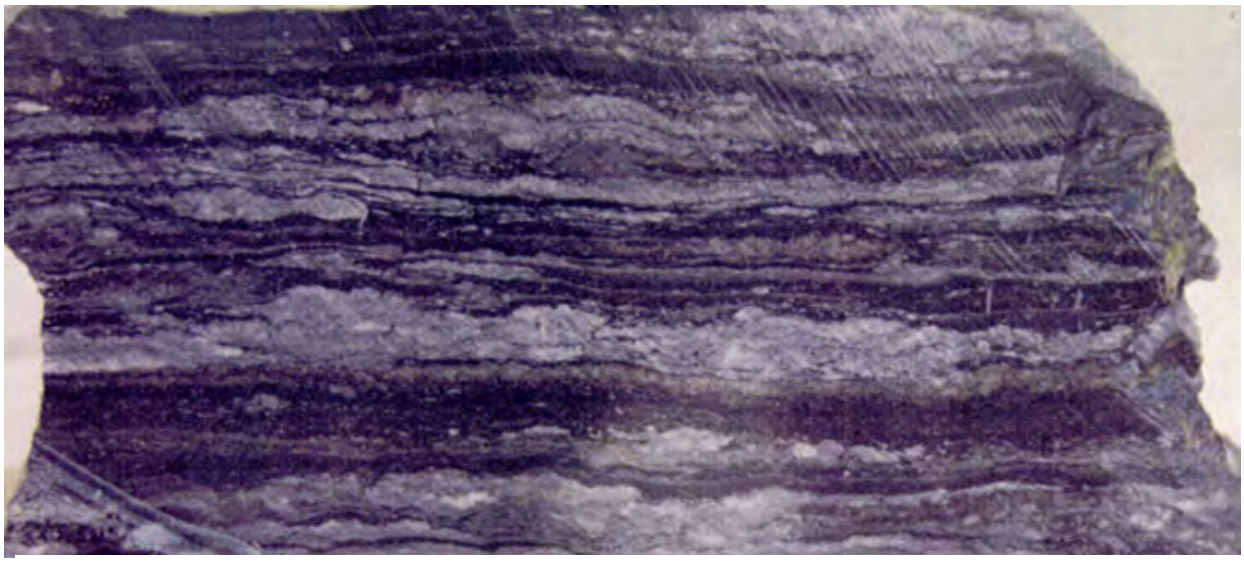

Figure 30: *Laminated barite and mudstone laterally equivalent to the Pyrite Zone mineralization to the north. Outcrop sample, Duddar, Pakistan (field of view 10cm).*

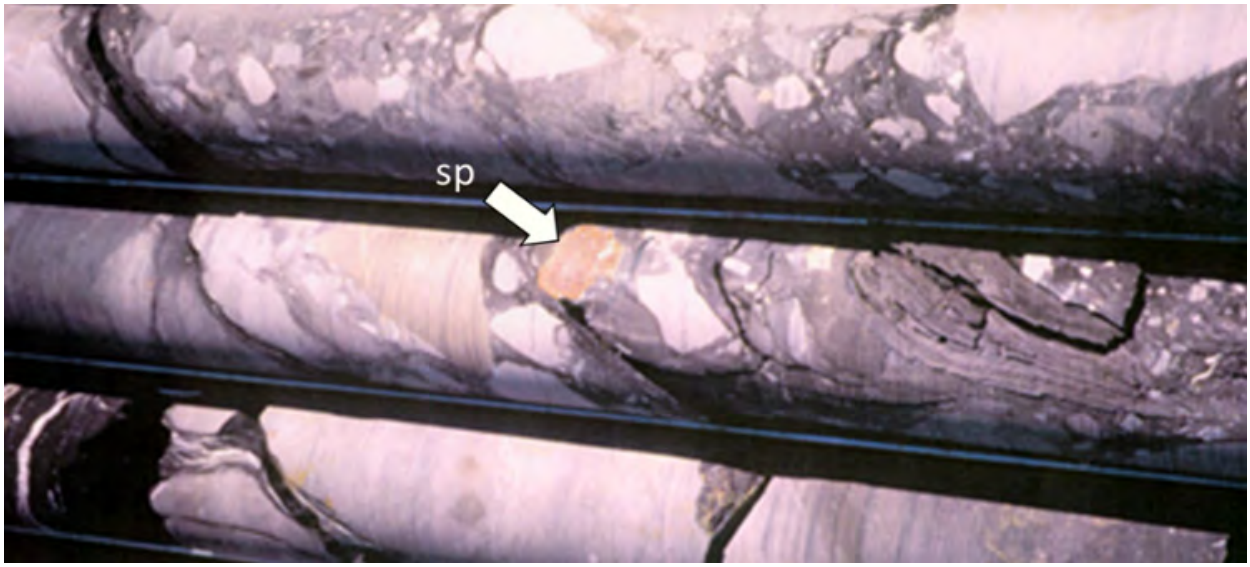

Figure 31: *Breccia containing sulphide and/or barite clasts occur in the hanging wall sequence at Duddar, Pakistan. A clast of orange sphalerite is marked with the white arrow. NQ core.*

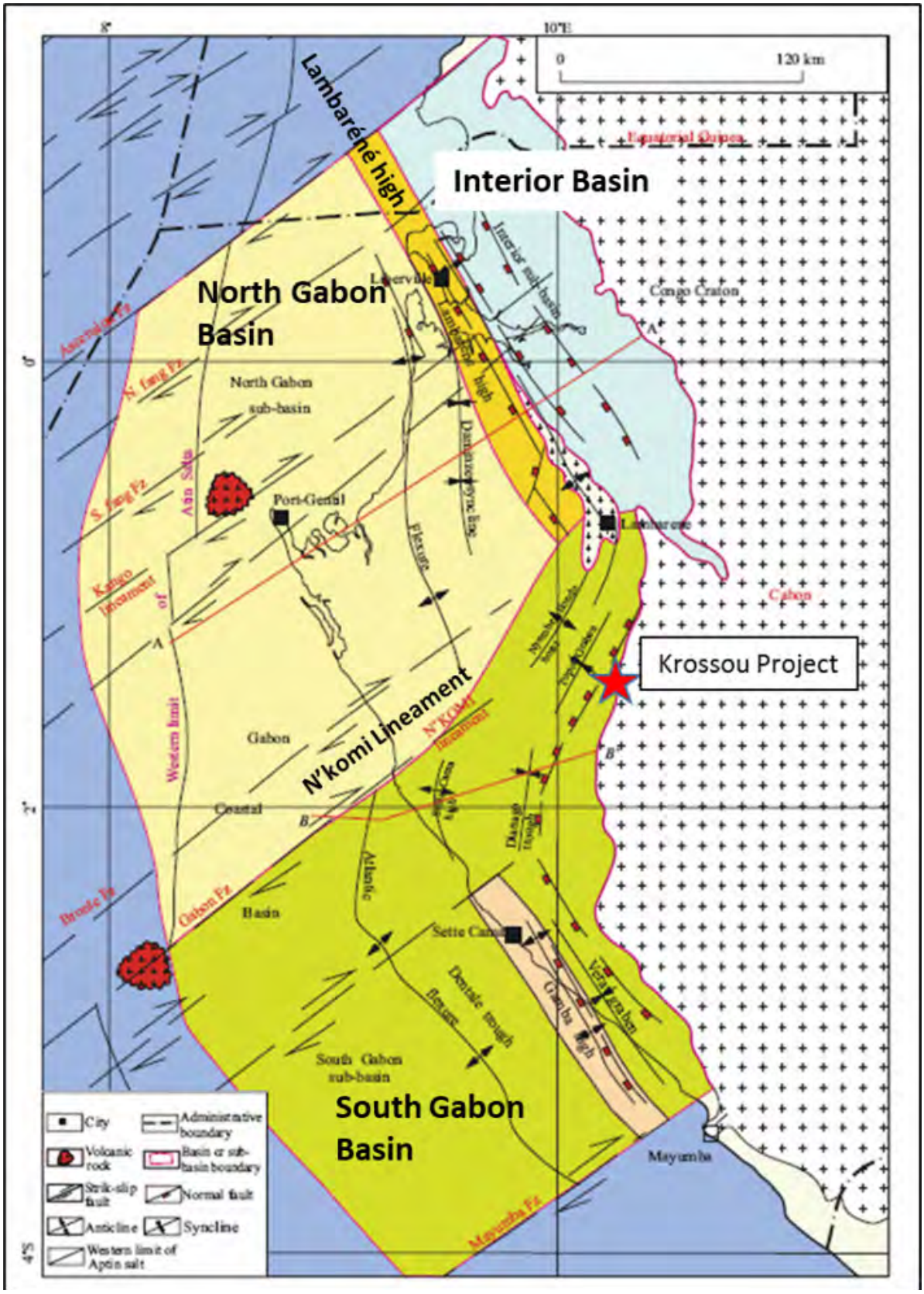

Figure 32. *Structural framework of the coastal basin in Gabon showing the right-stepping relay associated with the N'Komi lineament that separates the North and South Gabon sub-basins. From Chen et al., 2013.*

In the northern part of the deposit, the stratiform zone in underlain by a cross-cutting zone of stockwork vein-hosted sphalerite-galena mineralization with minor chalcopyrite. The sphalerite is darker in colour than in the stratiform zones, due to higher iron content, and coarser grained. Stockwork mineralization cuts upwards through the stratiform mineralization zone into the Middle and Upper Duddar Members. Clasts of this style of mineralization are observed in hangingwall sedimentary breccias (Figure 31).

Mineralization is associated with pervasive silicification and de-calcification halos to the stratiform zones on the scale of 1-5 metres. Mineralization is also associated with ankerite and dolomite alteration in the carbonate host rocks. Patchy ankerite alteration is evident in platform carbonates underlying mineralization for hundreds of metres and may be related to a basin scale process.

Interpretation

The Duddar deposit is interpreted to represent hydrothermal replacement of a reactive, reducing host rock that was deposited in the lower sag part of the basin by an oxidiz*ed* metalliferous brine derived from the underlying rift-stage clastic basin. Basin controlling faults provided cross-stratal permeability allowing access of deep basin fluids to the host rocks. Early marcasite-pyrite mineralization and carbonaceous limestone and mudstone are replaced by sphalerite and galena. Mineralization was localised in a fault-controlled sub-basin with a stockwork feeder zone at the north end of the deposit with higher-iron sphalerite and minor chalcopyrite.

Mineralization is interpreted to be of Early-Middle Jurassic age and related to extensional tectonics and the development of a rift-sag basin as the Indian continental plate separated from Gondwana (Allen, 1994). No mineralization occurs in the overlying the Late Jurassic-Cretaceous Mona-Jhal Group.

Coastal Basin of Gabon

The Coastal Basin (Basin Côtier) of Gabon is part of an extensive basin complex on the West African margin, often termed the 'Aptian Salt Basin', that developed as a rift-sag to passive margin basin during the opening of the South Atlantic from the Upper Jurassic to the present. The Coastal Basin from Cameroon south to Angola is an important hydrocarbon province.Exploration of platform carbonates at the edge of the basin by BRGM (Bureau de Recherches Géologiques et Minières) in the 1960s to 1980s led to the discovery of zinc-lead mineralization at a number of locations over a strike-length of more than 70 kilometres. Commencing in 2014, renewed assessment and exploration along the Kroussou trend was carried out by three Australian junior companies. The current holder, Apollo Minerals Group, released an Exploration Target of between 140 and 300 Mt at a grade between 2.0% and 3.4% zinc plus lead in November 2022 (https://apollominerals.com/investors/asx-announcements/).

Regional Geological Setting

The Coastal Basin in Gabon is divided into the Interior sub-basin, northeast of the Lambaréné basement high, the North Gabon sub-basin southwest of the basement high, and the South Gabon sub-basin south of the N'Komi lineament (Mbina Mounguengui & Guiraud, 2009; Chen *et al.*, 2013; Figure 32). Pre-rift sedimentation on Proterozoic basement saw up to 600 metres of Carboniferous to Jurassic continental clastic rocks deposited in the Interior sub-basin (Teisserenc and Villemin, 1990).

Lower Cretaceous rifting was accompanied by deposition of thick sequences of alluvial and lacustrine sandstones and shales, with accumulation of up to 4,000 metres of fluvial and organic-rich lacustrine sediments which are an important hydrocarbon source rock. Syn-rift sedimentation evolved through initial basement extensional block faulting and basin formation in the Neocomian, graben and block faulting in the late Neocomian to early Barremian and draping and growth faulting during the late Barremian and early Aptian (Teisserenc & Villemin, 1990). Syn-rift volcanism occurred in the Neocomian and early Aptian (Fernández *et al.*, 2020). Lithospheric breakup and formation of the first oceanic crust is interpreted to have occurred around the Aptian-Albian boundary.

In the South Gabon Basin (Figure 33), the Basal Sandstone unit, deposited in a braided-river environment, is overlain by the lacustrine Kissenda Shale with shale, thin carbonates, and minor siltstone, sandstone, and conglomerate. The overlying Melania Formation consists of shale and fine-grained, argillaceous sandstone deposited as turbidite channels and fans, transitioning upwards into organic-rich lacustrine shale, siltstone, and calcareous shale. The depocentre shifted westward during the late Barremian, marked by deposition of the 2000-3000 m thick Dentale Formation of lacustrine deltaic sandstone and shale. The middle Aptian Gamba Formation represents initiation of post-rift sag-phase sedimentation and is a transgressive unit consisting of fluvial sandstones with lagoonal shale interbedded with sandstone, dolomite, and anhydrite.

The syn-rift units are overlain by the 800-1000-metre-thick late Aptian evaporites of the Ezanga Formation in the Interior, North, and South Gabon sub-basins, which were affected by major subsequent salt tectonism. The overlying Albian to lower Cenomanian Madiéla Formation and the Turonian Sibang Limestone Member represent ramp- and shelf-carbonate deposition with lateral thickness variation resulting from initiation of salt diapirs.

Kroussou Structural and Lithostratigraphic Setting

The Kroussou mineralized trend lies along a north-northeast-trending segment of the eastern margin of the South Gabon sub-basin, which is north-northwest trending further to the north and south. This prominent north-northeast-trending right-step is coincident with the Gabon Fault or N'Komi lineament and is interpreted to represent a syn-rift relay zone. In outcrop, the basin margin is represented by an irregular unconformity with Lower Cretaceous sediments overlying Palaeoproterozoic basement of the Kimezian Supergroup (Noce *et al.*, 2007). The contact is characterized by kilometre-scale embayments or palaeochannels of Cretaceous sediment running broadly east-west into the basement. Present day topography is strongly controlled by the Cretaceous palaeotopography with present-day valleys over Cretaceous valleys. Zinc-lead and barite mineral occurrences have been identified at surface over a strike of about 135 kilometres along this trend (Figure 34).

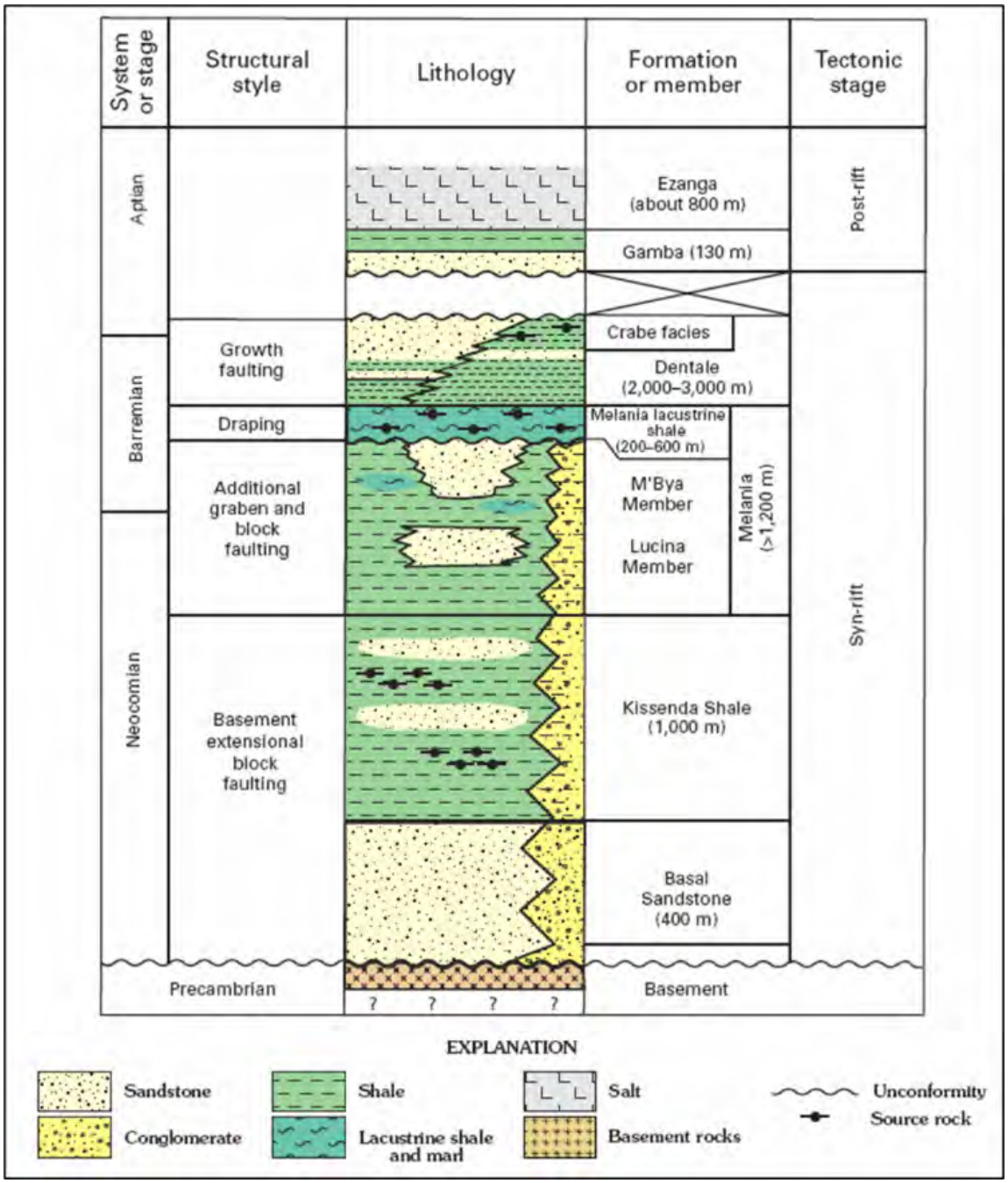

Figure 33: *Stratigraphic column for the South Gabon sub-basin. From Brownfield & Charpentier, 2006.*

Based on palynological dating, the BRGM assigned the Kroussou host sequence to the N'Zeme Asso Formation, equivalent to the middle Aptian Gamba Formation, comprising fluvial sandstone and lagoonal marl and mudstone. The entire rift sequence is therefore absent at Kroussou with basal sag-phase sedimentary rocks transgressing directly onto basement on the rift shoulder, where the overlying Ezanga evaporites were not developed.

The Dikaki embayment in the centre of the Kroussou trend has been one of the main targets for recent exploration (Figure 34) and drill data supports the interpretation of the lithostratigraphic setting of mineralization. The Palaeoproterozoic basement is overlain by a basal association of a coarse angular poorly sorted sedimentary breccia, laminated or nodular algal dolostone, and immature, reduced sandstone with carbonized detritus. This basal unit is interpreted to have been the result of strong topographical control possibly accompanied by faulting during sedimentation with fanglomerate breccias and alluvial channels impinging on a low-energy lacustrine environment with algal carbonate deposition.

The basal unit is overlain by a carbonate-cemented siliciclastic sequence which includes massive horizons of coarse polymict conglomerate, cycles of coarse polymict conglomerate fining up to arkosic pebbly sandstone and sandstone, and intervals of

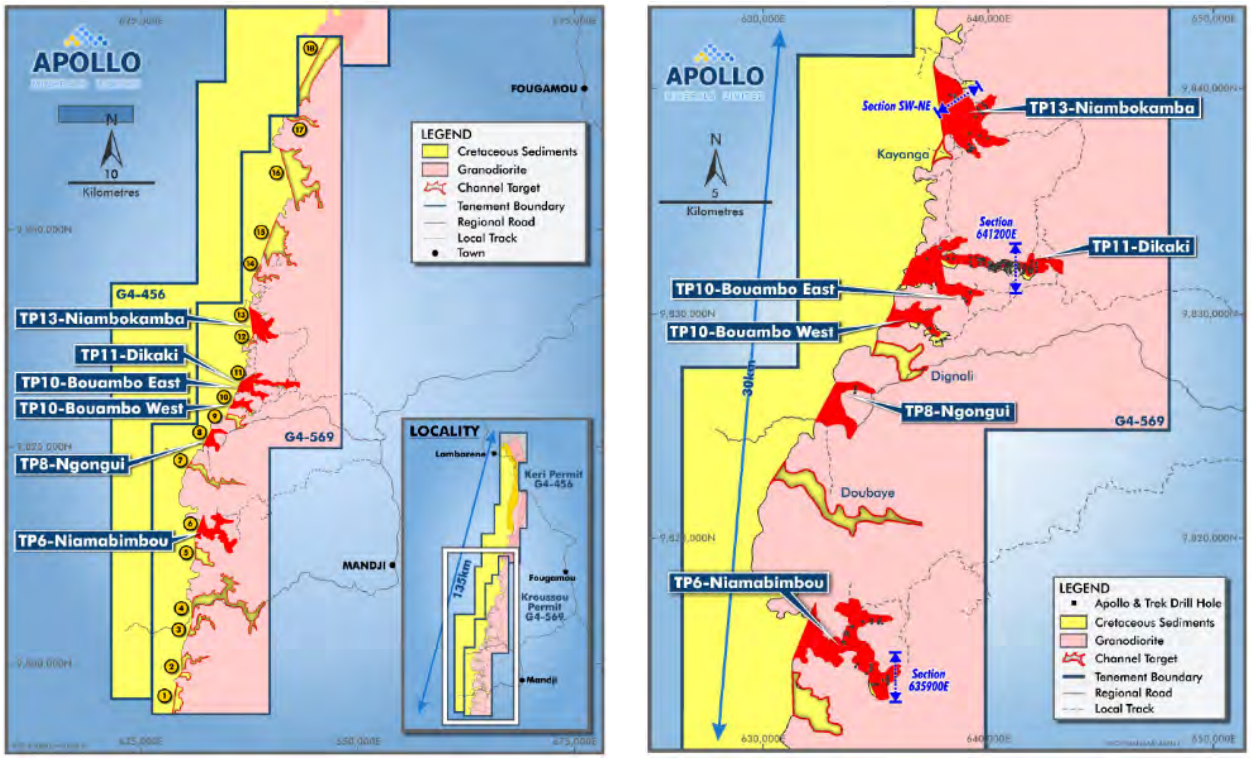

Figure 34: Kroussou trend showing the main prospects and the central Exploration Target. From Apollo Minerals ASX release 9 November 2022 (https://apollominerals.com/investors/asx-announcements).

clean carbonate-cemented sandstone and pebbly sandstone with thin-bedded dark fine-grained sandstone and organic-rich siltstone. Channel-fill conglomerate is highly variable in thickness, with the overlying facies deposited on a lower-relief post-channel surface with minor lacustrine dolostone interbeds, indicating a predominantly alluvial setting with restricted reduced playa lake deposition. The overlying sandstone and siltstone unit is dominated by calcareous immature sandstone and dark organic-rich siltstone.

The sequence is undeformed and bedding is consistently shallow dipping. The east to east-southeast orientation of the palaeochannels may be controlled by minor fault orientation, however no large-scale offsets are evident. The major rift-stage basin margin faults are interpreted to lie under cover to the east of the mapped unconformity. Oilwell RY2 (Madiela-2), 26 kilometres southwest of Dikaki, intersected Ezanga Formation evaporites from c. 540-630 metres implying a substantial basinward fault throw of at least 500 metres. Recent airborne electromagnetic surveys by Apollo Minerals suggest that smaller basin-parallel faults may control rotated fault blocks within the mineralized zones in the footwall of the main basin margin faults.

Mineralization

At the Dikaki prospect, stratabound disseminated galena and sphalerite mineralization occurs over a stratigraphic interval of at least 100 metres. The strongest mineralization occurs over thicknesses of 5 to 20 metres, replacing carbonate cement or carbonate clasts in clastic units, as disseminated to semi-massive replacement style in dolostone in the basal unit, and in veins in basement (Figure 35). The highest-grade mineralization is in clean, coarse arkosic sandstone horizons (2 to 8% Zn and 2 to 30% Pb). In coarser conglomerates, abundant marcasite mineralization with minor sphalerite and galena occurs in the matrix or as primary open-space fill between clasts, with dissolution of clasts and carbonate cement postdating mineralization. Weak mineralization in clean carbonate-cemented bituminous sandstone and in algal dolostone occurs in the upper unit, locally with chalcedonic silicification. Mineralization is strongly controlled by channel geometry and associated facies variation, with mineralized lenses elongated east-west in the central zone of the embayments.

Mineralization at Dikaki shows a very broad halo of zinc anomalism above 0.3% Zn, whereas lead anomalism is more constrained. Mineralization is associated with weak silver enrichment (max. 11 g/t Ag) but no clear-cut association with other trace elements. Copper and barite occurrences are reported elsewhere along the Kroussou trend, but the relationship with the zinc-lead mineralization has not been established.

Higher grade mineralization has been reported at the Niambokamba Prospect, seven kilometres north of Dikaki in a similar setting, including 6 metres at 16.1% Zn and 2.0% Pb, with 4.8 g/t Ag (https://apollominerals.com/investors/asx-announcements/). Mineralization is of similar style, replacing cement in calcareous clastic rocks and as more massive replacement in algal carbonate intervals (Figure 36).

Interpretation

The lateral extent, setting, style and chemistry of mineralization indicates that the Coastal Basin was a fertile basin for zinc lead mineralization and that a large-scale basinal fluid-flow

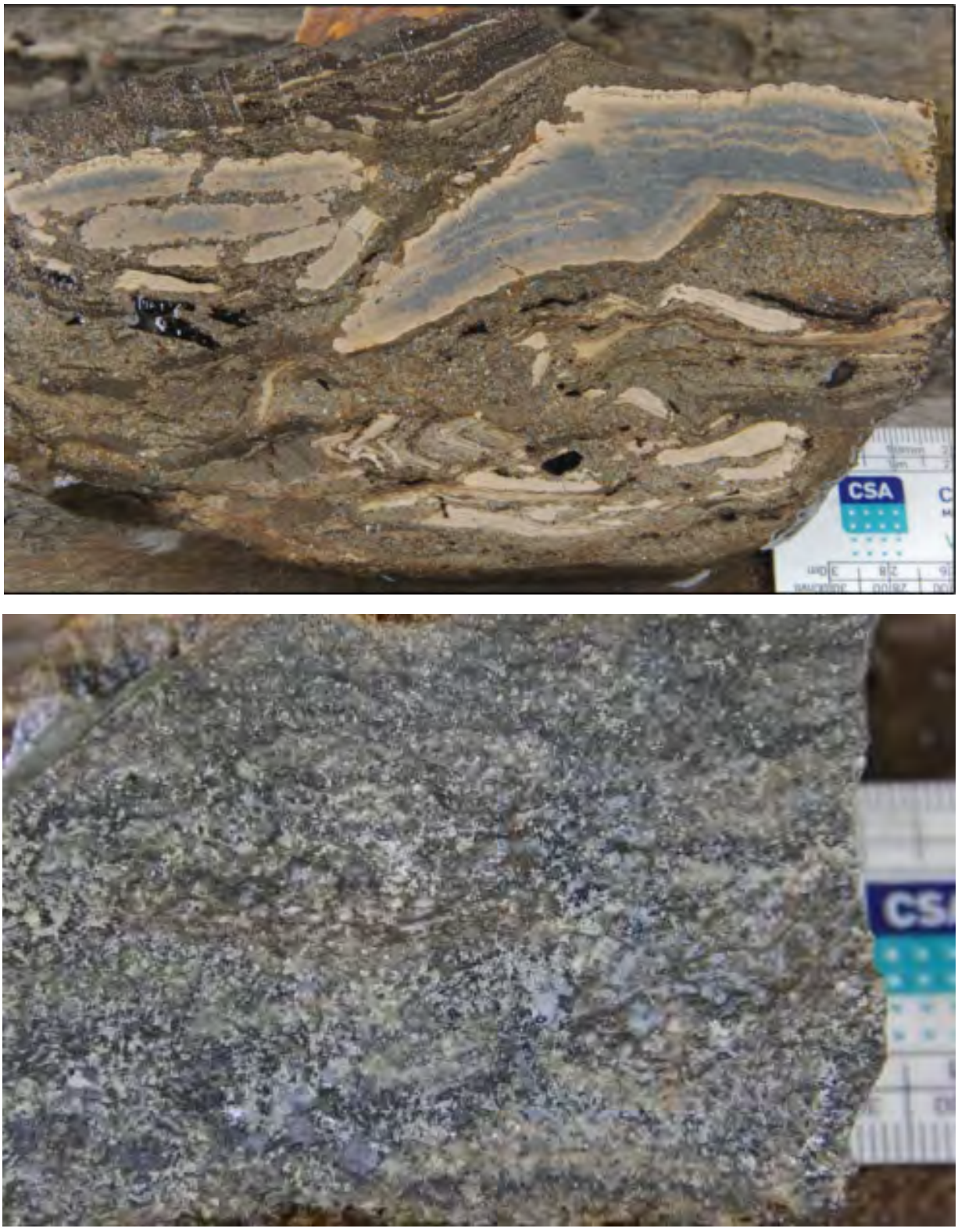

Figure 35: *Kroussou mineralization: At left, laminar lacustrine dolostone disrupted within coarse arkose with high grade galena-sphalerite replacement in dolostone and sandstone matrix. At right, coarse arkose with replacive pale sphalerite and galena in matrix.*

event brought mineralizing hydrothermal brines from the basin onto the eastern rift margin, mineralizing suitable host rocks through reaction with carbonate and/or through reduction of metalliferous brines due to interaction with hydrocarbons and the reduced host sequence. The fertility of the basin for zinc-lead may reflect the thick reduced arkosic rift sequence beneath the Ezanga Formation evaporites, with lacustrine sediments that include thick organic-rich shale horizons. The

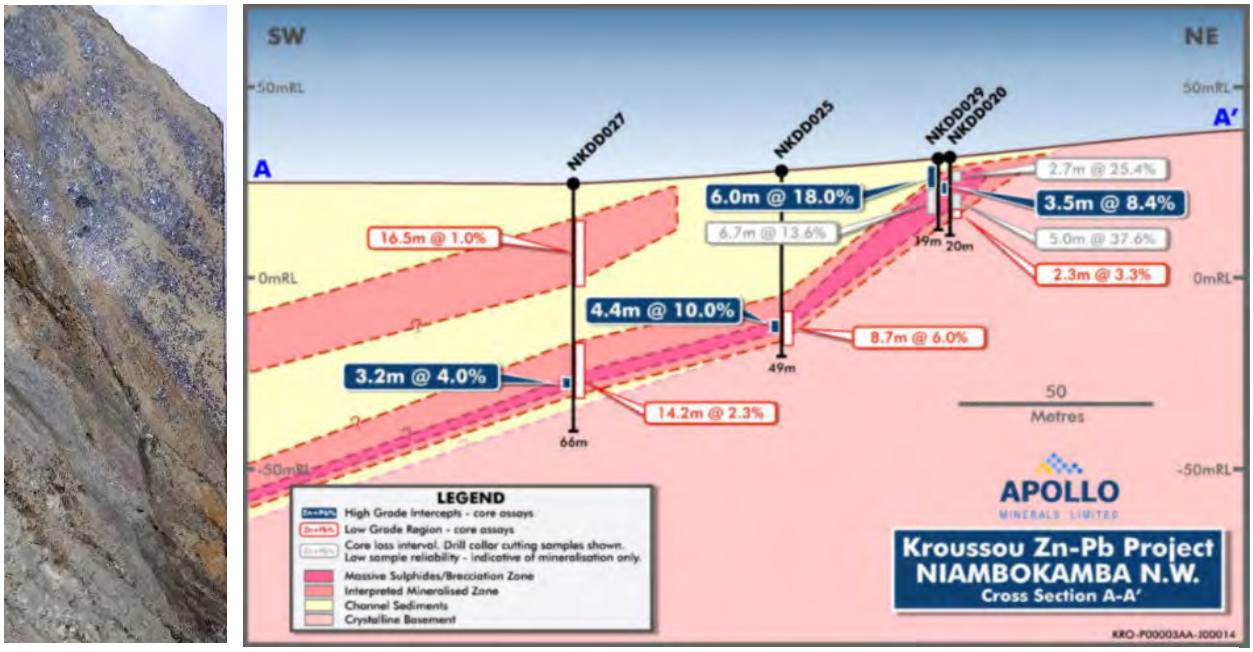

Figure 36 *At left, drill section through the Niambokamba Prospect. At right, high-grade sphalerite-galena at top totally replacing permeable algal carbonate unit at the Niambokamba prospect.*

evaporite unit at the base of the basin sag phase would have provided a hydrological seal allowing circulation of brines beneath the salt cap and effective extraction of metals.

The trigger event for fluid flow from the basin was most probably the initiation of halokinesis in the Upper Cretaceous in response to extension and sediment loading, with breaching of evaporite seals. An alternative trigger event could be the mild inversion in the Late Eocene that saw the end of major salt diapirism. The position of the Kroussou trend in a major fault-relay bend may have been a key focus for fluid flow from the basin. A combination of major and minor basin-parallel faults and relay structures would have channelled fluids onto the rift margin, where the basin margin pinch-out in earliest post-rift stratigraphy provided additional focus. Channels of clean, carbonate-cemented siliciclastics, and algal carbonates provided focus within the platform environment, as well as trap sites, with aquicludes provided by the shalier capping sequence. No remnant hydrocarbons have been identified with mineralization, but it is possible that sour gas expulsion occurred at the same time as mineralization and played a role as a trap reductant and sulphur source.

Atlas Miocene

The Atlas belt across Tunisia, Algeria and Morocco hosts numerous zinc-lead deposits within Jurassic to Eocene platform carbonates deposited on the Neotethys passive margin. These deposits have generally been interpreted to be MVT deposits related to fluid systems driven by Eocene to Miocene inversion, Atlas orogeny and uplift (e.g., Clayton & Baird, 1997; Bouabdellah *et al.*, 2012; Bouhlel *et al.*, 2013). However, in Tunisia, significant stratabound zinc-lead deposits also occur within Upper Miocene-Pliocene calcareous sandstones and lacustrine limestones deposited in late-orogenic pull-apart fault-controlled basins following the main Atlas orogeny (Reynolds & Mackay, 2007; Decrée *et al.*, 2008).

Bou Aouane is the largest known Mio-Pliocene deposit and supported an underground mine which closed in late 1986, with estimated production of c. 3 Mt at 5% Zn and Pb. On closure, the remaining 'resource' was reported as c. 1.35 Mt at 3.5% Zn and Pb at depth as well as a shallow 'resource' of 0.9 Mt at 4.9% Zn and Pb. The Sidi Driss open-pit mine produced lead and zinc until 1979 and a deeper lower-grade resource was the basis for a feasibility study by Alusuisse in 1985.

Regional Geological Setting

The geology of Tunisia is dominated by Mesozoic to Tertiary sedimentary rocks, variably affected by Alpine-age deformation through the Atlas fold and thrust belt. In the northwest, the Tell Atlas or Zone des Nappes. comprises Oligo-Miocene flysch structurally emplaced over deformed Permian to Eocene shelf sedimentary rocks. The Zone des Domes (or Majerda Zone) to the south is characterized by northeast-southwest elongated Triassic inliers within Cretaceous carbonates, interpreted to be of diapiric origin (Jallouli *et al.*, 2005), controlled by major basinal structures, and modified by Atlas thrusting.

Unconformities in the Late Cretaceous to Early Miocene reflect basin inversion accompanying the onset of Atlas deformation. Eocene marine carbonates are succeeded by regressive marginal marine to continental Oligocene to Early Miocene clastic rocks. The Middle to Late Miocene Atlas orogeny resulted from collision of a Eurasian-derived arc or microplate with the North Africa passive margin through subduction rollback (Rosenbaum *et al.*, 2002). The deep-water, passive-margin Oligo-Miocene ('Numidian') flysch was thrust southeast over the carbonate -dominated shelf sequences and the

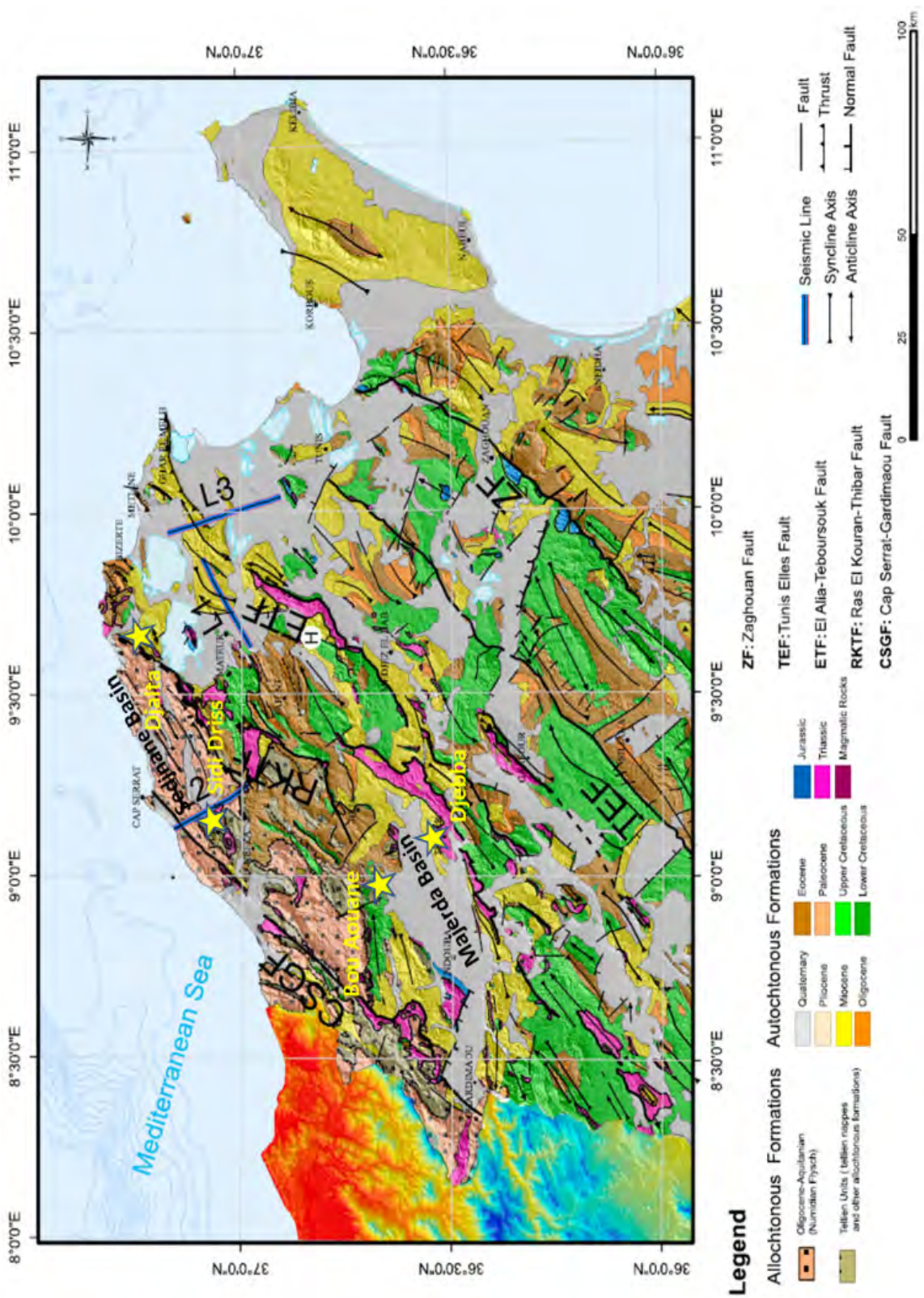

Figure 37: *Summary geology of northern Tunisia with Neogene basins, major faults and location of the main Mio-Pliocene deposits. Modified from Booth-Rea et al., 2018.*

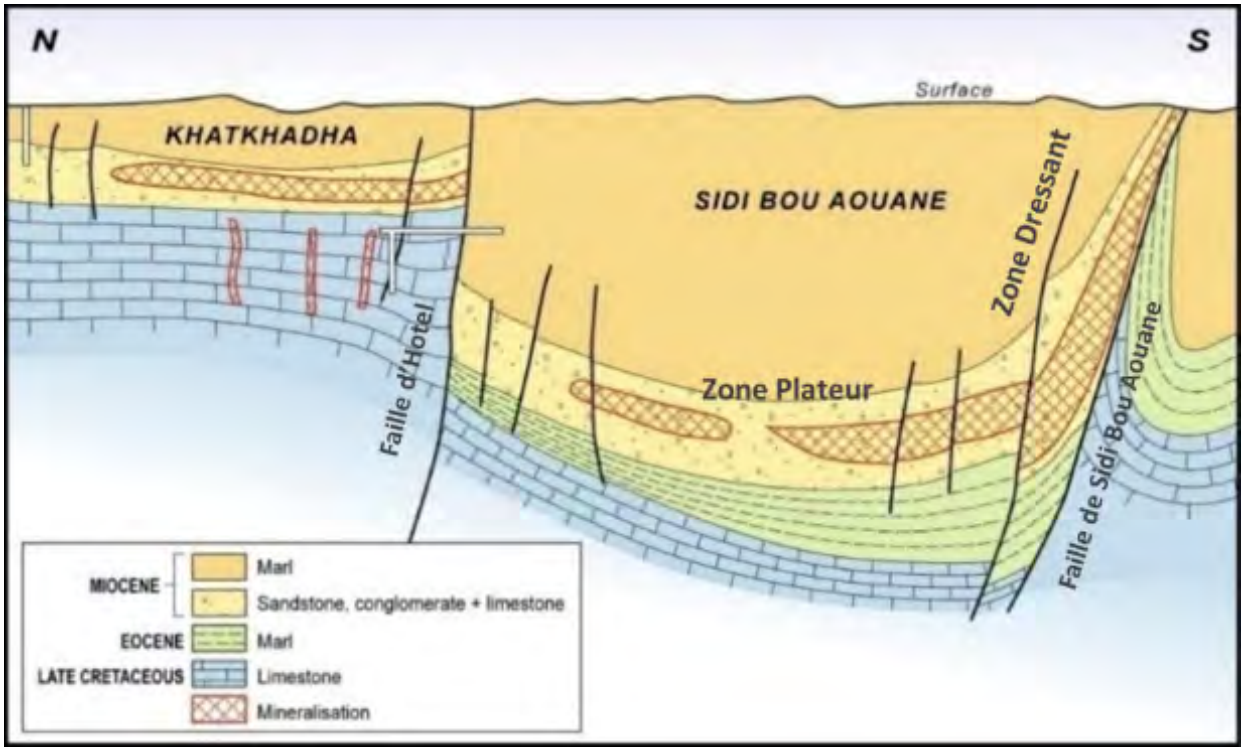

Figure 38: *Bou Aouane cross section modified from historical reports showing mineralized zones and inverted faults.*

carbonate platform was deformed in a foreland fold-and-thrust belt.

Internal basins of Late Miocene to Pleistocene age opened during a late-orogenic extensional collapse phase, which may reflect slab break-off, controlled by right-lateral transtensional movement on major east-northeast and northwest-trending faults (Figure 37; Azizi & Chihi, 2021). Continental molasse and lacustrine sediments, including carbonates and evaporites, were deposited in the basins accompanied by localised bimodal alkaline volcanism and intrusion (Rosenbaum *et al*., 2002; Booth-Rea et al, 2018; Decrée *et al*., 2014). These basins were inverted and uplifted prior to renewed extension and development of Quaternary alluvial rifts (Belguith *et al*., 2011).

Structural and Lithostratigraphic Setting

The Majerda Basin is a large Mio-Pliocene and Quaternary basin, extending about 100 kilometres along strike and up to 30 kilometres across, elongated northeast and swinging approximately east-west in its western part due to antithetic west-northwest structures and relays (Figure 37). The central part of the basin is largely covered by Quaternary sediments, but Miocene to Pliocene sedimentary rocks are exposed on its margins and in the east, north and southwest of the basin. These sequences were uplifted and locally deformed prior to Quarternary rifting and sedimentation. An oil well in the central western part of the basin intersected 700m of Quaternary and Neogene sediments above Triassic evaporites.

Mio-Pliocene sediments in the northeast of the basin were deposited in sub-basins controlled by northeast-trending basin-margin faults and west-northwest- to northwest-trending transfer or relay structures. Lacustrine carbonates and marls interbedded with carbonate-cemented alluvial sandstones and conglomerates pass upward into coarse siliciclastic sequences with alluvial fanglomerates, reflecting increasing fault-controlled uplift and coarse sediment supply. The stratabound Bou Aouane and El Haouaria zinc-lead deposits are hosted in the basal calcareous sediments on the northern margin of the basin, while the Djebba zinc-lead deposit occurs in a similar setting on the southern margin of the basin (Figure 37).

The smaller Sedjnane Basin lies about 35 kilometres north of the Majerda Basin and is controlled by a set of east-northeast-trending splays from the major northeast-trending Ghardimaou - Cap Serrat fault. The southwest edge of the basin is marked by the Oued Belief Triassic dome with associated evaporitic breccias, sediments, and the Tortonian-Messinian granodiorite and rhyolite, bounded by low-angle detachment structures and breccias (Decrée *et al.*, 2014; Booth-Rea *et al.*, 2018). The basal sediments in the basin include extensive lacustrine deposits with algal limestone, reduced bituminous limestone and marl, together with calcareous sandstones. The basin fill coarsens upwards with increasingly chaotic sedimentary breccias, and the basin is extensively covered by younger Quaternary conglomerates and sandstones.

Mineralization

The Bou Aouane deposit is located along a northeast-trending normal fault on the northern margin of the Majerda Basin. Mineralization occurs where the Cretaceous inlier in the footwall of the fault is terminated by a major northwest-trending

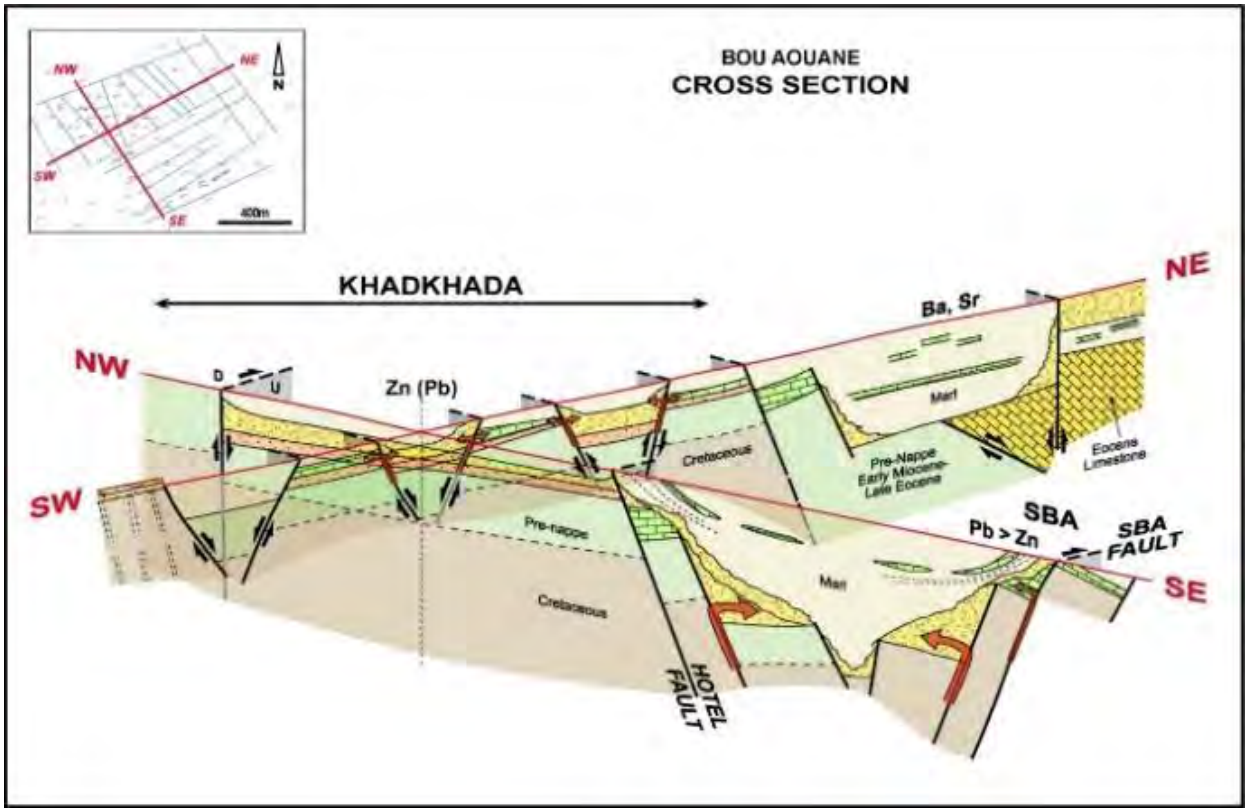

Figure 39: *Schematic illustration of the syn-mineralization geometry and structural controls on mineralization at Bou Aouane.*

extensional relay zone. The bulk of the mineralization is stratabound in Miocene calcareous siliciclastic and carbonate rocks with minor mineralization in veins within the Cretaceous Abiod limestone (Campanian-Maastrichtian) in the footwall of the main fault.

In the mine area, the northwest-trending Faille d'Hotel and the southeast-trending Faille de Sidi Bou Aouane (SBA) faults are interpreted to control Neogene mineralization (Figure 38, Figure 39). Both faults have been inverted after mineralization, with steepening of bedding and Eocene basement exposure along the SBA fault (Figure 38). The Neogene is mostly known from drilling which intersected a 50- to 100-metre-thick lower unit of lacustrine algal limestone, evaporite dissolution breccias, and calcareous sandstone, overlain by marl-dominated sequences and conglomerate. Algal limestone is mostly reddened, though some reduced bituminous limestone has also been intersected. Stratabound mineralized zones up to 30 metres thick in the lower unit were mined in the sub-horizontal Zone Plateur and the steeply dipping Zone Dressant close to the SBA fault (Figure 38). The Khadkhada sector on the northern hanging-wall side of the Faille d'Hotel is similar to the Zone Plateur.

Mineralization replaces limestone in favourable bands and laminae, as well as calcite matrix in sandstone, and also forms small-scale irregular cross-stratal veins and breccias (Figure 40). Ductile disruption of lamination in algal laminated limestone suggests mineralization before complete lithification, as does bladed barite that grows into soft sediment within micritic limestone with replacive galena laminae. Replacive sphalerite and galena is often cut by later vein and breccia mineralization with galena and calcite, which may display open-space growth textures. Mineralogy is simple with sphalerite and galena, very little pyrite, late calcite and minor Sr-rich barite. Sphalerite is low iron and pale cream to yellowish in colour. Mineralization in the Cretaceous has similar mineralogy occurring within cross-cutting brittle veins.

The Sidi Driss zinc-lead deposit is located on the southern faulted margin of the of the Sedjnane Basin (Decrée *et al.*, 2011) where the Neogene sequence is gently dipping, up to 160 metres thick, and lies unconformably on steeply dipping Eocene marl and limestone. In the west, the deposit is overlain by the Tamera supergene iron mine which exploited ferruginous breccias on the margin of the Oued Belif complex. The smaller Douahria and Gantra el Haichichi zinc-lead mines are located east of Sidi Driss on the southern side of the basin, along the major controlling east-northeast fault. The Djalta mine is located in the Mateur Basin along strike to the east from the Sedjnane Basin.

Mineralization at Sidi Driss is dominantly stratabound within argillaceous and silty marls with horizons of calcareous breccia, sandy limestone and algal limestone. Historical descriptions indicate that stratabound mineralization occurs at up to five favourable horizons, but is concentrated at two levels, one a limestone and the other a calcareous conglomerate. Grades and thickness increase to the southeast close to the basin-controlling fault. Minor vein mineralization occurs in limestone beds within the Eocene marl in the footwall of the controlling fault.

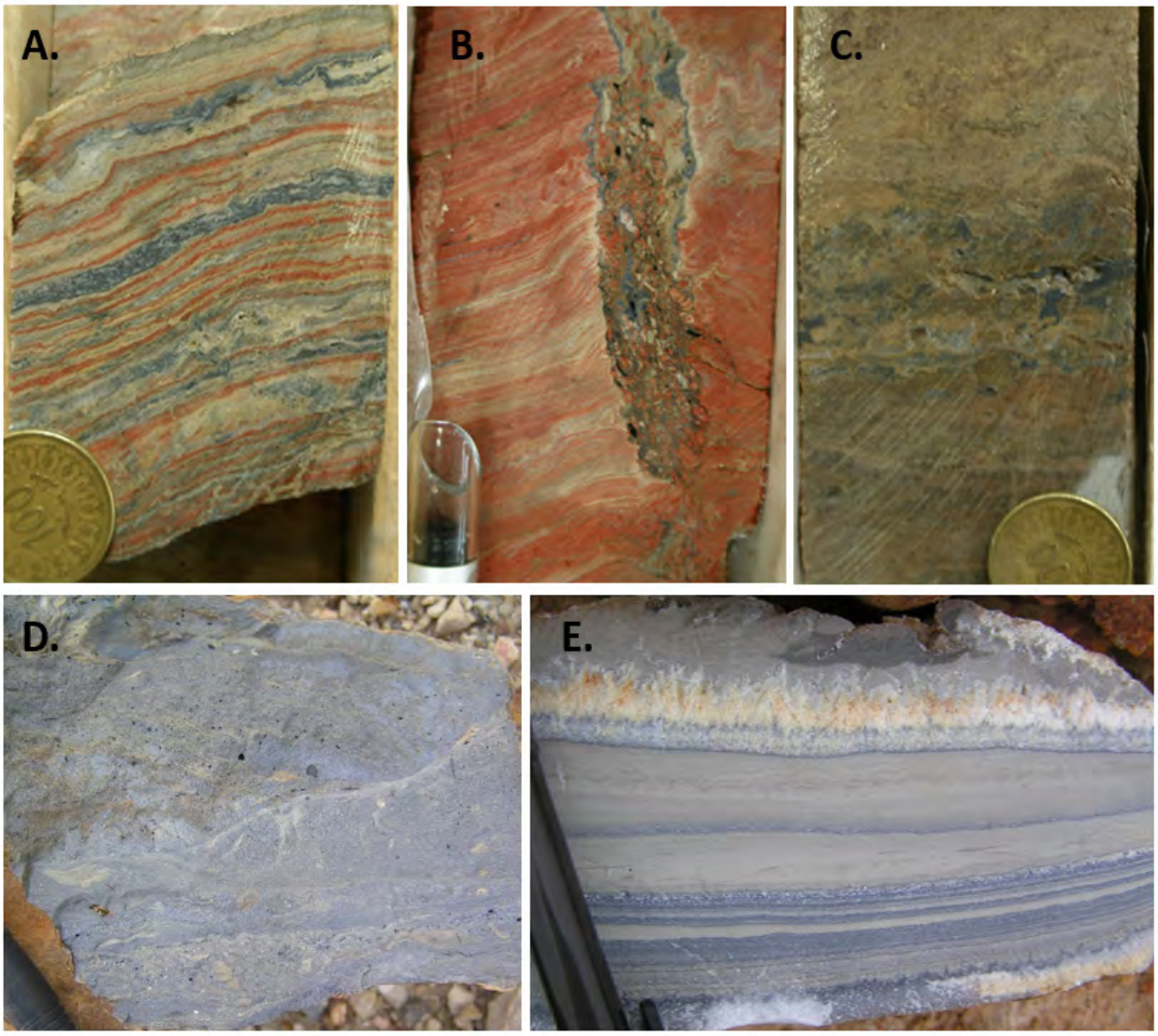

Figure 40: *Bou Aouane: **A).** Laminated algal limestone red bands and small-scale stratabound replacement by galena and very pale sphalerite. **B).** Thinly laminated red algal limestone cut by irregular galena-sphalerite mineralized breccia vein with thin bleached alteration rim; bending and contortion of lamination close to the vein suggests veining before complete lithification. **C)**. High-grade zinc-lead mineralization replacing limestone: pale sphalerite and late galena with some vuggy calcite. **D)**. Very high-grade lead-zinc mineralization replacing breccia, possibly of evaporite-dissolution origin. **E).** Fine-grained silty algal and silty limestone with laminated galena-rich replacement and, at top, bladed barite that appears to grow into and replace fine-grained micrite.*

Mineralization previously worked at Sidi Driss was low grade (c. 3.5% Zn and 1.3% Pb) but drilling has intersected potentially economic grade and thickness, for example 9m at 7.3% Zn and 0.7% Pb. Mineralization shows weakly elevated Ag, As, Sb and Tl. Barite-celestite horizons also occur in the sequence and predate sulphide mineralization (Decrée *et al.*, 2008), and possibly represents hydrothermal alteration of evaporite. Mineralization is characterized by sphalerite and galena with pyrite, which is interpreted to form a lateral and overlying halo to zinc-lead mineralization, and which may have been a precursor to the Tamera supergene iron deposit, which had elevated contents of zinc, lead and arsenic. Mineralization shows replacement and small-scale dissolution and open-space fill textures, replacing calcareous matrix in siliciclastic rocks and disseminated to massive replacement in limestone. Sphalerite is low iron and pale cream to yellowish in colour.

Lead isotope data for Sidi Driss, Douahria, and Djalta shows homogenous signatures with broadly conformable model ages (Decrée *et al.*, 2014; Jemmali *et al.*, 2011) which is compatible with homogenization of lead from the flysch basin. Negative sulphur isotope data from Djalta suggest BSR processes (Jemmali *et al.*, 2011) and similar signature at Sidi Driss with possible biogenic microspherultic textures in sphalerite which are strongly indicative of BSR (Decrée *et al.*, 2008, 2014).

Interpretation

Zinc-lead mineralization in Mio-Pliocene basins of northern

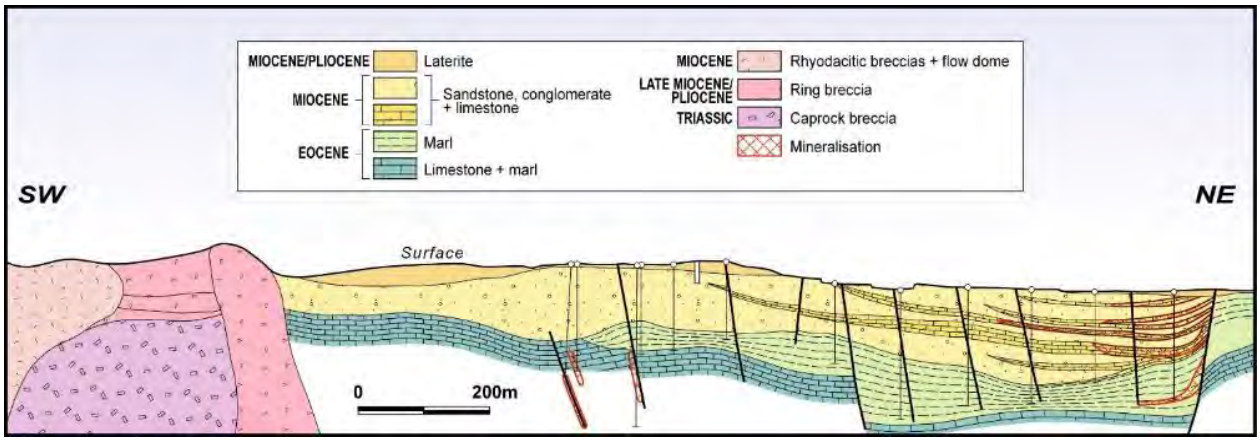

Figure 41: *Long section of the Sidi Driss deposit interpreted from historical sections and drilling. The breccia contact with the Oued Belif complex in the southwest has been interpreted as a structural décollement (Booth-Rea et al., 2018).*

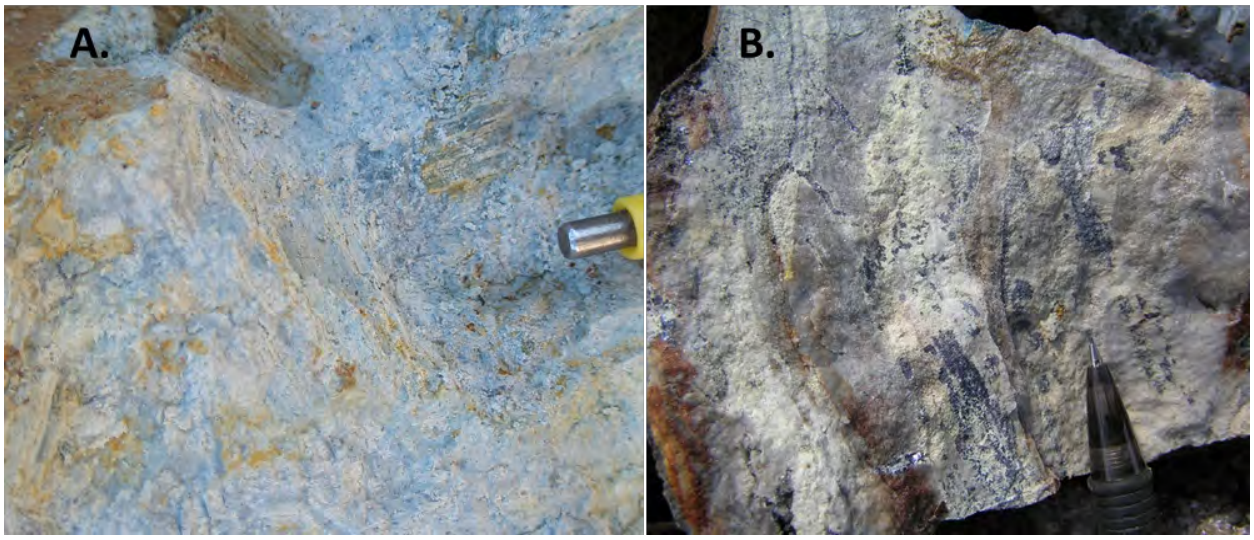

Figure 42: ***A)****. Sidi Driss limestone breccia, possibly of evaporite dissolution origin, with replacive galena and pale sphalerite concentrated in the matrix.* ***B)****. Gantra el Haichichi recrystallized limestone with bedding-parallel replacive galena and pale cream sphalerite.*

Tunisia postdates compressional Atlas deformation and is broadly contemporaneous with a period of extensional collapse and localised bi-modal alkaline magmatism. Although the known deposits are not large, the basins that host the deposits are not large enough to be the source of mineralizing fluids. The tectonically loaded Numidian flysch pile beneath and lateral to the late basins is a more likely source, with fluid flow triggered by the high heat-flow extensional event that followed Atlas thrust stacking. The transcurrent faults that control the basins focused fluid flow, and all the deposits and significant prospects are interpreted to be localised in jogs or fault relays between the major west-northwest and northeast fault sets.

Mineralization was trapped within algal, and probably evaporitic, limestones and calcite-cemented mature siliciclastic rocks. Reduced bituminous limestone and marl is present at Sidi Driss and there is strong evidence for a local sulphur source, possibly evaporitic, and BSR processes. This is compatible with an oxidized or mildly reduced basinal metal-bearing brine and sulphide deposition facilitated by reduction, reaction, and a local sulphur source. This mechanism is less clear at Bou Aouane where the host sequence is more oxidized with limestones commonly reddened. The occurrence of barite and celestite may reflect a local evaporitic source for sulphur, or mineralizing fluids may have been reduced by interaction with migrating hydrocarbons and sour gas.

Other Deposits and Districts

Previous workers have suggested that other carbonate-hosted deposits and districts have affinities with Irish-type rather than MVT deposits. Hitzman (1999) presented Morro Agudo in the Neoproterozoic Bambui Basin in Brazil, Gays River in the Lower Carboniferous of Nova Scotia, and Reocín in the

Cretaceous Basque-Cantabria Basin of northern Spain as examples and suggested other possible examples including Pend Oreille in the Cambrian Metalline district of northwest US, deposits in the Mackenzie platform of western Canada (the Misty Creek embayment of the Selwyn Basin), the Cretaceous of northern Mexico, and the Lower Palaeozoic of Thailand and Myanmar (described here as the Sibumasu Ordovician). A brief commentary about some of these deposits and other possible candidates is provided here.

The Morro Agudo zinc-lead sulphide deposit comprises several stratabound lenses hosted by dolostone interbedded with shaley dolostone, that is interpreted as a cycle boundary where carbonates are overlain by mudstones, located in the hangingwall of a complex fault zone (Misi *et al.*, 2005). The host rock includes oolitic and stromatolitic dolostone overlying dolostone breccia (Aldis *et al.*, 2022). A number of other sulphide zinc-lead deposits, as well as the Vazante willemite (zinc silicate) deposit, occur in the same stratigraphic position, in a sequence interpreted to lie above a Neoproterozoic glacial diamictite. Cordeiro *et al.* (2018) re-interpreted the host rocks as Mesoproterozoic age and proposed a two-stage mineralization event with Mesoproterozoic pyrite and Neoproterozoic zinc-lead mineralization, although invoking a Neoproterozoic seawater sulphur source. The lead isotope data for Morro Agudo data show a tightly constrained distribution compatible with a Neoproterozoic age and basinal metal source.

Recent work on the Yellowhead mineralization at the Cambrian-hosted Pend Oreille (Washington State, USA) deposit includes Re-Os dating of pyrite that supports a diagenetic age for mineralization (Paradis *et al.*, 2020). The replacive Yellowhead mineralization is pyrite-rich and stratabound within dolostones with localised brecciation. These deposits are stratigraphically below the iron-poor Josephine mineralization which occurs in cross-cutting breccias in bedded dolostone and has more typical MVT characteristics (St. Marie and Kesler, 2000).

Pend Oreille occurs within the Kootenay arc, a thrust-imbricated belt of Proterozoic to early Mesozoic metasedimentary and metavolcanic rocks that represents the platform to basin facies transition on the ancestral passive margin of Laurentia. The Cambrian platform carbonates host a number of additional zinc-lead deposits in British Columbia, extending north to the Quesnel Lake district (Paradis *et al.*, 2016). The same platform environment extends north to the Mackenzie platform on the eastern margin of the long-lived Selwyn Basin, well known for its substantial SHMS endowment of Upper Cambrian (Anvil), Lower Silurian (Howards Pass), and Upper Devonian (Macmillan Pass, Akie, Cirque) (Leach *et al.*, 2005). The Palaeozoic sag phase of the Selwyn Basin followed a thick Neoproterozoic rift sequence, although the sag phase platform remained tectonically unstable with significant extensional events and associated volcanism. The Mackenzie platform contains a number of carbonate-hosted zinc-lead deposits, generally described as MVT, within Neoproterozoic (Gayna River), Cambrian (Goz Creek, Monarch, Kicking Horse), and Silurian-Devonian (Robb Creek, Bear-Twit, Prairie Creek) carbonate rocks and associated with dolomitization (Paradis *et al.*, 2007). Stratabound replacive mineralization at the Prairie Creek deposit occurs in Ordovician-Silurian dolostone of the same age as the Howards Pass SHMS deposit and shows a similar lead isotope signature and similar sulphur isotope ratios indicative of TSR (Paradis, 2007).

The potential connection between the carbonate-hosted deposits of the Mackenzie Platform and the SHMS deposits of the Selwyn Basin has been previously recognized and formation of the carbonate-hosted deposits within the same syn-basinal fluid system has been proposed for Prairie Creek by Paradis (2007) and for other Cordilleran deposits including Robb Creek by Nelson *et al.* (2002). The Pend Oreille deposit is located in an analogous position on the ancestral North American margin and can be considered in the same context. The reinterpretation of Howards Pass (Gadd *et al.*, 2015) and Macmillan Pass (Magnall *et al.*, 2020) as syn-diagenetic replacement deposits also implies greater uncertainty in mineralization age ranges and increases the scope for different deposit types to form from the same, long lived, basinal fluid system in host rocks over a significant range in host rock ages.

The Gays River deposit in Nova Scotia was extensively studied in the 1980s and 1990s but this research has not been updated. Geological setting, localisation on a basin palaeohigh, temperature of mineralization, and isotopic characteristics are compatible with an early basinal fluid system tapping underlying siliciclastic sequences in the Visean, broadly analogous to the Irish Midlands.

Reocín and other late Aptian-hosted deposits in the Basque-Cantabrian Basin are generally interpreted to be of MVT affinity. The Basque-Cantabrian Basin accumulated at least 14 kilometres of Mesozoic sedimentary rocks in its deeper parts following initial Triassic rifting, a Jurassic sag phase, renewed major extension in the Aptian-Albian on the Atlantic passive margin, and slower subsidence in the Upper Cretaceous to Palaeogene (Gomez *et al.*, 2002). Inversion commenced in the southern basin in the early Eocene, culminating in full inversion and thrusting in the late Eocene to early Oligocene Pyrenean orogeny. The Aptian-Albian saw break-up of the platform and deposition of the Urgonian platform carbonates on fault-controlled intra-basin highs. At Reocín, cavity-fill and replacement mineralization is hosted in upper Aptian clean platform carbonates overlain by Albian mixed carbonate and siliciclastic rocks and predominantly siliciclastic Cenomanian rocks (Velasco *et al.*, 2003). Albian to Santonian alkaline volcanism is related to extensional faulting in the central domain of the basin (Castañares *et al.*, 2001). Mineralization is associated with a second stage of hydrothermal ferroan dolomitization and is interpreted to result from mixing of metalliferous basinal fluids with reduced sulphur-bearing brines (Velasco *et al.*, 2003), with fluid-inclusion chemistry indicating an evaporated brine origin (Grandia *et al.*, 2003). Based on isotopic signature, Velasco *et al.* (1996) interpreted a homogenized metal source in Palaeozoic sedimentary rocks for lead in Reocín, and a distinct less radiogenic source in the eastern part of the basin for the la Troya deposit.

The Basque-Cantabrian deposits show many similarities with the Irish Midlands, however the age of mineralization relative to sedimentation is generally interpreted to be substantially younger. Mineralization at Reocín is post-early Cenomanian in age, based on dolomitization of carbonates. Symons *et al.* (2009) interpreted a middle Miocene age for Reocín based on palaeomagnetic data. Perona *et al.* (2018) interpreted a

Campanian or older age for mineralization close to the Murguía and Orduña diapirs based on relationships with Albian to Campanian halokinesis in the basin. Velasco *et al.* (2003) interpreted a Palaeocene age which would coincide with early inversion in the basin. The bimodal lead isotope data indicate different sources in the eastern and western parts of the basin. The less radiogenic lead signature at la Troya is compatible with an Upper Cretaceous age, but this would imply an anomalously radiogenic source area for Reocín, or a younger age despite the similarity of the deposits.

The Mesozoic of Iran is host to multiple carbonate-hosted zinc-lead deposits, many in Aptian-Albian (Lower Cretaceous) platform carbonates, and mostly described as MVT deposits. Mehdi Abad is the largest deposit with a reported 'global resource' of about 218 Mt at 7.2% Zn, 2.3% Pb, and 51 g/t Ag (Magfouri *et al.*, 2016), hosted in platform carbonates deposited on the Yazd block of the Central-East Iranian Microcontinent. The platform was tectonically unstable with syn-sedimentary faulting and sub-basins with deep water carbonate and clastic deposition, accompanying oceanic rifting of the Sistan-Sabzevar ocean to the north in a broadly back-arc setting relative to the northward-subducting Neotethys to the south (Wilmsen *et al*., 2014). The largest sulphide-dominant bodies are hosted in a shallow water organic-rich sequence of mudstone, dolostone, and silty limestone of the Aptian Taft Formation. Sulphide mineralization forms stratabound replacive tabular bodies and breccias at two main horizons, interpreted to be related to the synsedimentary Black Hill Fault (Song *et al.*, 2017; Khan Mohammadi, *this volume*). Sulphide mineralization comprises sphalerite, galena, pyrite, minor chalcopyrite, and barite with associated ferroan dolomite or siderite alteration. The main stage of zinc-lead mineralization replaces earlier barite which contains minor chalcopyrite. Significant contents of silver, arsenic and antimony occur in oxide and sulphide mineralization (Reichert *et al.*, 2003). The setting, geometry, syn-diagenetic replacement textures, chemistry, and hydrothermal carbonate alteration suggest that the deposit should be considered as an Irish-type deposit, although it has also been previously described as 'SedEx'.

The Nanisivik zinc-lead deposit in the Canadian Arctic is hosted within Mesoproterozoic carbonates bordering the Borden Basin, interpreted as an 'impactogen' related to far-field stress accompanying Grenvillian orogeny and assembly of Rodinia (Turner *et al.*, 2016). The deposit is dominated by replacement of dolostone with less open-space fill, and pyrite replacement is much more extensive than zinc-lead mineralization (Patterson and Powis, 2002). The deposit is hosted in deep water laminated dolomicrite and coarse intraclastic dolostone, laterally equivalent to platform carbonates on fault controlled inter-basin highs, and disconformably overlain by reduced shale (Turner, 2011). The age of mineralization is constrained to slightly younger than the host rocks by broadly coincident Re-Os pyrite (Hnatyshin *et al.*, 2016), palaeomagnetic (Symons *et al.*, 2001) and Rb-Sr sphalerite (Christensen *et al*., 1993) ages. The setting and age suggest a mineralization event following extensional faulting in the basin and accompanying hydrocarbon migration, which has been invoked as a trapping mechanism (Turner, 2011), with fundamental similarities to the Irish Midlands deposits.

Discussion

Of the deposits and districts presented here, none are direct analogues for the 'type' deposits of the Irish Midlands, such as Navan, Lisheen and Silvermines. On this basis, we could conclude that Irish-type deposits are unique to the Irish Midlands. However, there is substantial variety in the deposits of the Irish Midlands, though formed within the same mineral system, and there are significant analogies between the Irish Midlands mineral system and the districts summarized in this overview. Applying the approach used in the petroleum industry, understanding the system is the foundation for targeting of discrete plays within that system. This is the preferred approach to understanding and targeting deposits formed in sedimentary basins.

Applying this approach, it is instructive to consider the empirical characteristics of Irish-type systems, the controls on these characteristics, and the implications for exploration from a basin selection to target (or play) scale. These characteristics can be addressed under the key components of a basinal mineral system: source (metals, sulphur, ligands, and fluid reservoir), transport trigger and driver (geodynamic), pathway (basin architecture), focus (trend-scale architecture), and trap.

In this context, there are substantial similarities, but also important differences, between Irish-type systems developing early in basin history and MVT systems formed later in orogens and orogenic forelands. Considering and naming the systems separately is warranted because the differences have implications for exploration, evaluation, and economic characteristics. It is also significant that the Irish-type mineral systems show substantial overlap with SHMS systems at a basin scale, and that some of the deposits described here have been previously described as SHMS deposits.

Irish-type and SHMS mineral systems require a large-scale hydrothermal fluid flow event in a rift-sag basin, typically occurring early in the sag phase. The classic MVT mineral systems, such as Viburnum, reflect large-scale fluid flow events during orogenic compression and uplift which postdates lithification of the host rocks and is normally much later in the history of the host basin. A rift-sag basin that is fertile for Irish-type or SHMS deposits may have remained intracratonic but more often evolved to a passive margin and may have undergone multiple rift-sag-inversion events. The scale of the rift basin must result in burial and heating of a large source volume of immature siliciclastic rocks to a level of maturity where metals are leached into basinal brines during progressive diagenesis. A homogenized metal source is indicated by the coherent lead isotope signature in Irish-type and SHMS deposits, with a model age close to sedimentation age. Empirically, deposits are associated with rifts that are over four kilometres thick, and with basin scale of hundreds of kilometres. Burial of the source sediments to depths greater than four kilometres suggests that metal maturity occurs at temperatures over 150°C, mostly above the hydrocarbon window of c. 80-160°C. Most fertile basins have evidence for volcanism in the rift phase, and maturity in high heat-flow basins may be reached at shallower depths.

Extraction and focused transport of metals to the overlying or lateral sag-phase platform requires large-scale fluid-flow.

Feature	Irish-type	MVT
Temperature	100-250ºC	80-150ºC
Age	Neoproterozoic to Phanerozoic	Palaeoproterozoic to Phanerozoic
Alteration	Dolomite, ferroan dolomite, ankerite	Dolomite (ferroan dolomite)
Zonation	Feeder zone Cu, Zn/Pb increase proximal to distal, distal Ba	Weakly zoned Zn/Pb increases proximal to distal
Major metals	Zn Pb Fe Ag (Cu Ba)	Zn Pb (Cu)
Associated element enrichment	Mn Sb As Tl (Ni Co)	Ag Cd Ge# Ga Cu In*
Host lithostratigraphy	Shallow to deep water mixed carbonate-clastic sequences	Clean shelf limestone sequences
Host Rocks	Clean or reduced limestones, micritic limestone	Clean limestone
Geometry	Single stratabound body or stacked lenses, good stratabound continuity	Irregular and discontinuous bodies, multiple zones, stratabound and cross-cutting
Style	Replacement, hydrothermal breccia, minor open-space fill	Open-space fill, breccia and palaeokarst, minor replacement+
Setting	Rift-sag basin, base of sag phase, passive margin or intracratonic basin	Passive margin to intracratonic basin in the foreland of a convergent margin.
Controls	Structural (fault) and stratigraphic	Stratigraphic, structural (joint ± fault) and palaeokarst
Lead isotope systematics	Broadly conformable model age and homogenous signature	Anomalously radiogenic and inhomogeneous signature
Sulphur isotope systematics	BSR or TSR	TSR
Zn/Pb ratio[1]	4	2.5
Contained Zinc kt[1]	1,536	230
Zn Grade[1]	7.9	4.9
Pb Grade[1]	2.2	2.8

Table 2 *Typical characteristics of Irish-type and MVT deposits*

*[1]Median of resource data from Penney et al. (2001). * See Leach et al. (2010) for a comprehensive list of trace elements present in selected carbonate-hosted deposits. # Holl et al. (2007). + Note that in huge systems such as Viburnum, replacement is a major form of mineralization.*

Moderately saline, weakly acidic basin brines are identified as the metal carrying fluids in many systems and show halogen signatures indicating that evaporated brines have been entrained in the basins from marginal shelves (Leach *et al.*, 2005; Emsbo, 2009). Carbonate shelves imply a low latitude setting favourable for marginal evaporative environments, interpreted to be a fundamental prerequisite for a fertile basin. Mineralizing fluids may be oxidizing or mildly reducing, which is interpreted to reflect the composition of the basinal sediments (Cooke *et al.*, 2000).

The trigger for large-scale fluid flow is interpreted to be an extensional or inversion event. In the Irish Midlands, mineralization follows major extension on the carbonate platform and overlaps with alkaline mafic volcanism in the Limerick Basin where magmatic heat has been postulated as an important driver for fluid circulation (Wilkinson & Hitzman, 2015). This may be a factor in the unique endowment of the province, where fluids are believed to have sourced metals largely from the older underlying flysch sedimentary rocks. In most of the districts described here, mineralization is interpreted to coincide with early extensional events, with or without volcanism.

Fluid flow in a basin will be focused by the rift architecture, where sub-orthogonal accommodation zones compartmentalize rift-bounding faults, control the distribution of sedimentary facies, including potential aquifers, and provide the basin-scale pathways towards basin-highs and platforms. When fluids enter the platform, other factors may play a role in fluid focus, including clastic and dolomitization aquifers, aquicludes, faults and pinch-outs. Empirically, for example in the Irish Midlands (Kyne *et al.*, 2020), the association between deposits

and fault relays and cross faults suggest that cross-stratal permeability provided by these structures is a critical factor in the creation of deposits. Irish-type deposits forming in tectonically active basin settings typically show a strong direct control by both faulting and lithology, as is exemplified by the Irish Midlands but also a feature of some lower temperature systems like the Lennard Shelf. This results in the typical Irish-type tabular stratabound geometry zoned away from a feeder structural zone.

Unlike hydrocarbon systems, mineral deposit formation requires that metal is effectively extracted from fluids that pass through the trap site and escape. Even within the same mineral system, trap controls may be quite different, as exemplified by the Lennard Shelf (Reynolds & Copp, 2017b). However, trap settings and mechanisms have broad similarities across Irish-type deposits and share many characteristics with MVT deposits.

Different fluid chemistries have been considered for metal transport (Giordano, 2002), but in most cases sulphide deposition is interpreted to result from the interaction of an oxidized or mildly reduced sulphur-poor acidic brine, carrying metals as chloride complexes, with a separate sulphur source. For a reduced metalliferous brine, low sulphur content is a prerequisite and fluid mixing with a sulphur-bearing fluid is essential for metal precipitation as sulphide (Zhong *et al.*, 2015). The local availability of sulphur is therefore a key trapping mechanism in most systems, combined with reaction and neutralization by carbonate rocks, and reduction of oxidized brines through interaction with hydrocarbons or reduced host rocks. Reduced sulphide may be generated by TSR, which requires temperatures above 100°C, or BSR which largely ceases above 80°C (Machel, 2001). BSR is the predominant sulphur reducing mechanism in the Irish Midlands and may be an important factor in optimum metal deposition to generate large, continuous deposits (Wilkinson & Hitzman, 2015; Ashton *et al.*, 2015). TSR is the predominant process in most SHMS and MVT deposits (Leach *et al.*, 2005).

The typical tabular geometry of Irish-type deposits may partly reflect favourable host lithology, but local hydrological conditions may also be an important factor. For example, the dense brines entering the dolomitized Waulsortian aquifer at Lisheen appear to have hugged the bottom of the aquifer and probably mixed with overlying evaporated seawater-derived fluids carrying BSR sulphur.

Conclusions

Mineral systems in sedimentary basins generate SHMS and Irish-type zinc-lead deposits early in basin history and classical MVT deposits much later in the host basin history during orogenesis and uplift. The fluid systems and fluid focus are therefore very similar in SHMS and Irish systems, but the deposit setting and trap environment is quite different for Irish-type deposits and shares some attributes with MVT trap settings. As a result, some deposits in the Irish-type spectrum show deposit-scale features similar to MVT deposits, though formed in a distinctly different type of mineral system. However, because of the differences between Irish-type and MVT systems and their timing, Irish-type deposits tend to form at relatively high temperatures, involve BSR and/or TSR, are dominated by replacement processes, show strong structural control, and form laterally continuous tabular replacement geometries. In contrast, MVT systems are typically lower temperature, involve TSR, are dominated by open-space fill, show limited structural control, and form irregular geometries often related to pre-existing palaeo-karst. The generalized, but by no means universal, features of Irish-type and classical MVT systems are tabulated in Table 2.

The mineral systems and deposits presented here illustrate the range and variability of mineralization that can occur within carbonate-hosted mineral systems formed early in basin history, whether we care to call them Irish-type or MVT. At one end of the spectrum, the Lennard Shelf deposits have always been described as MVTs, formed at low temperatures of 80-100°C, and include hydrothermal karst-fill deposits, massive replacement deposits, and fault-hosted deposits. The Admiral Bay deposit has also been described as MVT but is localised by a major fault zone, is dominated by replacement mineralization, shows fluid inclusion temperatures up to 156°C, and has a homogenous lead isotope signature with a broadly conformable model age. The deposits in the Ordovician carbonates of the Sibumasu terrane are deformed and metamorphosed, and attribution to an Irish-type system is based on broad characteristics in the absence of direct data on timing and fluids. The deposits are stratabound replacive, show probable fault control, and have a homogeneous lead isotope signature throughout the belt with a broadly conformable Lower Ordovician model age. Interestingly, the deposits are of similar age and have a similar lead isotope composition to Admiral Bay, and both systems were located in the northwest Australian part of Gondwana in the Ordovician.

The Alpine and Hakkâri deposits are hosted by Upper Triassic carbonates and formed during Neotethyan extension. Bleiberg shows fault control, stratabound replacement geometry, BSR sulphur isotope signature, and homogenous conformable lead isotope signature. The Hakkari deposits are strongly stratabound, have a lead isotope signature that overlaps the Alpine deposits, and have a sulphur isotope signature that is higher than the Alpine deposits but probably also represents BSR. Fault control is inferred at Hakkari but not demonstrated. The Duddar deposit is located in a very similar geological environment but accompanying younger late Triassic to Jurassic rifting between India and Arabian Gondwana. The deposit replaces shallow-water carbonates overlain by sedimentary breccias deposited in a fault-controlled basin, and mineralization is interpreted to be syn-diagenetic. The Alpine and Hakkari deposits are hosted in reduced sequences with evaporitic aspects within a regional sequence of platform carbonates. Duddar is hosted within a similar reduced unit capped with a sequence of mass-flow lithologies and argillaceous limestone.

The mineralization in the Coastal Basin of Gabon is at an early stage of evaluation. Interpretation of an Irish-type affinity is based on basin setting, evidence for early mineralization timing, and fault control. Additional work is required on this interesting passive-margin setting to understand the potential for large Irish-type or SHMS deposits. Similarly, the Miocene basins in the Atlas orogen have had limited evaluation but may have significant potential and show interesting similarities in setting and host rocks with the giant Jinding and Huoshaoyun zinc-lead deposits in China, hosted by Cenozoic intra-orogenic basins in the Himalayan orogen.

Effectively, carbonate-hosted deposits can be broadly sub-divided into those within basins where mineralization is unrelated to evolution of the host basin, including the classic MVT deposits from the interior basins of the USA and Canada such as the Viburnum Trend and Pine Point, and deposits whose development is linked directly to the evolution of the host basin. The latter are commonly situated near major basin architecture fault systems that separate a platform from a deep basin or rift, or on a platform that was cut by syn-sedimentary faults. This group includes the Irish Midlands deposits and can be broadened to encompass a global diaspora of 'Irish-type' deposits whose style varies depending on trap setting and system geodynamics and temperature. This diaspora ranges from low temperature replacement and open-space filling deposits of the Lennard Shelf to slightly hotter late diagenetic replacement deposits like Admiral Bay, Reocín and Nanisivik, to replacement deposits trapped in reduced facies like Bleiberg and Hakkari, to deposits such as Duddar and Mehdi Abad localised in fault-controlled platform sub-basins, to deposits in late orogenic successor basins like the Tunisian Atlas and potentially Jinding. The variability within these two groups depends on factors such as heat, the nature of the host rock and the degree of tectonism, where the Irish-type deposits tend to be higher temperature and more structurally controlled than the MVT deposits, and predominantly replacive rather than open-space fill, but due to the inherent variability of sedimentary basins can have characteristics in common with low temperature, structurally controlled mineralization like the Lennard Shelf

The implications of this mineral system approach and classification are significant for assessment of basin fertility, for targeting within basins, and for understanding the style and economic characteristics of the deposits that are likely to be found within specific basins and platforms. Criteria for basin fertility are largely shared between Irish-type and SHMS systems, such that basins with known SHMS deposits should have potential for Irish-type deposits, and vice versa. Examples of basins known to contain both deposit types include the Selwyn Basin (Howards Pass, Macmillan Pass and deposits in the Mackenzie platform including Prairie Creek); the Franklinian Basin (Citronen Fjord and Polaris); and possibly the McArthur Basin (HYC and the Cooley, Ridge and Coxco deposits). On the other hand, MVT-bearing basins fringed with foreland-type orogenic settings are likely to have little potential for SHMS or Irish-type deposits.

Targeting criteria within basins at a trend to deposit scale show less overlap between Irish-type and SHMS deposits due to the different geological environment, but large-scale structural criteria are largely shared. Within carbonate platforms, the approach to targeting Irish-type deposits should focus much more on structural architecture and favourable carbonate units than is the case for MVT deposits which are typically hosted in more uniform thicker carbonate sequences with less structural influence on sedimentary facies and on mineralization. Hydrocarbon can play a role in trapping of all these deposit types.

The Irish-type spectrum encompasses deposits that can be high-grade and form large tabular bodies that are economically attractive for mining. Irish-type deposits usually have favourable metallurgy with good recoveries and low-iron sphalerite resulting in high-grade concentrates. However, Irish-type concentrates can have elevated levels of deleterious elements including arsenic, antimony, mercury and thallium. MVT deposits are typically lower grade, more irregular and discontinuous, and less favourable for mining, however metallurgy is inevitably favourable with high quality zinc concentrates and low deleterious element content. Some Irish-type deposits share these MVT characteristics, and understanding the factors within the Irish-type spectrum that favour development of the most economically favourable deposits is important, potentially including system temperature and availability of abundant reduced sulphur through BSR.

Most importantly, as recognized by many previous reviews of low-temperature carbonate-hosted mineralization, these deposits show enormous variability regardless of how we attempt to classify them. A mineral system approach to targeting can factor in this variability and recognise that deposits that look different can form in the same type of mineral system, whereas deposits that look the same can form in different types of mineral system. Additionally, mineral systems, and especially plays within the mineral system, vary from basin to basin. Targeting in each basin should be based on understanding developed in that basin, in the context of a broader system model, rather than on attempting to classify deposits that defy easy classification.

References

Ahsan, S.N., & Qureshi, I., (1997) Mineral/rock resources of Lasbela and Khuzdar Districts, Balochistan, Pakistan. Geological Bulletin University of Peshawar 30, p. 41-51.

Akande, S. & Zentilli, M., (1984) Geologic, fluid inclusion, and stable isotope studies of the Gays River lead-zinc deposit, Nova Scotia, Canada. *Economic Geology* v.79, p. 1187-1211.

Aldis, C., Olivo, Gema. R., Arruda, Jessica, A.A.C. & Cevik, Ilkay, S., (2022) Proterozoic carbonate-hosted Morro Agudo sulfide Pb-Zn district, brazil: Mineralogical and geochemical evidence of fluid mixing during the ore stage. *Ore Geology Reviews* v.141, p. 1-25.

Allen, R.M. (1994) Final Report. Geology of the Duddar zinc-lead deposit. Duddar pre-feasibility study: United Nations Development Program (Project PAK/89/034)., unpublished report. In Allen, R. M., Gauthier, F., Jones, G. V., and Bhutani-Singh. 1994. Duddar. Prefeasibility study: UNDDSMS. New York. 5 volumes.

Allen, R.M. & Anwar, J., (1994) Geological setting of Duddar zinc-lead deposits: An exploration model for the Lasbela-Khuzdar belt. in Khan, A.U., Huda, Q. and Husain, V. (eds.) Proc. 2nd Soc. Econ. Geol. Mineral. Tech. (SEGMITE) Intern. Conf. on Industrial Minerals, p. 64-71.

Arain, A., Shakoormastoi, A., Ashgar, A., Hakro, R.A., Alias, D., Jamali, M.A., Bhatti, G.R., & Bhatti, W. (2021) A preliminary review on the metallogeny of sediment-hosted Pb-Zz deposits in Balochistan, Pakistan, *Earth Sciences Malaysia* v.5, p.19-26.

Ashton, J.H., Blakeman, R.J., Geraghty, J.F., Beach, A., Coller, D., & Philcox, M.E., (2015) The Giant Navan carbonate-hosted Zn–Pb deposit – A review, in Current Perspectives on Zinc Deposits, Archibald, S.M., Piercey, S.J., eds., *Irish Association for Economic Geology, Dublin, Ireland*, p. 85–122.

Azizi, R. & Chihi, L., (2021) Neogene basin of Northern Tunisia: new evidence of graben structures along E–W shear zone and geodynamic implications, *International Journal of Earth Sciences* v.110, p.2755–2778,

Bechstadt, T. (1979) The lead-zinc deposit of Bleiberg-Kreuth (Carinthia, Austria): palinspastic situation, paleogeography and ore mineralisation. *Verhandlungen Geologische Bundesanstalt Wien*, 1978, p. 221-235.

Belguith, Y., Geoffroy, L., Rigane, A., Gourmelen, C., & Ben Dhia, H., (2011) Neogene extensional deformation and related stress regimes in Central Tunisia. *Tectonophysics*, v.509(3-4), 198–207.

Beltrán-Triviño, A., Winkler, W., von Quadt, A., and Gallhofer1, D., 2016. Triassic magmatism on the transition from Variscan to Alpine cycles: evidence from U–Pb, Hf, and geochemistry of detrital minerals. *Swiss Journal of Geosciences* v.109.

Bender, F., (1983) Geology of Burma. Berlin: Gebruder Borntraeger, 299 pp.

Blevings, S., Kraft, J., Stemler, J., & Krolak, T., (2013) An overview of the structure, stratigraphy, and Zn-Pb-Ag deposits of the Red Dog District, northwestern Alaska, in Colpron, M., et al., eds., Tectonics, metallogeny, and discovery: The North American Cordillera and similar accretionary settings: *Society of Economic Geologists Special Publication* 17, p. 361–387.

Boast, A.M., Coleman, M.L. & Halls, C, (1981) Textural and stable isotopic evidence for the genesis of the Tynagh base metal deposit, Ireland. *Economic Geology*, v.76, p. 27–55.

Booth-Rea, G., Gaidi, S., Melki, F., & Marzougui, W., (2018) Late Miocene extensional collapse of northern Tunisia. Tectonics 37, p.1626–1647.

Bouhlel, S., Garnit, H., & Bejaoui, J., (2013) Lead isotopes signatures of the MVT lead-zinc (±F) deposits across Central-North Tunisia: Evidence for the heterogeneity in uranium component of the underlying source rocks. In, Jonsson et al. (eds.), Proceedings of the 12th Biennial SGA Meeting, Mineral deposit research for a high-tech world, Uppsala, Sweden. ISBN 978-91-7403-207-9. 1882 pp.

Bouabdellah, M., Sangster, D., Leach, D., Brown, A., Johnson, C., & Emsbo, P., (2012) The Touissit-Bou Beker Mississippi Valley-Type District of Northeastern Morocco: Relationships to the Messinian Salinity Crisis, Late Neogene-Quaternary alkaline magmatism, and buoyancy-driven fluid convection. *Economic Geology* v.110, p.1455-1484.

Boyce, A.J., (1990) Exhalation, sedimentation and sulphur isotope geochemistry of the Silvermines Zn + Pb + Ba deposits, County Tipperary, Ireland: Unpublished Ph.D. thesis, Glasgow, U.K., University of Strathclyde, 354 pp.

Boyce, A.J., Coleman, M. L., & Russell, M. J., (1983) Formation of fossil hydrothermal chimneys and mounds from Silvermines, Ireland. *Nature* v.306, p.545–550,

Bradley, D. & Leach, D., (2003) Tectonic controls of Mississippi Valley-type lead–zinc mineralization in orogenic forelands. *Mineralium Deposita* v.38, p.652-667.

Brannon, J.C., Podosek, F.A., & Cole, S.C., (1996) Radiometric dating of Mississippi Valley-type ore deposits. In: Sangster D.F. (ed), Carbonate-hosted lead-zinc deposit. *Soc Econ. Geol. Spec Publ* v.4, p.546-554.

Brigo, L. & Omenetto, P., (1978) The lead and zinc ores of the Raibl (Cave del Predil-Northern Italy) Zone: new metallogenic data. *Verhandlungen Geologische Bundesanstalt Wien*, 1978, p. 241-247.

Brigo L., Kostelka L., Omenetto P., Schneider H.J., Schroll E., Schulz O., & Strucl I., (1977) Comparative reflections on four alpine Pb-Zn deposits. In: Klemm D.D., Schneider H.J. (eds), Time and strata-bound ore deposits. Springer-Verlag, Berlin, p. 273–293.

Brownfield, M.E. & Charpentier, R., (2006) Geology and total petroleum systems of the West-Central Coastal province (7203), West Africa. *USGS Bull* 2207-B.

Castañares, L.M., Robles, S., Gimeno, D., & Vicente Bravo, J.C., (2001) The submarine volcanic system of the Errigoiti Formation (Albian-Santonian of the Basque-Cantabrian Basin, northern Spain): stratigraphic framework, facies, and sequences, *Journal of Sedimentary Research* v.71, p. 318–333,

Cerny, I. (1989) Current prospecting strategy for carbonate-hosted Pb-Zn mineralizations at Bleiberg-Kreuth (Austria). *Economic Geology* v.84, p. 1430-1435.

Ceyhan, N., (2003) Lead isotope geochemistry of Pb-Zn deposits from eastern Taurides, Turkey. M.Sc. thesis, Graduate School of Natural and Applied Sciences, Middle East Technical University, 90 pp.

Charusiri, P., Daorerk., V., Archibald., D., Hisada, K., & Ampaiwan, T., (2002) Geotectonic evolution of Thailand: A new synthesis, *Journal of the Geological Society of Thailand*, 1-20.

Chauvet, F., Lapierre, H., Maury, R.C., Bosch, D., Basile, C., Cotton, J., Brunet, P., & Campillo, S., (2011) Triassic alkaline magmatism of the Hawasina Nappes: post-breakup melting of the Oman lithospheric mantle modified by the Permian Neotethyan plume, *Lithos* v.122, p.122-136

Chen, A., Jin, C., Lou, Z., Chen, H., Xu, S., Huang, K., & Hu, S., (2013) Salt tectonics and basin evolution in the Gabon Coastal Basin, West Africa. *Journal of Earth Science* v.24, p. 903–917.

Christensen, J.N., Halliday, A.N., Kesler, S.E., & Sangster, D.F., (1993) Further evaluation of the Rb-Sr dating of sphalerite: the Nanisivik Precambrian MVT deposit, Baffin Island, Canada [abs.]: *Geological Society of America Abstracts with Programs* v. 25, p.471.

Clayton, C.J., & Baird, A.W., (1997) Fluid flow, Pb-Zn mineralization, hydrocarbon maturation and migration in the Tunisian Atlas [ext. abs.]: Geofluids II '97, *International Conference on Fluid Evolution, Migration, and Interaction in Sedimentary Basins and Orogenic Belts, 2nd, Extended Abstracts*, p. 457-460.

Cooke, D. R., Bull, S.W., Large, R.R., & McGoldrick, P.J., (2000) The importance of oxidized brines for the formation of Australian Proterozoic stratiform sediment-hosted Pb-Zn (Sedex) deposits. *Economic Geology* v.95, p.1–18.

Cordeiro, P.F.O., Oliveira, C.G,. Paniago, L.N., Romagna, G., & Santos, R.V., (2018) The carbonate-hosted MVT Morro Agudo Zn-Pb deposit, central Brazil. *Ore Geology Reviews*v. 101, p.437–452.

Decrée, S., Marignac, C., De Putter, Th., Deloule, E., Liégeois, J.P., & Demaiffe, D., (2008) Pb–Zn mineralization in a Miocene regional extensional context: The case of the Sidi Driss and the Douahria ore deposits (Nefza mining district, northern Tunisia). *Ore Geology Reviews* v.34, p.285–303.

Decrée, S., Marignac, C., Liégeois, J-P., Yans, J., Ben Abdallah, R., & Demaiffe, D., 2014. Miocene magmatic evolution in the Nefza district (Northern Tunisia) and its relationship with the genesis of polymetallic mineralizations. *Lithos* v.192–195, p.240–258.

Dewing, K., Turner, E. & Harrison. (2007) Geological history, mineral occurrences and mineral potential of the sedimentary rocks of the Canadian Arctic Archipelago, in *Geological Association of Canada, Mineral Deposits Division, Special Publication* No. 5, p733-754

Diehl, P.& Kern, H., (1981) Geology, mineralogy and geochemistry of some carbonate-hosted lead-zinc deposits in Kanchanaburi Province, western Thailand. *Economic Geology* v.76, p. 2128-2146.

Dörling, S.L., Dentith, M.C., Groves, D.I. & Vearncombe, J.R., (1995) Extensional, synsedimentary deformation and compaction-driven fluid-flow: an alternative mechanism for MVT deposit formation on the Lennard Shelf, Western Australia [abstract]. *Society of Economic Geologists, International Field Conference on Carbonate-Hosted Lead-Zinc Deposits, St Louis, Missouri*, 76-80.

Dörling, S.L., Groves, D.I. & Muhling, P., (1998) Lennard Shelf Mississippi Valley-type (MVT) Pb–Zn deposits, Western Australia, *AGSO Journal of Australian Geology and Geophysics*, v.17, p. 115–120.

Dzulynski, S., & Sass-Gustkiewicz, M., (1985) Hydrothermal karst phenomena as a factor in the formation of Mississippi Valley type deposits. In: Wolf, K.H. (Ed.), Handbook of Strata Bound and Stratiform Ore Deposits, Elsevier, Amsterdam, 13: p. 391-439.

Elliott, H.A.L., Gernon, T.M., Roberts, S., Boyce, A.J. & Hewson, C., (2019) Diatremes Act as Fluid Conduits for Zn-Pb Mineralization in the SW Irish Ore Field. *Economic Geology* v. 114, p. 117–125.

Emsbo, P., (2009) Geologic Criteria for the Assessment of Sedimentary Exhalative (Sedex) Zn-Pb-Ag Deposits. *U.S. Geological Survey Open-File Report* 2009−1209, 21 p.

Erik, N.Y., Özçelik, O., Altunsoy, M., & Illeez, H.I., (2005) Source-rock hydrocarbon potential of the Middle Triassic—Lower Jurassic Cudi Group units, eastern Southeast Turkey, *International Geology Review*, v.47, p.398-419,

Etminan, H., McCracken, S. R., Jaireth, S., & Ferguson, J., (1995 Geology and genesis of Admiral Bay Fault carbonate hosted Zn-Pb deposit (Canning Basin, Western Australia), in Leach, D. L., and Goldhaber, M. B., *International Field Conference on Carbonate Hosted Lead-Zinc Deposits, St. Louis. Missouri, Extended Abstracts*, p. 73-75.

Ferguson, K.M., (1999) Lead, zinc and silver deposits of Western Australia. Geological Survey of Western Australia. *Mineral Resources Bulletin* v.15.

Fernández, O., Olaiz, A. Cascone, L., Hernandez, P., Faria, A., Tritlla, J., Ingles, M., Aida, B., Pinto, I., Rocca, R., Sanders, C., Herrá, A., & Tur, N., (2020) Geophysical evidence for breakup volcanism in the Angola and Gabon passive margins. *Marine and Petroleum Geology* v.116..

Gadd, M.G., Layton-Matthews, D., Peter, J.M., & Paradis, S., (2015) In situ trace element and sulphur isotope analyses of pyrite constrain timing of mineralization and sources of sulphur in the Howard's Pass SEDEX Zn-Pb District, Yukon. In Paradis, S., ed., Targeted Geoscience Initiative 4: sediment-hosted Zn-Pb deposits: processes and implications for exploration: *Geological Survey of Canada Open File*, 7838, p. 58-74.

Giordano, T.H., (2002) Transport of Pb and Zn by carboxylate complexes in basinal ore fluids and related petroleum-field brines at 100°C: the influence of pH and oxygen fugacity. *Geochem Trans*. v.3:56.

Gomez, M., Vergés, J., & Riaza, C., (2002) Inversion tectonics of the northern margin of the Basque Cantabrian Basin, *Bull. Soc. géol. France*, v.173, p. 449-459,

Goossens, P.J. (1978) The metallogenic provinces in Burma; their definitions, geologic relationships and extensions into China, India and Thailand. Proceedings of the 3rd Regional Conference on Geology and Mineral Resources of Southeast Asia,14–18 November 1978, Bangkok, p. 431–492

Grandia, F., Canals, À., Cardellach, E., Banks, D.A., & Perona, J., (2003) Origin of ore-forming brines in sediment-hosted Zn-Pb deposits of the Basque-Cantabrian basin, northern Spain. *Economic Geology*, v.98, p. 1397–1411.

Hahn, l., Koch, K. E. & Wittekindt, H., (1986) Outline of the Geology and the Mineral Potential of Thailand. *Geologisches Jahrbuch* v.59B, 49 pp.

Hanilçi, N., Öztürk, H., & Banks, D., (2020) Geological, geochemical and microthermometric characteristics of the Hakkari region Zn-Pb deposits, SE Turkey. *Ore Geology Reviews* v.125.

Henjes-Kunst, E., Raith, J.G., & Boyce, A.J., (2017) Micro-scale sulfur isotope and chemical variations in sphalerite from the Bleiberg Pb-Zn deposit, Eastern Alps, Austria, *Ore Geology Reviews* v.90, p. 52–62,

Herlec, U., Spangenberg, J.R., & Lavrič, J.V., (2010) Sulfur isotope variations from orebody to hand-specimen scale at the Mežica lead–zinc deposit, Slovenia: a predominantly biogenic pattern. *Mineralium Deposita*, v.45 p.531–547.

Hitzman, M.W, (1999) Characteristics and worldwide occurrences of Irish-type Zn-Pb-Ag deposits. In, Holm, O., Pongratz, J., and McGoldrick, P. (eds), Basins, Fluids and Zn-Pb ores, *CODES Special Publication* v.2, p.93-116.

Hnatyshin, D.J., Kontak, D., Turner, E.C., Creaser, R.A., Morden, R., & Stern, R.A., (2016) Geochronologic (Re-Os) and fluid-chemical constraints on the formation of the Mesoproterozoic-hosted Nanisivik Zn-Pb deposit, Nunavut, Canada: Evidence for early diagenetic, low-temperature conditions of formation. *Ore Geology Reviews* v.79, p.189-217.

Hocking, R.M., Copp, I.A., Playford, P.E., & Kempton, R.H., (1996) The Cadjebut Formation: A Givetian Evaporitic Precursor to Devonian Reef Complexes of the Lennard Shelf, Canning Basin, Western Australia. *Geological Survey of Western Australia 1995–96 Annual Review*, p.48-55.

Holl, R., Kling, M. & Schroll, E., (2007) The metallogenesis of germanium-A review. *Ore Geology Reviews* v.30, p. 145-180.

Hutchison, C. S., (1989) Geological evolution of South-East Asia. *Geological Society of Malaysia*, 433pp.

Jallouli, C., Chikhaoui, M., Braham, A., Turki, M., Mickus, K., & Benassi, R., (2005) Evidence for Triassic salt domes in the Tunisian Atlas from gravity and geological data. *Tectonophysics* v.396, p.209–225.

Jemmali, N., Souissi, F., Villa, I.M., & Vennemann, T.M., (2011) Ore genesis of Pb–Zn deposits in the Nappe zone of Northern Tunisia: Constraints from Pb–S–C–O isotopic systems, *Ore Geology Reviews* v.40, p.41–53,

Jitpiromsri, P. & Kanjanapayont, P., (2012) Morphotectonic Indices of the Mae Ping Fault Zone, Northwestern Thailand. *Bulletin of Earth Sciences of Thailand* v.5, p. 30-38.

Jones, G.V., (1994) Final mission report: Economic geology. Duddar pre-feasibility study: United Nations Development Program (Project PAK/89/034), unpublished report. In Allen, R.M., Gauthier, F., Jones, G.V., and Bhutani-Singh. 1994. Duddar. Prefeasibility study: UNDDSMS. New York. 5 volumes.

Jones, G.V. & Sajjad, A., (1994) Duddar Zn-Pb-Fe-Ba mineralization. In Khan, A.U., Huda, Q. and Husain, V. (eds.) Proc. 2nd Soc. Econ. Geol. Mineral. Tech. (SEGMITE) *Intern. Conf. on Industrial Minerals*, 58–63, Karachi.

Kennard, J. M., Jackson, M. J., Romine, K. K., Shaw, R. D. & Southgate, P. N., (1994) Depositional sequences and associated petroleum systems of the Canning Basin, W.A. In, Purcell, P. G. and Purcell, R. R. (eds), West Australian Basin Symposium: *Proceedings of the Petroleum Exploration Society of Australia Symposium, Perth*, p.657-676.

Khin Zaw, Aung Pwa, & Thet Aung Zan, (1984) Lead-zinc mineralization at Theingon Mine, Bawsaing, Southern Shan State, Burma: A Mississippi Valley-type deposit? *Geol. Soc. Malaysia* v.17, p. 283-306,

Kucha, H., Schroll, E., Raith, J.G., & Halas, S., (2010) Microbial sphalerite formation in carbonate-hosted Zn-Pb ores, Bleiberg, Austria: micro- to nanotextural and sulfur isotope evidence. *Economic Geology* v.105 p.1005–1023.

Kuhlemann, J., Vennemann, T., Herlec, U., Zeeh, S.,& Bechstaedt, T., (2001) Variations of sulfur isotopes, trace element compositions, and cathodoluminescence of Mississippi Valley-Type Pb-Zn ores from the Drau Range, Eastern Alps (Slovenia-Austria): Implications for ore deposition on a regional versus microscale: *Economic Geology* v.,96, p. 1931–1941.

Kuhlemann, J., & Zeeh, S., (1995) Sphalerite stratigraphy and trace element composition of East Alpine Pb-Zn deposits (Drau Range, Austria-Slovenia): *Economic Geology* v.90, p. 2073–2080.

Kyne, R., Torremans, K., Güven, J., Doyle, R., & Walsh, J., (2020) 3-D modeling of the Lisheen and Silvermines deposits, County Tipperary, Ireland: insights into structural controls on the formation of Irish Zn-Pb deposits, *Economic Geology* v.114 p.93-116.

LeHuray A.P., Caulfield, J. B. D., Rye, D.M., & Dixon, R., (1987) Basement controls on sediment-hosted Zn-Pb deposits: A Pb isotope

study of Carboniferous mineralization in Central Ireland, *Economic Geology* v.82, p.1695–1709.

Leach, D.L.& Sangster, D.F., (1993) Mississippi Valley-type lead-zinc deposits. In Kirkham, R.V., Sinclair, W.D., Thorp, R.I., and Duke, J.M. (eds) Mineral Deposit Models. *Geol. Assoc. Canada Spec. Paper* 40, p.289-314

Leach, D.L., Bradley, D.C., Lewchuk, M.T., Symons, D.T.A., de Marsily, G., & Brannon, J.C., (2001) Mississippi Valley-Type lead-zinc deposits through geological time: implications from recent age-dating research: *Mineralium Deposita* v.,36, p. 711–740.

Leach, D.L., Bechstaedt, T., Boni, M., & Zeeh, S., (2003) Triassic-hosted MVT Zn-Pb ores of Poland, Austria, Slovenia and Italy, in Kelly, J.G., Andrew, C.J., Ashton, J.H., Boland, M.B., Earls, G., Fusciardi, L., and Stanley, G., eds., Europe's major base metal deposits: *Dublin, Irish Association for Economic Geology*, p. 169–213.

Leach, D.L., Sangster, D.F., Kelley, K.D., Large, R.R., Garven, G., Allen, C.R., Gutzmer, J., & Walters, S., (2005) Sediment-hosted lead-zinc deposits: A global perspective: *Economic Geology 100th Anniversary Volume*, p. 561–607. doi: 10.5382/AV100.18

Leach, D.L., Taylor, R.D., Fey, D.L., Diehl, S.F. & Saltus, R.W., (2010) A deposit model for Mississippi-Valley type lead-zinc ores, Chapter A of Mineral deposit models for resource assessment, *U.S Geological Survey Scientific investigations report* 2010-5070-A , 52p.

Machel, H.G., (2001) Bacterial and thermochemical sulfate reduction in diagenetic settings — old and new insights, *Sedimentary Geology* v.140, p.143-175.

Magfouri, S., Hosseinzadeh, M.R., Choulet, F., & Rajabi, A., (2016) Mineralogical characterization of non-sulfide Zn–Pb mineralization at Mehdiabad deposit, Iran, Conference *Abstract, 35th International Geological Congress, Cape Town, South Africa*, Volume 1.

Magnall, J. M., Gleeson, S. A., Creaser, R. A., Paradis, S., Glodny, J., & Kyle, J. R., (2020) The mineralogical evolution of the clastic dominant-type Zn-Pb ± Ba deposits at Macmillan Pass (Yukon, Canada)—tracing subseafloor barite replacement in the layered mineralization. *Economic Geology* v.115, p. 961–979,

Maldonado, F., Mengal, J.M., Khan, S.H.,& Warwick, P.D., (2011) Summary of the stratigraphy and structural elements related to plate convergence of the Quetta-Muslim Bagh-Sibi region, Balochistan, west-central Pakistan: *USGS Open-File Report* 2011–1224, 19 pp.

Maucher, A., & Schneider, H. J., (1967) The Alpine lead-zinc ores: *Economic Geology Monograph* 3, p. 71–89.

McCracken, S.R., (1997) Stratigraphic, diagenetic, and structural controls of the Admiral Bay carbonate-hosted Zn-Pb-Ag deposit, Canning Basin, Western Australia, Unpublished PhD Thesis, University of Western Australia, 352pp.

McCracken, S.R., Etminan, H., Connor, A.G. & Williams, V.A., (1996) Geology of the Admiral Bay carbonate-hosted zinc-lead deposit, Canning Basin, Western Australia. In: Sangster, D.F. (Ed) Carbonate-Hosted Lead-Zinc Deposits: *Society of Economic Geologists, Special Publication*, 4, p.330-349.

Metcalfe, I., (2009) Late Palaeozoic and Mesozoic tectonic and palaeogeographical evolution of SE Asia. In: Buffetaut, E., Cuny, G., Le Loeuff, J. and Suteethorn, V. (eds) Late Palaeozoic and Mesozoic Ecosystems in SE Asia. *The Geological Society, London, Special Publications*, v.315, p. 7–23.

Metcalfe, I., (2011) Tectonic framework and Phanerozoic evolution of Sundaland. *Gondwana Research* v.19, p.3–21.

Middleton, H. & Wallace, M.W., (2003) The evolution of fluid flow systems prior to, during, and post MVT mineralization in the Givetian–Frasnian carbonates of the Emanuel Range, Western Australia, *Journal of Geochemical Exploration* v.78– 79, p.91– 97,

Mills, H., Halliday, A., Ashton, J., Anderson, K. & Russell, M. J., (1987) Origin of a giant orebody at Navan, Ireland. *Nature* v.327, p. 223–226.

Misi, A., Iyer, S.S.S., Coelho, C.E.S., Tassinari, C.G.C., Franca-Rocha, W.J.S., de Abreu Cunha, I., Rocha Gomes, A.S., de Oliveira, T.F., Teixeira, J.B.G., & Filho, V.M.C., (2005) Sediment hosted lead–zinc deposits of the Neoproterozoic Bambuí Group and correlative sequences, São Francisco Craton, Brazil: A review and a possible metallogenic evolution model. *Ore Geology Reviews*, v.26, p. 263-304.

Mohn, G., Manatschal, G., Müntener, O., Beltrando, M., & Masini, E., (2010) Unravelling the interaction between tectonic and sedimentary processes during lithospheric thinning in the alpine Tethys margins. *Int J Earth Sc*i v. 99 (Geol Rundsch), p. 75–101,

Morton, S.N. de, Wallace, M.W., Reed, C.P., Hewson, C., Redmond, P., Cross, E., & Moynihan, C., (2015) The significance of Tournaisian tectonism in the Dublin Basin: Implications for basin evolution and zinc-lead mineralization in the Irish Midlands, *Sedimentary Geology* v.330, p. 32-46.

Mory, (2017) A Palaeozoic perspective of Western Australia. *Geological Survey of Western Australia*: 58 pp.

Mueller, A.G., (2022) The Rammelsberg shale-hosted Cu-Zn-Pb sulfide-barite deposit, Germany: Linking SEDEX and Kuroko-type massive sulfides. Slide presentation and explanatory notes. https://e-sga.org/index.php?id=199

Nelson, J., Paradis, S., Christensen, J., & Gabites, J., (2002) Canadian Cordilleran Mississippi Valley-type deposits: A case for Devonian-Mississippian back-arc hydrothermal origin: *Economic Geology* v.97, p. 1013-1036,

Noce, C.M., Pedrosa-Soares, A.C., da Silva, L.C., Armstrong, R., & Piuzana, D., (2007) Evolution of polycyclic basement complexes in the Araçuaí Orogen, based on U–Pb SHRIMP data: Implications for Brazil–Africa links in Paleoproterozoic time. *Precambrian Research* v.159, p. 60-78.

O'Keefe, W.G. (1986) Age and postulated source rocks for mineralization in central Ireland, as indicated by lead isotopes. In: C.J. Andrew, R.W.A. Crowe, S. Finlay, W.M. Pennell and J.F. Pyne (eds), The geology and genesis of mineral deposits in Ireland. *Irish Association of Economic Geology*, p. 617–624.

Paradis, S., (2007) Isotope geochemistry of the Prairie Creek carbonate-hosted zinc-lead-silver deposit, southern Mackenzie Mountains, Northwest Territories. In, Mineral and energy resource potential of the proposed expansion to the Nahanni National Park Reserve, North Cordillera, Northwest Territories, (ed.) Falck, H., Wrigh, D.F. and Harrist, J., *Geological Survey of Canada, Open File* 5344, p

Paradis, S., Hannigan, P., & Dewing, K., (2007) Mississippi Valley-type lead-zinc deposits, in Goodfellow, W.D., ed., Mineral Deposits of Canada: A Synthesis of Major Deposit-Types, District Metallogeny, the Evolution of Geological Provinces, and Exploration Methods: *Geological Association of Canada, Mineral Deposits Division, Special Publicatio*n No. 5, p. 185-203.

Paradis, S., Simandl, G.J., Keevil, H., & Raudsepp, M., (2016) Carbonate-hosted nonsulfide Pb-Zn deposits of the Quesnel Lake District, British Columbia, Canada. *Economic Geology* v.111 p. 179–198.

Paradis, S., Hnatyshin, D., Simandl, G.J., & Creaser, R.A., (2020) Re-Os pyrite geochronology of the Yellowhead-type mineralization, Pend Oreille mine, Kootenay Arc, Metaline District, Washington, *Economic Geology* v.115, p. 1373–1384

Parker, R., Brady, B., Hayden, A., & Watts, G., (2013) Technical report and Preliminary Economic Assessment of the Song Toh – Boh Yai Properties, Kemco Project, Thong Phaphum District, Kanchanaburi Province, Thailand; NI 43-101 Technical Report, A.C.A. Howe International Limited report for Southeast Asia Mining Corp.

Parra-Garcia, M., Sanchez, G., Dentith, M.C. & George, A.D., (2014) Regional structural and stratigraphic study of the Canning Basin, Western Australia, *GSWA report* 140, 215 p.

Pasminco, (1998) Annual Report. Pasminco Limited, 18 September 1998.

Peace, W.M., & Wallace, M.W., (2000) Timing of mineralisation at the Navan Zn-Pb deposit: a post-Arundian age for Irish mineralisation. *Geology* v.28(8), p. 711–714.

Penney, S.R., Allen, R.M., Harrisson, S., Lees, T.C., Murphy, F.C. Norman, A.R. & Roberts, P.A. (2003) The global distribution of zinc mineralisation, an analysis based on a new zinc deposits database. *Transactions of the Institute of Mining and Metallurgy, Applied Earth Science*, v.113, p. B183.

Perinçek, D., (1990) Stratigraphy of the Hakkkari region, Southeastern Anatolia, *Bull. Turk. Pet. Geol. Assoc.* v.2, p. 21–68.

Perona, J., Canals, A., & Cardellach, (2018) Zn-Pb mineralization associated with salt diapirs in the Basque-Cantabrian Basin, Northern Spain: geology, geochemistry, and genetic model, *Economic Geology*, v.113, p. 1133–1159,

Playford, P.E., (1980) Devonian 'Great Barrier Reef' of the Canning Basin, Western Australia: *AAPG Bulletin*, v. 64, p. 814–840.

Playford, P.E.& Wallace, M., (2001) Exhalative mineralization in Devonian reef complexes of the Canning Basin, Western Australia, *Economic Geology*, v.96, p.595–1610,

Playford, P.E., Hocking, R.M., & Cockbain, A. E., (2009) Devonian reef complexes of the Canning Basin, Western Australia, *GSWA Bulletin*, v.,145/444.

Reichert, J., Borg, G. & Rashidi, B., (2003) Mineralogy of calamine ore from the Mehdi Abad zinc-lead deposit, Central Iran, In, Eliopoulos, D.G., et al. (eds), Mineral Exploration and Sustainable Development: *Proceedings of the Seventh Biennial SGA Meeting*, Athens, Greece.

Reynolds, N.A., (2017) Zn-Pb-Ag Mineral systems of Southeast Asia and South China – tectonic context and discovery opportunities, (abs) Ore deposits of Asia and beyond, *SEG 2017 Conference Proceedings*, Beijing China.

Reynolds, N.A. & Mackay, W., (2007) The Atlas zinc-lead province and analogies within the Tethyan zinc belt, In Andrew, C.J. et al., eds, Digging Deeper: *Proceedings of the Ninth Biennial SGA Meeting, Dublin, Ireland*, p.101-103.

Reynolds, N. A. & Copp, I.A., (2017a) Admiral Bay Zn-Pb-Ag deposit of the Canning Basin. *Australasian Institute of Mining and Metallurgy Monograph* 32, p.445–448.

Reynolds, N.A. & Copp, I.A, (2017b) Zn-Pb-Ag deposits of the Lennard Shelf, Canning Basin, In *Australasian Institute of Mining and Metallurgy Monograph* 32, p. 441–444.

Rosenbaum, G., Lister, G. S. & Duboz, C. (2002) Reconstruction of the tectonic evolution of the western Mediterranean since the Oligocene. In: Rosenbaum, G. and Lister, G. S. 2002. Reconstruction of the evolution of the Alpine-Himalayan Orogen. *Journal of the Virtual Explorer*, v.8, p. 107 - 126.

Russell, M.J. (1972a) The geological environment of post-Caledonian base-metal mineralization in Ireland. PhD thesis, Durham University, UK.

Sangster, D.F. (1976) Carbonate-hosted lead-zinc deposits. In, Wolf, K.H. (ed) Handbook of stratabound and stratiform ore deposits v.6, p.447-454.

Sangster, D.F., (1983) Mississippi Valley-type deposits: a geological melange. In: Kisvarsanyi, G., Grant, S.K., Pratt W.P., and Koenig, J.W. (eds) International conference on Mississippi Valley type lead-zinc deposits. University of Missouri Press, Rolla, Missouri, p. 7-19.

Sangster, D.F, (1990) Mississippi Valley-type and Sedex lead-zinc deposits: a comparative examination, *Transactions of the Institution of Mining and Metallurgy, Applied Earth Scienc*e, v.99, p. B21−B42.

Schroll, E., (1996) The Triassic carbonate-hosted Pb–Zn mineralization in the Alps (Europe). The metallogenetic position of Bleiberg type. In: Sangster, D.F. (ed) Carbonate-hosted lead–zinc deposits. *Society of Economic Geologists Special Publication*, p.182–194

Schroll, E., Köppel, V., & Cerny, I., (2006) Pb and Sr isotope and geochemical data from the Pb–Zn deposit Bleiberg (Austria): constraints on the age of mineralization, *Mineralogy and Petrology* v.86, p.129-156,

Schroll, E. & Rantitsch, G., (2005) Sulphur isotope patterns in the Bleiberg deposit (Eastern Alps) and their implications for genetically affiliated lead-zinc deposits. *Contributions to Mineralogy and Petrology* v.84. P. 1-18.

Schulz, O., (1964) Lead-zinc deposits in the Calcareous Alps as an example of submarine hydrothermal formation of mineral deposits. In: Amstutz G.C. (ed) Sedimentology and ore genesis 2. Elsevier, Amsterdam, p. 47–52.

Schultz, R. W., (1966) Lower Carboniferous cherty ironstones at Tynagh, Ireland. *Economic Geology* v.61, p. 311–342.

Selverstone, J., (2005) Are the Alps collapsing? *Annu. Rev. Earth Planet. Sci.* 2005. 33:113–32,

Shaw, R.D., Sexton, M.J. & Zeilinger, I., (1995) The tectonic framework of the Canning Basin, W.A., including 1:2 million structural elements map of the Canning Basin. **Geoscience Australia Record** 1994/048.

Slezak, P., Hitzman, M. W., van Acken, D., Dunlevy, E., Chew, D., Drakou, F., & Holdstock, M., (2022) Petrogenesis of the Limerick Igneous Suite: insights into the causes of post-eruptive alteration and the magmatic sources underlying the Iapetus Suture in SW Ireland, *Journal of the Geological Society*, v.180,

Song, Y.C., Liu, Y., Hou, Z., & Fard, M., (2017) Geology and mineralization of the world-class Mehdiabad Pb-Zn deposit, central Iran, SEG 2017 Conference Proceedings, Ore Deposits of China and Beyond, Beijing, China,

Song, Y.C., Liu, Y., Hou, Z., Fard, M., Zhang, H., & Zhuang, L.L., (2019) Sediment-hosted Pb–Zn deposits in the Tethyan domain from China to Iran: Characteristics, tectonic setting, and ore controls. *Gondwana Research* v.75, p.249-281,

Spangenberg, J.E. & Herlec, U, (2006) Hydrocarbon biomarkers in the Topla-Mežica zinc–lead deposits, Northern Karavanke/Drau range, Slovenia: paleoenvironment at the site of ore formation. *Economic Geology* v.101 p.997–1021

Spinks, S.C., Pearce, M.A., Liu, W., Kunzmann, M., Ryan, C.G., Moorhead, G.F., Kirkham, R., Blaikie, T. Sheldon, H.A., Schaubs, P.M. & Rickard, W.D.A., (2021) Carbonate replacement as the principal ore formation process in the Proterozoic McArthur River (HYC) sediment-Hosted Zn-Pb Deposit, Australia. *Economic Geology* v.116, p. 693–718.

St. Marie, J., & Kesler, S.F., (2000) Iron-rich and iron-poor Mississippi Valley-type mineralization, Metaline district, Washington: *Economic Geology*, v.95, p. 1091–1106.

Stampfli, G.M. & Borel, G.D., (2002) A plate tectonic model for the Paleozoic and Mesozoic constrained by dynamic plate boundaries and restored synthetic oceanic isochrons, *Earth and Planetary Science Letters* v.196, p.17-33,

Strogen, P. (1995) Lower Carboniferous volcanic rocks of the Limerick syncline, In Anderson, K., Ashton, J., Earls, G., Hitzman, M., and Tear, S., Irish Carbonate-Hosted Zn-Pb Deposits, *Society of Economic Geologists Guidebook Series* Volume 21

Symons, D.T.A., Symons, T.B.,& Sangster, D.F., (2001) Paleomagnetism of the Society Cliffs dolostone and the age of the Nanisivik zinc deposits, Baffin Island, Canada. *Mineralium Deposita* 36 p.412-459,

Symons, D.T.A & Arne, D.C., (2005) Paleomagnetic constraints on Zn–Pb ore genesis of the Pillara mine, Lennard shelf, Western Australia. *Mineralium Deposita* v.39, p.944–959,

Symons, D.T.A., Lewchuk, M.T., Kawasaki, K., Velasco, F., & Leach, D.L., (2009) The Reocín zinc–lead deposit, Spain: paleomagnetic dating of a late Tertiary ore body, *Mineralium Deposita* v.44, p. 867–880,

Teisserenc, P. & Villemin, J., (1989) Sedimentary Basin of Gabon-Geology and Oil Systems. In: Edwards, J.D. and Santogrossi, P.A., Eds., Divergent/Passive Margin Basins, Volume 46, *American Association of Petroleum Geologists Memoir*, p. 117-199.

Than Htun, Aung Kyin, & Khin Zaw, (2017) Lead–zinc–silver deposits of Myanmar, in Barber, A. J., Khin Zaw, and Crow, M. J. (eds), Myanmar: Geology, Resources and Tectonics, *Geological Society, London, Memoirs*, v.48, p.589–623, DOI : 10.1144/M48.27

Tompkins, L.A., Rayner, M.J., Groves, D.I. & Roche, M. T. (1994a) Evaporites; in situ sulfur source for rhythmically banded ore in the Cadjebut Mississippi Valley-type Zn-Pb deposit, Western Australia: *Economic Geology*, v.89, p. 467-492

Tompkins, L.A., Pedone, V.A., Roche, M.T.,& Groves, D.I., (1994b) The Cadjebut deposit as an example of Mississippi Valley-Type mineralisation on the Lennard Shelf, Western Australia-Single episode or multiple events. *Economic Geology* v.89, p. 450-466

Torremans, K., Kyne, R., Doyle, R., Güven, J., & Walsh, J.J., (2018) Controls on metal distributions at the Lisheen and Silvermines deposits: Insights into fluid flow pathways in Irish-type Zn-Pb deposits. *Economic Geology*, v.113, p.1455-1477,

Turner, E.C. (2011) Structural and stratigraphic controls on carbonate-hosted base metal mineralization in the Mesoproterozoic Borden Basin (Nanisivik District), Nunavut, *Economic Geology*, v.106, p. 1197–1223,

Turner E.C., Long, D.G.F., Rainbird, R.H., Petrus, J.A., & Rayner, N.M., (2016) Late Mesoproterozoic rifting in Arctic Canada during Rodinia assembly: impactogens, trans-continental far-field stress and zinc mineralisation, *Terra Nova* v.28, P.188-194,

Velasco, F., Herrero, J.M., Yusta, IñakiI., Alonso, J.A., Seebold, IgnacioI., & Leach, D.L., (2003) Geology and geochemistry of the Reocin zinc-lead deposit, Basque-Cantabrian basin, northern Spain: *Economic Geology*, v. 98, p. 1371–1396.

Velasco, F., Pesquera, A., & Herrero, J.M., (1996) Lead isotope study of Zn-Pb ore deposits associated with the Basque-Cantabrian basin and Paleozoic basement, Northern Spain, *Mineralium Deposita* v.31, p.84-92,

Warren, J. K. & Kempton, R., (1997) Evaporite sedimentology and the origin of evaporite-associated Mississippi Valley-type sulfides in the Cadjebut mine area, Lennard Shelf, Canning Basin, Western Australia. In: SEPM Special Publication 57, Basin-Wide Diagenetic Patterns: Integrated Petrologic, Geochemical, and Hydrologic Considerations Edited by: Montañez, I.P., Gregg, J.M., and Shelton, K.L., p. 183-205,

Walker, N., (2005) The distribution patterns of pathfinder elements in the Upper Dark Limestone cover sequence above the SWEX-B mineralisation. MSc Thesis, National University of Ireland, Galway, 150 p.

Wallace, M.W., Middleton, H.A., Johns, B. & Marshallsea, S., (2002) Hydrocarbons and Mississippi Valley-type sulfides in the Devonian Reef Complexes of the eastern Lennard Shelf, Canning Basin, Western Australia, in The Sedimentary Basins of WA 3 (ed M. Keep and S.J. Moss), Petroleum Exploration Society of Australia, pp. 795-816.

Wilkinson, J., (2014) Sediment-hosted zinc–lead mineralization: processes and perspectives, In: Holland H.D. and Turekian K.K. (eds.) *Treatise on Geochemistry*, *Second Edition*, vol. 13, pp. 219-249. Oxford:

Wilkinson, J., & Hitzman, M., (2015) The Irish Zn-Pb Orefield: The View from 2014. In Archibald, S. M. and Piercey, S. J., Current Perspectives on Zinc Deposits, IAEG,

Wilmsen, M., Fürsich, F.T., & Majidifard, M.R., (2014) An overview of the Cretaceous stratigraphy and facies development of the Yazd Block, western Central Iran, *Journal of Asian Earth Sciences* v.102, p.73–91,

Wogwanich, T., (1990) Lithostratigraphy, sedimentology, and diagenesis of the Ordovician carbonates, Southern Thailand. Ph.D. Thesis, University of Tasmania, 215 pp.

Zhong, R., Brugger, J., Chen, Y., & Li, W., (2015) Contrasting regimes of Cu, Zn and Pb transport in ore-forming hydrothermal fluids, *Chemical Geology* v.395, p. 154-164.

Ziegler, M.A., (2001) Late Permian to Holocene paleofacies evolution of the Arabian Plate and its hydrocarbon occurrences, *GeoArabia*, Vol. 6, No. 3, 2001, p.445-504.